# Simulation Techniques for Intense Beams*

Steven M. Lund
Lawrence Livermore National Laboratory (LLNL)

Steven M. Lund and John J. Barnard
"Beam Physics with Intense Space-Charge"

US Particle Accelerator School

University of Maryland, held at Annapolis, MD
16-27 June, 2008
(Version 20080622)

* Research supported by the US Dept. of Energy at LLNL and LBNL under contract Nos. DE-AC52-07NA27344 and DE-AC02-05CH11231.



## Simulation Techniques for Intense Beams: Outline

Why Numerical Simulation
Classes of Intense Beam Simulations
Overview of Basic Numerical Methods
Numerical Methods for Particle and Distribution Methods
Diagnostics
Initial Distributions and Particle Loading
Numerical Convergence
Practical Considerations
Overview of the WARP Code
Example Simulations
References



## Simulation Techniques for Intense Beams: Detailed Outline

1) Why Numerical Simulation?
2) Classes of Intense Beam Simulations
- A. Overview
- B. Particle Methods
- C. Distribution Methods
- D. Moment Methods
- E. Hybrid Methods

3) Overview of Basic Numerical Methods
- A. Discretization
- B. Discrete Numerical Operations
  - Derivatives
  - Quadrature
  - Irregular Grids and Axisymmetric Systems
- C. Time Advance
  - Overview
  - Euler and Runge-Kutta Advances
  - Solution of Moment Methods



## Detailed Outline - 2

4) Numerical Methods for Particle and Distribution Methods
- A. Overview
- B. Integration of Equations of Motion
  - Leapfrog Advance for Electric Forces
  - Leapfrog Advance for Electric and Magnetic Forces
  - Numerical Errors and Stability of the Leapfrog Method
  - Illustrative Examples
- C. Field Solution
  - Electrostatic Overview
  - Green's Function Approach
  - Gridded Solution: Poisson Equation and Boundary Conditions
  - Methods of Gridded Field Solution
  - Spectral Methods and the FFT
- D. Weighting: Depositing Particles on the Field Mesh and Interpolating Gridded Fields to Particles
  - Overview of Approaches
  - Approaches: Nearest Grid Point, Cloud in Cell, Area, Splines
- E. Computational Cycle for Particle in Cell Simulations

## Detailed Outline - 3

5) Diagnostics

6) Initial Distributions and Particle Loading

7) Numerical Convergence

8) Practical Considerations

A. Overview
B. Fast Memory
C. Run Time
D. Machine Architectures

9) Overview of the WARP Code

10) Example Simulations

A. ESQ Injector
B. ....

Contact Information
Acknowledgments
References



## S1: Why Numerical Simulation?

Builds intuition of intense beam physics

- "The purpose of computation is insight, not numbers"
  Richard Hamming, chief mathematician of the Manhattan Project and Turning Award recipient
- Advantages over laboratory experiments:
  - Full nonintrusive beam diagnostics are possible
  - Effects can be turned on and off

Allows analysis of more realistic situations than analytically tractable

- Realistic geometries
- Non-ideal distributions
- Combined effects
- Large amplitude (nonlinear) effects

Insight obtained can motivate analytical theories

- Suggest and test approximations and models to most simply express relevant effects



## Why Numerical Simulation? (2)

Can quantify expected performance of specific machines

- Machines and facilities expensive – important to have high confidence that systems will work as intended

Computers and numerical methods/libraries are becoming more powerful

Enables both analysis of more realistic problems and/or better numerical convergence

- Bigger and faster hardware
  - Processor speed increasing
  - Parallel machine architectures
  - Greater memory
- More developed software
  - Improved numerical methods
  - Libraries of debugged code modules
  - Graphics and visualization tools



## Why Numerical Simulation? (3)

Simulations are increasingly powerful and valuable in the analysis of intense beams, but should not be used to exclusion

- Parametric scaling is *very* important in machine design
  - Often it is hardest to understand what specific choices should be made in physical aperture sizes, etc.
  - Although scaling can be explored with simulation, analytical theory often best illustrates the trade-offs, sensitivities, and relevant combinations of parameters
- Concepts often fail due to limits of technology (e.g., fabrication tolerances, material failures, and unanticipated properties) and hence full laboratory testing is vital
  - Many understood classes of errors can be probed with simulation.
  - Unanticipated error sources are most dangerous
- Economic realities often severely limit what can be constructed
  - Simulating something unattainable may serve little purpose

## Why Numerical Simulation? (4)

The highest understanding and confidence is achieved when results from analytic theory, numerical simulation, and experiment all converge

- Motivates model simplifications and identification of relevant sensitivities

Numerical simulation skills are highly sought in many areas of accelerator and beam physics

- Specialists readily employable
- Skills transfer easily to many fields of physics and engineering

Numerous programming languages are employed in numerical simulations of intense beams

- Most common today: Fortran, Fortran 90, C, C++, Java, ...
- Strengths and weaknesses depend on application, preferences, and history (legacy code)

Results are analyzed with a variety of graphics packages:

- Commonly used: NCAR, Gist, Gnuplot, IDL, Narcisse...
- Plot frames combine into movies
- Use can greatly simplify construction of beam visualization diagnostics



## Why Numerical Simulation? (5)

A modern and flexible way to construct simulation packages is to link routines in fast, compiled code with an interactive interpreter such as:

- Examples: Python, Basis, Yorick, ...

Advantages of using interactive interpreters:

- Allows routines to be coded in mixed languages
  - Renders choice of programming languages less important
- Flexible reconfiguration of code modules possible to adapt for specific, unanticipated needs
  - Reduces need for recompilation and cumbersome structures for special uses
  - Aids cross-checking problems and debugging
- "Steering" of code during runs to address unanticipated side effects
- In the case of Python, facilitates modern, object-oriented structure



## Why Numerical Simulation? (6)

Discussing particular programming languages and graphics packages is beyond the scope of this class. Here our goal is to survey numerical simulation methods employed without presenting details of specific implementations.

However, we will show examples based on the "WARP" particle-in-cell code developed for intense beam simulation at LLNL and LBNL

- WARP is so named since it works on a "warped" Cartesian mesh with bends
- WARP is a family of particle-in-cell code tools built around a common Python interpreter for flexible operation
- Optimized for the simulation of intense beams with self-consistent electrostatic space-charge forces
- Actively maintained and extended:
  - Diagnostics
  - E-cloud
  - Electromagnetic effects and dense plasmas

    ⋮

More on WARP later after discussion of methods, etc.



## S2: Classes of Intense Beam Simulations

### S2A: Overview

There are three distinct classes of modeling of intense ion beams applicable to numerical simulation

1) Particle methods (see: S2B)
2) Distribution methods (see: S2C)
3) Moment methods (see: S2D)

All of these draw heavily on methods developed for the simulation of neutral plasmas. The main differences are:

- Lack of overall charge neutrality
  - Single species typical, though electron + ion simulations are common too
- Directed motion of the beam along accelerator axis
- Applied field descriptions of the lattice
  - Optical focusing elements
  - Accelerating structures

We will review and contrast these methods before discussing specific numerical implementations

## S2B: Particle Methods: Equations of Motion

Classical point particles are advanced with self-consistent interactions given by the Maxwell Equations

- Most general: If actual number of particles are used, this is approximately the physical beam
- Often intractable using real number of beam particles due to numerical work and problem size

Equations of motion (time domain, 3D, for generality)

ith particle:

$$\frac{d\mathbf{p}_i}{dt} = \mathbf{F}_i = q_i\left(\mathbf{E} + \frac{d\mathbf{x}_i}{dt}\times\mathbf{B}\right)$$

$$m_i\gamma_i\frac{d\mathbf{x}_i}{dt} = \mathbf{p}_i \quad ; \quad \gamma_i = \left[1 + \frac{\mathbf{p}_i^2}{(m_i c)^2}\right]^{1/2}$$

Initial conditions

$\mathbf{x}_i(t=0)$

$\mathbf{p}_i(t=0)$

Particle orbits $\mathbf{x}_i(t)$, $\mathbf{p}_i(t)$ solved as a function of time



## S2B: Particle Methods: Fields

Fields (electromagnetic in most general form)

Charge Density

$$\nabla\cdot\mathbf{E} = \frac{\rho}{\epsilon_0}$$

$$\nabla\times\mathbf{E} = -\frac{\partial\mathbf{B}}{\partial t}$$

$$\rho(\mathbf{x},t) = \rho_{\text{ext}}(\mathbf{x},t) + \sum_i q_i\delta[\mathbf{x}-\mathbf{x}_i(t)]$$

external (applied)

particle beam

Current Density

$$\nabla\cdot\mathbf{B} = 0$$

$$\nabla\times\mathbf{B} = \mu_0\mathbf{J} + \mu_0\epsilon_0\frac{\partial\mathbf{E}}{\partial t}$$

$$\mathbf{J}(\mathbf{x},t) = \mathbf{J}_{\text{ext}}(\mathbf{x},t) + \sum_i q_i\frac{d\mathbf{x}}{dt}\delta[\mathbf{x}-\mathbf{x}_i(t)]$$

+ boundary conditions on $\mathbf{E}$, $\mathbf{B}$



## S2C: Distribution Methods: Equations of Motion

Distribution Methods

- Based on reduced (statistical) continuum models of the beam
- Two classes: (microscopic) kinetic models and (macroscopic) fluid models
- Here, distribution means a function of continuum variables
- Use a 3D collision-less Vlasov model to illustrate concept
  Obtained from statistical averages of particle formulation

Example Kinetic Model: Vlasov Equation of Motion

$q_i = q$ ; $m_i = m$ ; easy to generalize for multiple species (see later slide)

$$\left\{\frac{\partial}{\partial t} + \mathbf{v}\cdot\frac{\partial}{\partial x} + q\left(\mathbf{E}+\mathbf{v}\times\mathbf{B}\right)\right\} f(\mathbf{x},\mathbf{p},t) = 0$$

$$\mathbf{v} = \frac{\mathbf{p}}{\gamma m} = \frac{\mathbf{p}/m}{[1+\mathbf{p}^2/(mc)^2]^{1/2}}$$

Initial condition

$f(\mathbf{x},\mathbf{p},t=0)$

$f(\mathbf{x},\mathbf{p},t)$ evolved from t = 0

$\mathbf{x}$, $\mathbf{p}$, $t$ independent variables



## S2C: Distribution Methods: Fields

Fields: Same as in particle methods but with $\rho$, $\mathbf{J}$ expressed in proper form for coupling to the distribution

Charge Density

$$\nabla\cdot\mathbf{E} = \frac{\rho}{\epsilon_0}$$

$$\nabla\times\mathbf{E} = -\frac{\partial\mathbf{B}}{\partial t}$$

$$\rho(\mathbf{x},t) = \rho_{\text{ext}}(\mathbf{x},t) + q\int d^3p\, f(\mathbf{x},\mathbf{p},t)$$

external (applied)

beam

Current Density

$$\nabla\cdot\mathbf{B} = 0$$

$$\nabla\times\mathbf{B} = \mu_0\mathbf{J} + \mu_0\epsilon_0\frac{\partial\mathbf{E}}{\partial t}$$

$$\mathbf{J}(\mathbf{x},t) = \mathbf{J}_{\text{ext}}(\mathbf{x},t) + q\int d^3p\, \mathbf{v} f(\mathbf{x},\mathbf{p},t)$$

+ boundary conditions on $\mathbf{E}$, $\mathbf{B}$

## S2C: Distribution Methods: Vlasov Equation

The Vlasov Equation is essentially a continuity equation for an incompressible "fluid" in 6D phase-space. To see this, note that

$$\frac{\partial}{\partial \mathbf{p}} \cdot \mathbf{v} \times \mathbf{B} = 0$$

The Vlasov Equation can be expressed as

$$\frac{\partial f}{\partial t} + \frac{\partial}{\partial \mathbf{x}} \cdot (\mathbf{v} f) + \frac{\partial}{\partial \mathbf{p}} \cdot (q[\mathbf{E} + \mathbf{v} \times \mathbf{B}] f) = 0$$

$$\Rightarrow \frac{\partial f}{\partial t} + \frac{\partial}{\partial \mathbf{x}} \cdot \left( \frac{d\mathbf{x}}{dt}\bigg|_{\text{orbit}} f \right) + \frac{\partial}{\partial \mathbf{p}} \cdot \left( \frac{d\mathbf{p}}{dt}\bigg|_{\text{orbit}} f \right) = 0$$

which is manifestly the form of a continuity equation in 6D phase-space, i.e., probability is not created or destroyed



## S2C: Distribution Methods: Collision Corrections

The effect of collisions can be included by adding a collision operator:

$$\boxed{\left\{ \frac{\partial}{\partial t} + \mathbf{v} \cdot \frac{\partial}{\partial \mathbf{x}} + \frac{\partial}{\partial \mathbf{p}} \cdot (q[\mathbf{E} + \mathbf{v} \times \mathbf{B}]) \right\} f = \frac{\partial f}{\partial t}\bigg|_{\text{coll}}}$$

For most applications in beam physics, $\frac{\partial f}{\partial t}\bigg|_{\text{coll}}$ can be neglected.

- See: estimates in J.J. Barnard, Intro Lectures

For exceptional cases, specific forms of collisions terms can be found in Nicholson, *Intro to Plasma Theory*, Wiley 1983, and similar plasma physics texts



## S2C: Distribution Methods: Comment on the PIC Method

The common Particle-in-Cell (PIC) method is *not* really a particle method, but rather a distribution method that uses a collection of smoothed "macro" particles to simulate Vlasov's Equation. This can understood roughly by noting that Vlasov's Equation can be interpreted as

$$\frac{d}{dt} f(\mathbf{x}, \mathbf{p}, t) = 0$$

Total derivative along a test particle's path

$\Longrightarrow$ Advance particles in a continuous field "fluid" to eliminate particle collisions

Important Point:

PIC is a method to solve Vlasov's Equation, *not* a discrete particle method

This will become clear after these lectures



## S2C: Distribution Methods: Multispecies Generalizations

Subscript species with $j$. Then in the Vlasov equation replace:

$$f \longrightarrow f_j$$
$$m \longrightarrow m_j$$
$$q \longrightarrow q_j$$

and there is a separate Vlasov equation for each of the $j$ species.

Replace the charge and current density couplings in the Maxwell Equations with and appropriate form to include charge and current contributions from all species:

$$\rho(\mathbf{x}, t) = \rho_{\text{ext}}(\mathbf{x}, t) + \sum_j q_j \int d^3p\, f_j(\mathbf{x}, \mathbf{p}, t)$$

$$\mathbf{J}(\mathbf{x}, t) = \mathbf{J}_{\text{ext}}(\mathbf{x}, t) + \sum_j q_j \int d^3p\, \mathbf{v} f_j(\mathbf{x}, \mathbf{p}, t)$$

Also, if collisions are included the collision operator should be generalized to include collisions between species as well as collisions of a species with itself

## S2C: Fluid Models

Fluid Models

- Obtained from further averages of kinetic model
- Described in terms of "macroscopic" variables (density, flow velocity, pressure...) that vary in ***x*** and *t*
- Models must be closed (truncated) at some order via physically motivated assumptions (cold, negligible heat flow, ...)

Moments:

Density $\quad n: \quad n(\mathbf{x},t) = \int d^3p\ f(\mathbf{x},\mathbf{p},t)$

Flow velocity $\quad \mathbf{V}: \quad n\mathbf{V}(\mathbf{x},t) = \int d^3p\ \mathbf{v} f(\mathbf{x},\mathbf{p},t)$

Flow momentum $\quad \mathbf{P}: \quad n\mathbf{P}(\mathbf{x},t) = \int d^3p\ \mathbf{p} f(\mathbf{x},\mathbf{p},t)$

Pressure tensor $\quad \mathcal{P}_{ij}: \quad n\mathcal{P}_{ij}(\mathbf{x},t) = \int d^3p\ [p_i - P_i(\mathbf{x},t)] \times [v_j - V_j(\mathbf{x},t)] f(\mathbf{x},\mathbf{p},t)$

Higher rank objects $\quad \vdots \quad \vdots \quad \vdots$



## S2C: Fluid Models: Equations of Motion

Equations of Motion (Eulerian approach)

Continuity:

$$\frac{\partial n}{\partial t} + \frac{\partial}{\partial \mathbf{x}} \cdot [n\mathbf{V}] = 0$$

Force: ith component

$$n\left(\frac{\partial}{\partial t} + \mathbf{V}\cdot\frac{\partial}{\partial \mathbf{x}}\right) P_i + \sum_j \frac{\partial}{\partial x_j}\mathcal{P}_{ij} = qn[\mathbf{E} + \mathbf{V}\times\mathbf{B}]_i$$

Field:

Maxwell Equations with charge and current density coupling to fluid variables given by:

$$\rho(\mathbf{x},t) = \rho_{\text{ext}}(\mathbf{x},t) + qn(\mathbf{x},t)$$
$$\mathbf{J}(\mathbf{x},t) = \mathbf{J}_{\text{ext}}(\mathbf{x},t) + qn(\mathbf{x},t)\mathbf{V}(\mathbf{x},t)$$



## S2C: Fluid Model: Multispecies Generalization

Subscript species with *j*. Then in the continuity, force, pressure, ... equations replace

| Particle Properties | Moments |
|---|---|
| $m \longrightarrow m_j$ | $n \longrightarrow n_j$ |
| $q \longrightarrow q_j$ | $\mathbf{V} \longrightarrow \mathbf{V}_j$ |
| | $\vdots$ |

Replace the charge and current density couplings in the Maxwell Equations with

$$\rho(\mathbf{x},t) = \rho_{\text{ext}}(\mathbf{x},t) + \sum_j q_j n_j(\mathbf{x},t)$$

$$\mathbf{J}(\mathbf{x},t) = \mathbf{J}_{\text{ext}}(\mathbf{x},t) + \sum_j q_j n_j(\mathbf{x},t)\mathbf{V}_j(\mathbf{x},t)$$



## S2C: Lagrangian Formulation of Distribution Methods

In kinetic and especially fluid models it can be convenient to adopt *Lagrangian* methods. For fluid models these can be distinguished as follows:

Eulerian Fluid Model:

Flow quantities are functions of space (***x***) and and evolve in time (*t*)

- Example: density *n*(***x***, *t*) and flow velocity **V**(***x***, *t*)

Lagrangian Fluid Model:

Identify parts of evolution (flow) with objects (material elements) and follow the flow in time (*t*)

- Shape and position of elements must generally evolve to represent flow
- Example: envelope model edge radii $r_x(s),\ r_y(s)$

Many distribution methods for Vlasov's Equation are hybrid Lagrangian methods

- Macro particle "shapes" in PIC (Particle in Cell) method to be covered can be thought of as Lagrangian elements representing a Vlasov flow

## S2C: Example Lagrangian Fluid Model

1D Lagrangian model of the longitudinal evolution of a cold beam

- Discretize fluid into longitudinal elements with boundaries
- Derive equations of motion for elements

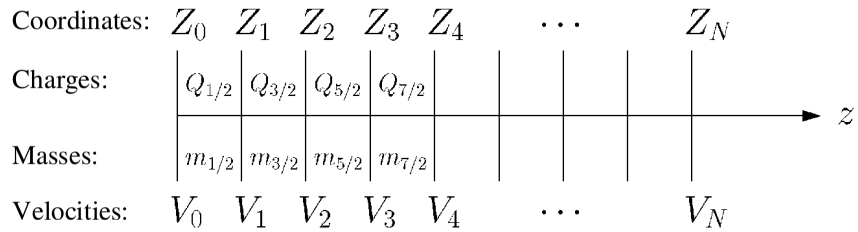


| | | | | |
|---|---|---|---|---|
| $z = Z_i$ | slice boundaries | $Q_{i+1/2}$ | fixed | $\frac{q}{m} = \text{const}$ |
| $\frac{dZ_i}{dt} = V_i$ | velocities of slice boundaries | $m_{i+1/2}$ | fixed | for single species (set initial coordinates) |



## Example Lagrangian Fluid Model, Continued (2)

Solve the equations of motion

$$\frac{dZ_i(t)}{dt} = V_i(t)$$
$$\frac{dV_i(t)}{dt} = \frac{q}{m} E_z(Z_i, t)$$

for all the slice boundaries. Several methods might be used to calculate $E_z$:

1) Take "slices" to have some radial extent modeled by a perpendicular envelope etc. and deposit the $Q_{i+1/2}$ onto a grid and solve:

$$\nabla^2 \phi = -\frac{\rho}{\epsilon_0} \qquad E_z = -\frac{\partial \phi}{\partial z}$$

subject to $E_z \to 0$ as $|z| \to \infty$

2) Employ a "g-factor" model

$$E_z = -\frac{g}{4\pi\epsilon_0}\frac{\partial \lambda}{\partial z}$$

$\lambda$ calculated from $Q_{i+1/2}$ and radial extent of the elements etc.

3) Pure 1D model using Gauss' Law



## S2D: Moment Methods

Moment Methods

- Most reduced description of an intense beam
  - Often employed in lattice designs
- Beam represented by a finite (closed and truncated) set of moments that are advanced from initial values
  - Here by moments, we mean functions of a single variable *s* or *t*
- Such models are not generally self-consistent
  - Some special cases such as a stable transverse KV equilibrium distribution (see: S.M. Lund lectures on Transverse Equilibrium Distributions) are consistent with truncated moment description (rms envelope equation)
  - Typically derived from assumed distributions with self-similar evolution
- See: S.M. Lund lectures on Transverse Equilibrium Distributions for more details on moment methods



## S2D: Moment Methods: 1st Order Moments

Many moment models exist. Illustrate with examples for transverse beam evolution

Moment definition:

$$\langle \ldots \rangle_\perp \equiv \frac{\int d^2x_\perp \int d^2x'_\perp \ldots f}{\int d^2x_\perp \int d^2x'_\perp f}$$

1st order moments:

| | |
|---|---|
| $\mathbf{X} = \langle \mathbf{x} \rangle_\perp$ | Centroid coordinate |
| $\mathbf{X}' = \langle \mathbf{x}' \rangle_\perp$ | Centroid angle |
| $\Delta = \left\langle \frac{\delta p_s}{p_s} \right\rangle_\perp \equiv \langle \delta \rangle_\perp$ | Off momentum |
| $\vdots$ | $\vdots$ |

## S2D: Moment Methods: 2nd and Higher Order Moments

2nd order moments:

| x moments | y moments | x-y cross moments | dispersive moments |
|---|---|---|---|
| $\langle x^2 \rangle_\perp$ | $\langle y^2 \rangle_\perp$ | $\langle xy \rangle_\perp$ | $\langle x\delta \rangle_\perp$ , $\langle y\delta \rangle_\perp$ |
| $\langle xx' \rangle_\perp$ | $\langle yy' \rangle_\perp$ | $\langle x'y \rangle_\perp$ , $\langle xy' \rangle_\perp$ | $\langle x'\delta \rangle_\perp$ , $\langle y'\delta \rangle_\perp$ |
| $\langle x'^2 \rangle_\perp$ | $\langle y'^2 \rangle_\perp$ | $\langle x'y' \rangle_\perp$ | $\langle \delta^2 \rangle_\perp$ |

It is typically convenient to subtract centroid from higher-order moments

$$\tilde{x} \equiv x - X \qquad \tilde{x}' \equiv x' - X'$$
$$\tilde{y} \equiv y - Y \qquad \tilde{y}' \equiv y' - Y'$$

$$\langle \tilde{x}^2 \rangle_\perp = \langle (x - X)^2 \rangle_\perp = \langle x^2 \rangle_\perp - X^2, \text{ etc.}$$

3rd order moments: Analogous to 2nd order case, but more for each order

$$\langle x^3 \rangle_\perp , \ \langle x^2 y \rangle_\perp , \ \ldots$$



## S2D: Moment Methods: Common 2nd Order Moments

Many quantities of physical interest are expressed in terms of moments

Statistical beam size: (rms edge measure)

$$r_x = 2 \langle \tilde{x}^2 \rangle_\perp^{1/2}$$
$$r_y = 2 \langle \tilde{y}^2 \rangle_\perp^{1/2}$$

Statistical emittances: (rms edge measure)

$$\varepsilon_x = 4 \left[ \langle \tilde{x}^2 \rangle_\perp \langle \tilde{x}'^2 \rangle_\perp - \langle \tilde{x}\tilde{x}' \rangle_\perp^2 \right]^{1/2}$$
$$\varepsilon_y = 4 \left[ \langle \tilde{y}^2 \rangle_\perp \langle \tilde{y}'^2 \rangle_\perp - \langle \tilde{y}\tilde{y}' \rangle_\perp^2 \right]^{1/2}$$



## S2D: Moment Methods: Equations of Motion

Equations of Motion

- Can be expressed in terms of moments of combinations of moments that are of physical interest
- Moments are advanced from specified initial conditions

Form equations:

$$\frac{d}{ds}\mathbf{M} = \mathbf{F}(\mathbf{M})$$

**M** = vector of moments, generally infinite

**F** = vector function of **M**, generally nonlinear

Moment methods generally form an infinite chain of equations that do *not* truncate. To be useful the system must be truncated. Truncations are usually carried out by assuming a specific form of the distribution that can be described by a finite set of moments

- Self-similar evolution: form of distribution assumed not to change
  - Analytical solutions often employed
- Neglect of terms

A simple example will be employed to illustrate these points



## S2D: Moment Methods: Example: Transverse Envelope Eqns.

Truncation assumption: unbunched uniform density elliptical beam in free space

- $\delta = 0$ , no axial velocity spread
- All cross moments zero, i.e. $\langle \tilde{x}\tilde{y} \rangle_\perp = 0$

Centroid: $X = \langle x \rangle_\perp$, $Y = \langle y \rangle_\perp$

Envelope: $r_x = 2 \langle \tilde{x}^2 \rangle_\perp^{1/2}$, $r_y = 2 \langle \tilde{y}^2 \rangle_\perp^{1/2}$

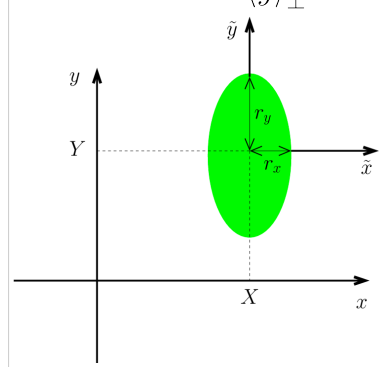


For: $\dfrac{\tilde{x}^2}{r_x^2} + \dfrac{\tilde{y}^2}{r_y^2} < 1$

$$E_{\tilde{x}} = \frac{\lambda}{\pi\epsilon_0} \frac{\tilde{x}}{(r_x + r_y) r_x}$$

$$E_{\tilde{y}} = \frac{\lambda}{\pi\epsilon_0} \frac{\tilde{y}}{(r_x + r_y) r_y}$$

$\lambda =$ line charge density

These results are employed to derive the moment equations of motion

(See S.M. Lund lectures on Transverse Centroid and Envelope Models)

## Example Continued (2) - Equations of Motion in Matrix Form

$$\frac{d}{ds}\begin{bmatrix} X \\ X' \\ Y \\ Y' \end{bmatrix} = \begin{bmatrix} X' \\ -\kappa_x(s)X \\ Y' \\ -\kappa_y(s)Y \end{bmatrix}$$

$$\frac{d}{ds}\begin{bmatrix} \langle\tilde{x}^2\rangle_\perp \\ \langle\tilde{x}\tilde{x}'\rangle_\perp \\ \langle\tilde{x}'^2\rangle_\perp \\ \langle\tilde{y}^2\rangle_\perp \\ \langle\tilde{y}\tilde{y}'\rangle_\perp \\ \langle\tilde{y}'^2\rangle_\perp \end{bmatrix} = \begin{bmatrix} 2\langle\tilde{x}\tilde{x}'\rangle_\perp \\ \langle\tilde{x}'^2\rangle_\perp - \kappa_x(s)\langle\tilde{x}^2\rangle_\perp + \frac{Q\langle\tilde{x}'^2\rangle_\perp}{[4\langle\tilde{x}^2\rangle_\perp^{1/2}(\langle\tilde{x}^2\rangle_\perp^{1/2}+\langle\tilde{y}^2\rangle_\perp^{1/2})]} \\ -2\kappa_x(s)\langle\tilde{x}\tilde{x}'\rangle_\perp + \frac{2Q\langle\tilde{x}\tilde{x}'\rangle_\perp}{[4\langle\tilde{x}^2\rangle_\perp^{1/2}(\langle\tilde{x}^2\rangle_\perp^{1/2}+\langle\tilde{y}^2\rangle_\perp^{1/2})]} \\ 2\langle\tilde{y}\tilde{y}'\rangle_\perp \\ \langle\tilde{y}'^2\rangle_\perp - \kappa_y(s)\langle\tilde{y}^2\rangle_\perp + \frac{Q\langle\tilde{y}'^2\rangle_\perp}{[4\langle\tilde{y}^2\rangle_\perp^{1/2}(\langle\tilde{x}^2\rangle_\perp^{1/2}+\langle\tilde{y}^2\rangle_\perp^{1/2})]} \\ -2\kappa_y(s)\langle\tilde{y}\tilde{y}'\rangle_\perp + \frac{2Q\langle\tilde{y}\tilde{y}'\rangle_\perp}{[4\langle\tilde{y}^2\rangle_\perp^{1/2}(\langle\tilde{x}^2\rangle_\perp^{1/2}+\langle\tilde{y}^2\rangle_\perp^{1/2})]} \end{bmatrix}$$

- Form truncates due to assumed distribution form
- Self-consistent with the KV distribution. See: S.M. Lund lectures on Transverse Equilibrium Distributions



## Example Continued (3) - Reduced Form Equations of Motion

Using 2nd order moment equations we can show that

$$\frac{d}{ds}\varepsilon_x^2 = 0 = \frac{d}{ds}\varepsilon_y^2$$

$$\Longrightarrow \quad \boxed{\begin{aligned} \varepsilon_x^2 &= 16\left[\langle x^2\rangle_\perp\langle x'^2\rangle_\perp - \langle xx'\rangle_\perp^2\right] = \text{const} \\ \varepsilon_y^2 &= 16\left[\langle y^2\rangle_\perp\langle y'^2\rangle_\perp - \langle yy'\rangle_\perp^2\right] = \text{const} \end{aligned}}$$

The 2nd order moment equations can be equivalently expressed as

$$\boxed{\begin{aligned} \frac{dr_x}{ds} &= r_x' \;; \quad \frac{d}{ds}r_x' + \kappa_x r_x - \frac{2Q}{r_x+r_y} - \frac{\varepsilon_x^2}{r_x^3} = 0 \\ \frac{dr_y}{ds} &= r_y' \;; \quad \frac{d}{ds}r_y' + \kappa_y r_y - \frac{2Q}{r_x+r_y} - \frac{\varepsilon_y^2}{r_y^3} = 0 \end{aligned}}$$



## Example Continued (4) : Contrast Form of Matrix and Reduced Form Moment Equations

Relative advantages of the use of coupled matrix form versus reduced equations can depend on the problem/situation

Coupled Matrix Equations

$$\frac{d}{ds}\mathbf{M} = \mathbf{F}$$

**M** = Moment Vector

**F** = Force Vector

- Easy to formulate
  - Straightforward to incorporate additional effects
- Natural fit to numerical routine
  - Easy to code

Reduced Equations

$$X'' + \kappa_x X = 0$$

$$r_x'' + \kappa_x r_x - \frac{2Q}{r_x+r_y} - \frac{\varepsilon_x^2}{r_x^3} = 0$$

etc.

Reduction based on identifying invariants such as

$\varepsilon_x^2 = 16\left[\langle\tilde{x}^2\rangle_\perp\langle\tilde{x}'^2\rangle_\perp - \langle\tilde{x}\tilde{x}'\rangle_\perp^2\right]$

helps understand solutions

- Compact expressions



## S2E: Hybrid Methods

Beyond the three levels of modeling outlined earlier:

1) Particle methods
2) Distribution methods
3) Moment methods

there exist numerous "hybrid" methods that combine features of several methods.

Examples:

- Particle-in-Cell (PIC) models with shaped particles
- Gyro-kinetic models
  - Average over fast gyro motion in magnetic fields: common in plasma physics
- Delta-f models
  - Evolve perturbed distribution with marker particles

⋮

## Hybrid Methods Continued (2)

General comments:

- Particle and distribution methods are appropriate for higher levels of detail
- Moment methods are used for rapid iteration of machine design
  - Moments also typically calculated as diagnostics in particle and distribution methods
- Even within one (e.g. particle) there are many levels of description:
  - Electromagnetic and electrostatic, with many field solution methods
  - 1D, 2D, 3D
  - ⋮
- Employing a hierarchy of models with full diagnostics allows cross-checking (both in numerics and physics) and aids understanding
  - No single method is best in all cases



## S3: Overview of Basic Numerical Methods

### S3A: Discretizations

General approach is to discretize independent variables in each of the methods and solve for dependent variables which in some cases may be discretized as well

time (or $s$)

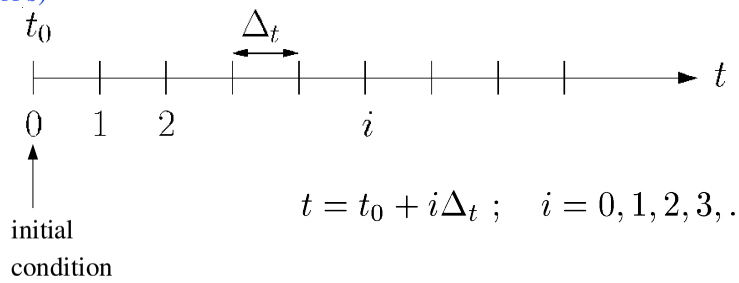


$$t = t_0 + i\Delta_t \; ; \quad i = 0, 1, 2, 3, ...$$

- Nonuniform meshes also possible
  - Can add resolution where needed
  - Increases complexity

In typical applications may apply these descriptions in a variety of ways

- Move a transverse thin slice of a beam...



## Transverse Coordinate Discretization

Spatial Coordinates (transverse)

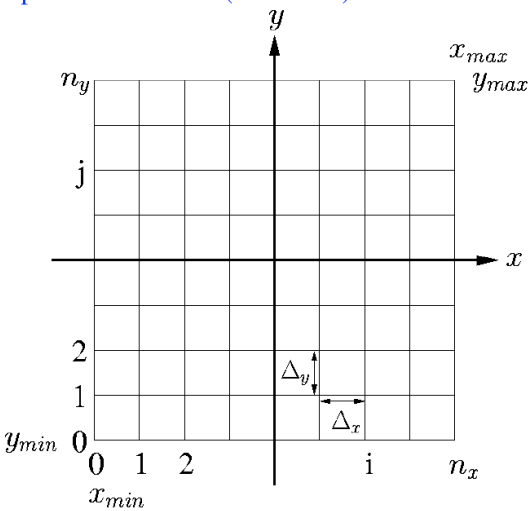


$$x_i = x_{min} + i\Delta_x$$
$$y_j = y_{min} + j\Delta_y$$

$$\Delta_x = (x_{max} - x_{min})/n_x$$
$$\Delta_y = (y_{max} - y_{min})/n_y$$

$$i = 0, 1, 2, ..., n_x$$
$$j = 0, 1, 2, ..., n_y$$

Analogous for 3D, momentum coordinates, etc.



## Transverse Coordinate Discretization – Applications

In typical applications may apply these discretizations in a variety of ways:

Transverse Slice Simulation:

- Move a transverse thin "slice" of beam along the axial coordinate $s$ of a reference particle

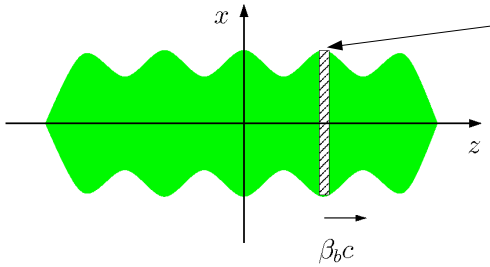


Thin slice of a long pulse is advanced and the transverse grid moves with the slice

- Limitations:
  - This "unbunched" approximation is not always possible
  - 3D effect can matter, e.g. in short pulses and/or beams ends

## Transverse Coordinate Discretization – Applications (2)

Steady State Simulation:

- Simulate the middle of a long pulse where a time stationary beam fills the grid

Example: Mid-Pulse Diode

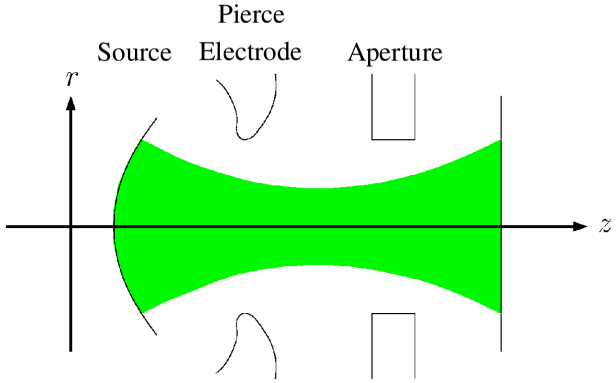


- Mesh is stationary, leading to limitations
  - Beam pulse always has ends: see J.J. Barnard lectures on Longitudinal Physics
  - Assumes that the mid-pulse in nearly time-independent in structure



## Transverse Coordinate Discretization – Applications (3)

Full 3D Simulation

- Simulate a 3D beam with a moving mesh that follows a reference particle (possibly beam centroid).

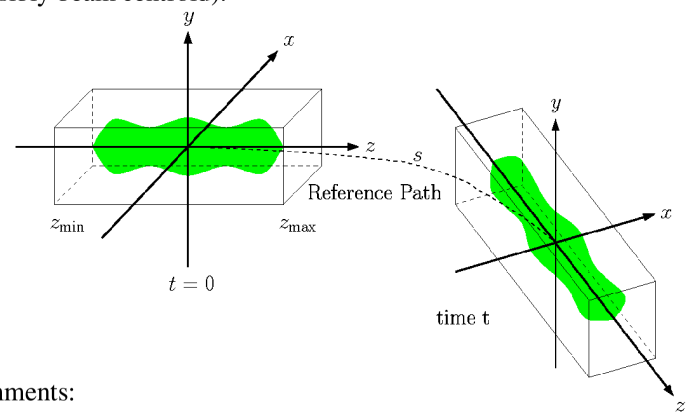


- Comments:
  - Most realistic level of modeling, but also most numerically intensive
  - Grid can be moved in discretized jumps so that applied fields maintain alignment with the grid



## S3B: Discrete Numerical Operations

Let x represent a spatial coordinate and $f(x)$ some continuous function of $x$

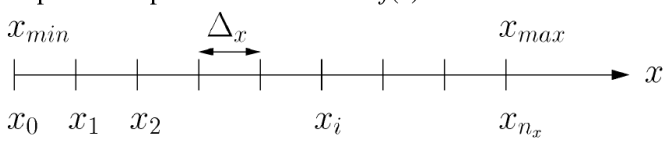


$$x_i = x_{min} + i\Delta_x; \quad \Delta_x = (x_{max} - x_{min})/n_x$$

$$i = 0, 1, 2, ..., n_x$$

Denote $f_i \equiv f(x_i)$, etc. and Taylor expand one grid point forward and backward about $x = x_i$

$$f_{i+1} = f_i + \left.\frac{\partial f}{\partial x}\right|_i \Delta_x + \frac{1}{2!}\left.\frac{\partial^2 f}{\partial x^2}\right|_i \Delta_x^2 + \frac{1}{3!}\left.\frac{\partial^3 f}{\partial x^3}\right|_i \Delta_x^3 + \ldots$$

$$f_{i-1} = f_i - \left.\frac{\partial f}{\partial x}\right|_i \Delta_x + \frac{1}{2!}\left.\frac{\partial^2 f}{\partial x^2}\right|_i \Delta_x^2 - \frac{1}{3!}\left.\frac{\partial^3 f}{\partial x^3}\right|_i \Delta_x^3 + \ldots$$

The same methodology can be applied to other spatial ($x$, $y$, etc.), axial ($s$), and temporal ($t$) coordinates



## Discrete Numerical Operations: Derivatives

Simple, but inaccurate expressions for 1st order derivatives follow immediately from the forward and backward expansions

2 point:
(non-centered)

Forward: $$\left.\frac{\partial f}{\partial x}\right|_i = \frac{f_{i+1} - f_i}{\Delta_x} + \mathcal{O}(\Delta_x)$$

Backward: $$\left.\frac{\partial f}{\partial x}\right|_i = \frac{f_i - f_{i-1}}{\Delta_x} + \mathcal{O}(\Delta_x)$$

A more accurate, centered discretization for a 1st order derivative is obtained by subtracting the two expansions.

3 point:
(centered)

$$\left.\frac{\partial f}{\partial x}\right|_i = \frac{f_{i+1} - f_{i-1}}{2\Delta_x} + \mathcal{O}(\Delta_x^2)$$

- More accuracy generally will require the use of more function points

## Discrete Numerical Operations: Derivatives (2)

The expansions can be relabeled ($i$ -> $i$+1, etc.) and the resulting set of equations can be manipulated to obtain 5-point and other higher-order forms with higher accuracy:

5 point: (centered)

$$\boxed{\left.\frac{\partial f}{\partial x}\right|_i = \frac{f_{i-2} - 8f_{i-1} + 8f_{i+1} - f_{i+2}}{12\Delta_x} + \mathcal{O}(\Delta_x^4)}$$

Still higher order, and more accurate, forms are possible but rapidly become cumbersome and require more points.

Similar methods can be employed to obtain discretizations of higher order derivatives. For example,

3 point: (centered)

$$\boxed{\left.\frac{\partial^2 f}{\partial x^2}\right|_i = \frac{f_{i+1} - 2f_i + f_{i-1}}{\Delta_x^2} + \mathcal{O}(\Delta_x^2)}$$



## Discrete Numerical Operations: Integrals/Quadrature

Take $n_x$ even, then $\int_{x_{min}}^{x_{max}} d\tilde{x}\, f(\tilde{x})$ can be composed as sub-integrals of the form

$$\int_{x_{i-1}}^{x_{i+1}} d\tilde{x}\, f(\tilde{x})$$

Using a linear approximation (Trapezoidal Rule):

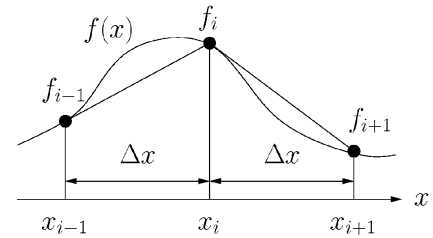


$$\boxed{\int_{x_{i-1}}^{x_{i+1}} dx\, f(x) = \frac{f_{i-1} + 2f_i + f_{i+1}}{2}\Delta_x + \mathcal{O}(\Delta_x^3)}$$



## Discrete Numerical Operations: Integrals/Quadrature (2)

Better approximations can be found (e.g., Simpson's Rule) using Taylor series expansions and the previous discrete derivatives:

$$f(x) = f_i + \frac{f_{i+1} - f_{i-1}}{2\Delta_x}x + \frac{f_{i+1} - f_i + f_{i-1}}{\Delta_x^2}x^2 + \ldots$$

giving:

$$\boxed{\int_{x_{i-1}}^{x_{i+1}} dx\, f(x) = \frac{f_{i-1} + 4f_i + f_{i+1}}{3}\Delta_x + \mathcal{O}(\Delta_x^5)}$$

In the examples given, uniform grids have been employed and the formulas presented for derivatives and integrals are readily generalized to multiple dimensions.



## Discrete Numerical Operations: Irregular Grids

Nonuniform grids can be used to effectively concentrate resolution where it is needed

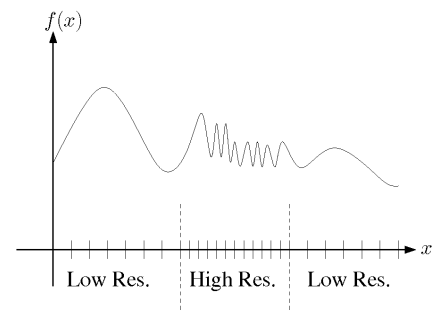


- Can be used most effectively when high resolution is needed only in limited regions and simulation domains are large
- Nonuniform grids make discretized formulas more complicated, particularly with respect to ordering errors
  - A simple example of nonuniform derivative calculation is included in the homework to illustrate methods

## Discrete Numerical Operations: Axisymmetric Systems

To be added: Slide to discuss how to solve cylindrically symmetric problems pointing out origin problems. Suggest that it is often better to simply do in 2D *x-y* geometry and use conserved angular momentum.



## S3C: Numerical Solution of Moment Methods – Time Advance

We now have the tools to numerically solve moment methods. The moment equations may always be written as an N-dimensional set of coupled 1st order ODEs (see: S2C and S.M. Lund lectures on Transverse Envelope Equations):

$$\mathbf{M} = \left(\langle x\rangle_\perp, \cdots, \langle x^2\rangle_\perp, \cdots\right) \qquad \text{N-dim vector of moments}$$

$$\frac{d\mathbf{M}}{ds} = \mathbf{F}(\mathbf{M}, s) \qquad \text{vector equation of motion}$$

- Methods developed to advance moments can also be used for advances in particle and distribution methods

/// Example: Axisymmetric envelope equation for a continuously focused beam

$$\frac{d^2R}{ds^2} + k_{\beta 0}^2 R - \frac{Q}{R} - \frac{\varepsilon_x^2}{R^3} = 0 \qquad R = 2\sqrt{\langle x^2\rangle_\perp}$$

$$\frac{d}{ds}\begin{bmatrix} R \\ R' \end{bmatrix} = \begin{bmatrix} R' \\ -k_{\beta 0}^2 R + \frac{Q}{R} + \frac{\varepsilon_x^2}{R^3} \end{bmatrix} \qquad k_{\beta 0}^2,\ Q,\ \varepsilon_x^2,\ \text{constants}$$

///



## S3C: Numerical Solution of Moment Methods – Euler Advance

Euler's Method:

Apply the forward difference formula

$$\left.\frac{d\mathbf{M}}{ds}\right|_i = \frac{\mathbf{M}_{i+1} - \mathbf{M}_i}{\Delta_s} + \mathcal{O}(\Delta_s) = \mathbf{F}(\mathbf{M}_i, s_i)$$

Rearrange to obtain 1st order Euler advance:

$$\mathbf{M}_{i+1} = \mathbf{M}_i + \mathbf{F}(\mathbf{M}_i, s_i)\Delta_s + \mathcal{O}(\Delta_s^2)$$

- Moments advanced in discrete steps in s from initial values

Note that $N_s$ steps will lead to a total error

$$\text{error} \sim N_s \cdot \mathcal{O}(\Delta_s^2) \sim \frac{s_{max} - s_{min}}{\Delta_s}\mathcal{O}(\Delta_s^2) \sim \mathcal{O}(\Delta_s)$$

- Error decreases only linearly with step size
- Numerical work for each step is only one evaluation of **F**



## S3C: Numerical Solution of Moment Methods – Order Advance

Definition:

A discrete advance with error $\mathcal{O}(\Delta_s^n)$ is an ($n$-1)th order method

- Euler's method is a 1st order method
- Higher order methods are generally used for ODE's in moment methods
  - Cheap to evaluate **F**
- Low order methods are generally used for particle and distribution methods
  - Expensive to evaluate **F**

## S3C: Numerical Solution of Moment Methods – Runge-Kutta Advance

Runge-Kutta Method:

Integrate from $s_i$ to $s_{i+1}$:

$$\frac{d\mathbf{M}}{ds} = \mathbf{F}(\mathbf{M}, s)$$

$$\mathbf{M}_{i+1} = \mathbf{M}_i + \int_{s_i}^{s_{i+1}} ds\, \mathbf{F}(\mathbf{M}, s)$$

Approximate **F** with a Taylor expansion through the midpoint of the step, $s_{i=1/2}$

$$\mathbf{F}(\mathbf{M}, s) = \mathbf{F}(\mathbf{M}_{i+1/2}, s_{i+1/2}) + \left.\frac{\partial \mathbf{F}}{\partial s}\right|_{s_{i+1/2}} (s - s_{i-1/2}) \quad + \ldots$$

The linear term integrates to zero, leaving

$$\Rightarrow \mathbf{M}_{i+1} = \mathbf{M}_i + \mathbf{F}(\mathbf{M}_{i+1/2}, s_{i+1/2}) \cdot \Delta_s + \mathcal{O}(\Delta_s^3)$$



## Runge-Kutta Advance (2)

Note: only need $\mathbf{M}_{i+1/2}$ to $\mathcal{O}(\Delta_s^2)$ for $\mathcal{O}(\Delta_s^3)$ accuracy
Apply Euler's method for the two-step procedure:

2nd Order Runge-Kutta Method:

Step 1: $\mathbf{K} = \mathbf{F}(\mathbf{M}_i, s_i)\Delta_s$

Step 2: $\mathbf{M}_{i+1} = \mathbf{M}_i + \mathbf{F}\left(\mathbf{M}_i + \frac{\mathbf{K}}{2}, s_i + \frac{\Delta_s}{2}\right)\Delta_s + \mathcal{O}(\Delta_s^3)$

- Requires two evaluations of **F** per advance
- 2nd order accurate in $\Delta_s$

Higher order Runge-Kutta schemes are derived analogously from various quadrature formulas. Such formulas are found in standard numerical methods texts

- Typically, methods with error $\mathcal{O}(\Delta_s^{N+1})$ will require N evaluations of **F**



## S3C: Numerical Solutions of Moment Methods

Many methods are employed to advance moments and particle orbits.

A general survey of these methods is beyond the scope of this lecture. But some general comments can be made:

- Many higher-order methods with adaptive step sizes exist that refine accuracy to specified tolerances and are optimized for specific classes of equations
- Choice of numerical method often relates to numerical work and stability considerations
- Certain methods can be formulated to exactly preserve relevant single-particle invariants
  - "Symplectic" methods preserve Hamiltonian structure of dynamics
- Accelerator problems can be demanding due to multiple frequency scales and long tracking times/distances
  - Hamiltonian dynamics; phase space volume does not decay



## S3C: Numerical Solutions of Moment Methods – Numerical Stability

"Numerical Reversibility" test of stability:

In this method, the final value of an advance is used as an initial condition. Then the problem is run backwards to the original starting point and deviations from the initial conditions taken in the original advance are analyzed.

- Often a simple, but stringent test of accuracy
- Will ultimately fail due to roundoff errors and cases where there is a sensitive dependence on initial conditions
- Orbits can be wrong but qualitatively right. We will quantify this notion better later. So lack of full convergence does not necessarily mean that useless results will be obtained.

We will now briefly overview an application of moment equations, namely the KV envelope equations, to a practical high current transport lattice that was designed for Heavy Ion Fusion applications at Lawrence Berkeley National Laboratory.

## S3C: Moment Equation Application: Perp. KV Envelope Eqns

Neglect image charges and nonlinear self-fields (emittance constant) to obtain moment equations for the evolution of the beam envelope radii

$$\frac{d^2 r_x}{ds^2} + \kappa_q r_x - \frac{2Q}{r_x + r_y} - \frac{\varepsilon_x^2}{r_x^3} = 0 \qquad r_x = 2\sqrt{\langle x^2 \rangle_\perp}$$

$$\frac{d^2 r_y}{ds^2} - \kappa_q r_y - \frac{2Q}{r_x + r_y} - \frac{\varepsilon_y^2}{r_y^3} = 0 \qquad r_y = 2\sqrt{\langle y^2 \rangle_\perp}$$

$$Q = \frac{qI}{2\pi\epsilon_0 m c^3 \gamma_b^3 \beta_b^3}$$

Dimensionless Perveance measures space-charge strength

$$\varepsilon_x = 4\left[\langle x^2 \rangle_\perp \langle x'^2 \rangle_\perp - \langle x x' \rangle_\perp^2\right]^{1/2}$$

$$(\varepsilon_{xn} = \gamma_b \beta_b \varepsilon_x \text{ normalized})$$

RMS Edge Emittance measures x-x' phase-space area ~(beam size)sqrt(thermal temp.)

The matched beam solution together with parametric constraints from engineering, higher-order theory, and simulations are used to design the lattice.



## Application Example Continued (2) – Focusing Lattice

Take an alternating gradient FODO doublet lattice

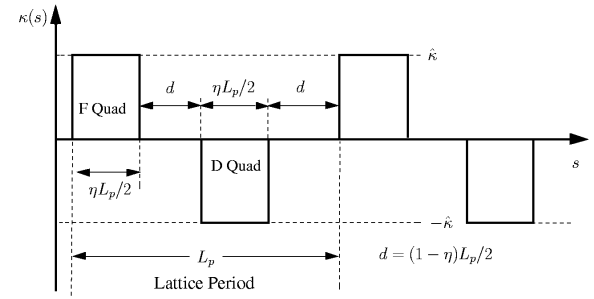


$$d = (1-\eta)\frac{L_p}{2} \qquad \eta = \text{Quadrupole Occupancy } (0 < \eta \le 1)$$

Focusing Strength

$$\hat{\kappa} = \begin{cases} \frac{1}{[B\rho]}\left|\frac{dB_x}{dy}\right|, & \text{Magnetic Quadrupole} \\ \frac{1}{[B\rho]\beta_b c}\left|\frac{dE_x}{dy}\right|, & \text{Electric Quadrupole} \end{cases}$$

Rigidity $[B\rho] = m\gamma_b\beta_b c/q$



## Application Example Contd. (3) – Matched Envelope Properties

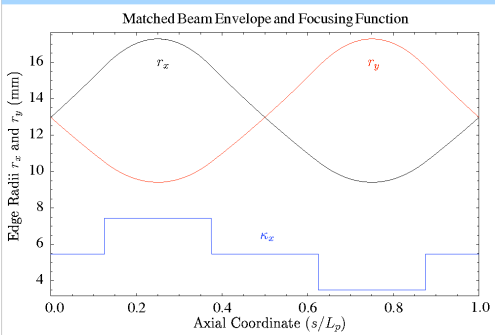


Ion
$K^+$, E = 2 MeV
Current
I = 800 mA
Lattice
$L_p = 0.5\text{m}$
$\eta = 1/2$
$\sigma_0 = 80^\circ/\text{Lattice Period}$

Envelope Properties:

1) Low Emittance Case: $\varepsilon_x = \varepsilon_y = 50$ mm-mrad; $\sigma = 9.42^\circ/\text{Lattice Period}$

$\text{Max}[r_x] = \text{Max}[r_y] = 17.3$ mm $\qquad \text{Max}[r'_x] = -\text{Min}[r'_y] = 47.5$ mrad

$\text{Min}[r_x] = \text{Min}[r_y] = 9.41$ mm $\qquad \text{Max}[r'_y] = -\text{Min}[r'_x] = 47.5$ mrad

2) High Emittance Case: $\varepsilon_x = \varepsilon_y = 200$ mm-mrad; $\sigma = 32.13^\circ/\text{Lattice Period}$

$\text{Max}[r_x] = \text{Max}[r_y] = 18.9$ mm $\qquad \text{Max}[r'_x] = -\text{Min}[r'_y] = 52.4$ mrad

$\text{Min}[r_x] = \text{Min}[r_y] = 10.1$ mm $\qquad \text{Max}[r'_y] = -\text{Min}[r'_x] = 52.4$ mrad



## S4: Numerical Solution of Particle and Distribution Methods

## S4A: Overview

Particle Methods – Generally not used at high space-charge intensity

Distribution Methods – Preferred (especially PIC) for high space-charge. We will motivate why now.

Why are direct particle methods are not a good choice for typical beams?

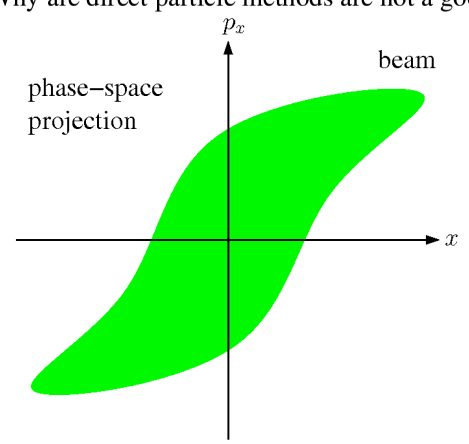


$N$ particle coordinates $\{\mathbf{x}_i, \mathbf{p}_i\}$

Physical beam (typical) $N \sim 10^{10} - 10^{14}$ particles

Although larger problems are possible every year with more powerful computers, current processor speeds and memory limit us to $N \lesssim 10^8$ particles

## Numerical Solution of Particle and Distribution Methods (2)

Represent the beam by Lagrangian "macroparticles" advanced in time

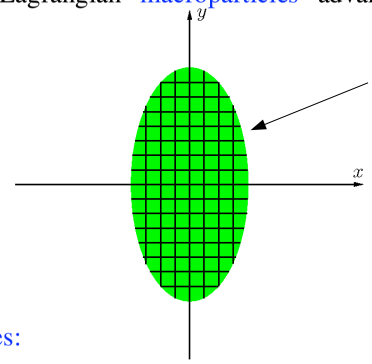


Partition local density into macroparticles

Macroparticle Properties:

- Same $q/m$ ratio as real particle
  - Gives same single particle dynamics in the applied field
- More collisions due to macroparticles having more close approaches
  - Enhanced collisionality is unphysical
  - Controlled by smoothing the macroparticle interaction with the self-field. More on this later.



## Numerical Solution of Particle and Distribution Methods (3)

Direct Vlasov as an example:

Discretize grid points $\{\boldsymbol{x}_i, \boldsymbol{p}_i\}$

Advance distribution $f(\boldsymbol{x},\boldsymbol{p},t)$ at discrete grid points in time

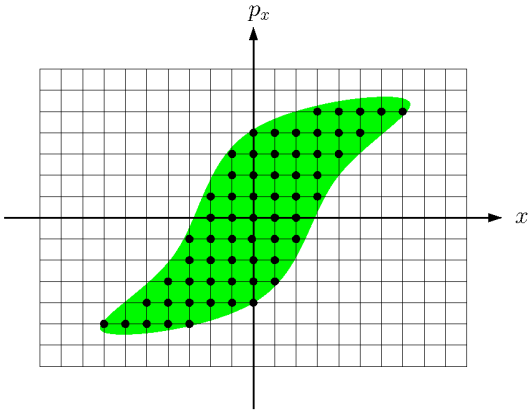


- Continuum distribution advanced on a discrete phase-space mesh
  - Extreme memory for high resolution. Example: for 4D $x$-$p_x$, $y$-$p_y$ with 100 mesh points on each axis -> $100^4 = 10^8$ values to store in fast memory (RAM)
- Discretization errors can lead to aliasing and unphysical behavior (negative probability, etc.)



## Numerical Solution of Particle and Distribution Methods (4)

Both particle and distribution methods can be broken up into two basic parts:

1) Moving particles or distribution evaluated at grid points through a finite time (or axial space) step
2) Calculation of beam self-fields consistently with the distribution of particles

In both methods, significant fractions of run time may *be devoted to diagnostics*

- Moment calculations can be computationally intensive and may be "gathered" frequently for evolution "histories"
- Phase space projections ("snapshot" in time)
- Fields (snapshot in time)

Diagnostics are also critical!

- Without appropriate diagnostics runs are useless, even if correct
- Must accumulate and analyze/present large amounts of data in an understandable format

Significant code development time may also be devoted to creating (loading) the initial distribution of particles to simulate

- Loading will usually only take a small fraction of total run time



## S4B: Integration of Equations of Motion

Higher order methods require more storage and numerical work per time step

- Fieldsolves are expensive, especially in 3D, and several fieldsolves per step can be necessary for higher order accuracy

Therefore, low-order methods are typically used for self-consistent space-charge.

The "leapfrog" method is most common

- Only need to store prior position and velocity
- One fieldsolve per time step

Illustrate the leapfrog method for non-relativistic particle equations of motion:

- Develop methods for particles but can be applied to moments, distributions,...

$$m\frac{d\mathbf{v}}{dt} = \mathbf{F} = q(\mathbf{E} + \mathbf{v} \times \mathbf{B})$$
$$\frac{d\mathbf{x}}{dt} = \mathbf{v}$$

## Leapfrog Method for Electric Forces

Leapfrog Method: for *velocity independent* (Electric) forces

Leapfrog Advance (time centered): Advance velocity and position out of phase

$$1) \quad m\frac{\mathbf{v}_{i+1/2}-\mathbf{v}_{i-1/2}}{\Delta_t} = \mathbf{F}_i \qquad \mathbf{F}=\mathbf{F}(\mathbf{x})$$

$$2) \quad \frac{\mathbf{x}_{i+1}-\mathbf{x}_i}{\Delta_t} = \mathbf{v}_{i+1/2}$$

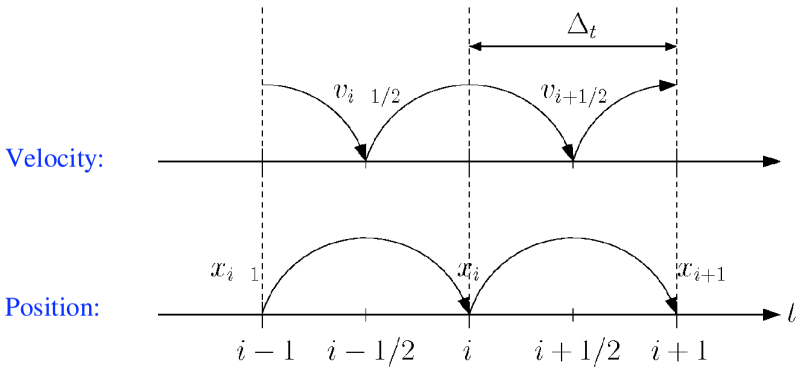




### Leapfrog Method: Order

To analyze the properties of the leapfrog method it is convenient to write the map in an alternative form:

$$i \to i+1 \ : \quad \begin{cases} \dfrac{\mathbf{x}_{i+1}-\mathbf{x}_i}{\Delta_t} = \mathbf{v}_{i+1/2} \\ \dfrac{\mathbf{x}_i-\mathbf{x}_{i-1}}{\Delta_t} = \mathbf{v}_{i-1/2} \end{cases}$$

Subtract the two equations above and apply the other leapfrog advance formula:

$$\Longrightarrow \quad m\frac{\mathbf{v}_{i+1/2}-\mathbf{v}_{i-1/2}}{\Delta_t} = \boxed{m\frac{\mathbf{x}_{i+1}-2\mathbf{x}_i+\mathbf{x}_{i-1}}{\Delta_t^2} = \mathbf{F}_i}$$

Note correspondence of formula to discretized derivative:

$$\left.\frac{\partial^2 f}{\partial x^2}\right|_i = \frac{f_{i+1}-2f_i+f_{i-1}}{\Delta_x^2} + \mathcal{O}(\Delta_x^2)$$

- $\mathbf{x}_{i+1}$ fixed from $\mathbf{x}_i,\ \mathbf{x}_{i-1},\ \mathbf{F}_i$ to $\mathcal{O}(\Delta_t^4)$
- Leapfrog method is 2nd order accurate



## Initial conditions must be desynchronized in leapfrog method

### Leapfrog Method: Synchronization

Since **x** and **v** are not evaluated at the same time in the leapfrog method synchronization is necessary both to start the advance cycle and for diagnostics

- Initial conditions: typically, **v** is pushed back half a cycle

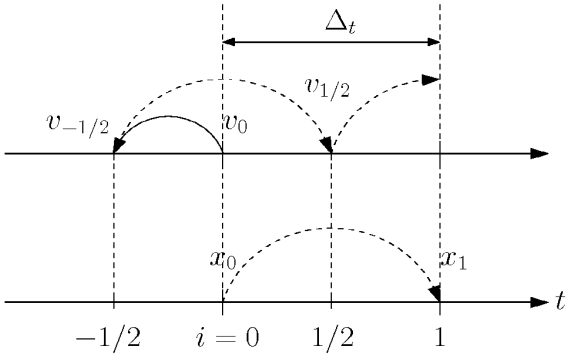


- When evaluating diagnostic quantities such as moments the particle coordinates and velocities should first be synchronized analogously to above



## Leapfrog Method for Magnetic and Electric Forces -- The Boris Method

### Velocity Dependent Forces

Another complication in the evolution ensues when the force has velocity dependence, as occurs with magnetic forces. This complication results because ***x*** and ***v*** are advanced out of phase in the leapfrog method

$$\boxed{\mathbf{F} = q\mathbf{E} + q\mathbf{v}\times\mathbf{B}}$$

velocity term

- Electric field **E** accelerates
- Magnetic field **B** bends particle trajectory without change in speed |**v**|

A commonly implemented time centered scheme for magnetic forces is the following 3-step "Boris" method:

J. Boris, in *Proceedings of the 4th Conference on the Numerical Simulation of Plasmas* (Naval Research Lab, Washington DC 1970)

## The Boris Advance

Boris Advance: 3-step, time-centered

1) Half-step acceleration in electric field

$$\mathbf{v}^{(1)}_{i+1/2} = \mathbf{v}_{i-1/2} + \frac{q}{m}\mathbf{E}_i\frac{\Delta_t}{2}$$

2) Rotation in magnetic field. Here choose coordinates so that

$$\mathbf{B}_i = B_i\hat{z}\ ,\ \omega_{ci} = \frac{qB_i}{m}$$

$$\parallel \mathbf{B}_i\ :\quad v^{(2)}_{z_{i+1/2}} = v^{(1)}_{z_{i+1/2}}$$

$$\perp \mathbf{B}_i\ :\quad \begin{bmatrix} v^{(2)}_{z_{i+1/2}} \\ v^{(1)}_{z_{i+1/2}} \end{bmatrix} = \begin{bmatrix} \cos(\omega_{ci}\Delta_t) & \sin(\omega_{ci}\Delta_t) \\ -\sin(\omega_{ci}\Delta_t) & \cos(\omega_{ci}\Delta_t) \end{bmatrix} \begin{bmatrix} v^{(2)}_{z_{i+1/2}} \\ v^{(1)}_{z_{i+1/2}} \end{bmatrix}$$

3) Half-step acceleration in electric field

$$\mathbf{v}_{i+1/2} = \mathbf{v}^{(3)}_{i+1/2} = \mathbf{v}^{(2)}_{i+1/2} + \frac{q}{m}\mathbf{E}_i\frac{\Delta_t}{2}$$



## Boris Advance Continued (2)

Complication: on startup, how does one generate the out-of-phase **x**, **v** advance from the initial conditions?

- Calculate **E**, **B** with initial conditions
- Move **v** backward half a time step
  - Rotate with **B** a half-step
  - Decelerate a half-step in **E**

Similar comments hold for synchronization of **x**, **v** for diagnostic accumulation

Now we will look at the numerical properties of the leapfrog advance cycle

- Only use a simple "electric" force example to illustrate issues



## Leapfrog Advance: Errors and Numerical Stability

To better understand the leapfrog method consider the simple harmonic oscillator:

$$\boxed{\frac{d^2x}{dt^2} = -\omega^2 x,\ \omega = \text{const}} \implies \begin{aligned} x &= C_0\cos\omega t + C_1\sin\omega t \\ &= x_0\cos(\omega t + \psi_0) \end{aligned}$$

Exact solution

Discretized equation of motion

$$\boxed{\frac{x_{i+1} - 2x_i + x_{i-1}}{\Delta_t^2} = -\omega^2 x_i}$$

Try a solution of the form $x_i = ce^{j\tilde{\omega}i\Delta_t}$, $j \equiv \sqrt{-1}$

$$\Rightarrow e^{j\tilde{\omega}\Delta_t} - 2 + e^{-j\tilde{\omega}\Delta_t} = -\omega^2\Delta_t^2$$

$$2 - 2\cos(\tilde{\omega}\Delta_t) = \omega^2\Delta_t^2$$

$$\sin^2\left(\frac{\tilde{\omega}\Delta_t}{2}\right) = \frac{\omega^2\Delta_t^2}{4}$$

$$\Rightarrow \boxed{\sin\left(\frac{\tilde{\omega}\Delta_t}{2}\right) = \frac{\omega\Delta_t}{2}}$$

This has solutions for $\omega\Delta_t < 2$ and it is straightforward to show via expansion that for small $\omega\Delta_t$

$$\boxed{\omega\Delta_t = \tilde{\omega}\Delta_t + \frac{(\tilde{\omega}\Delta_t)^3}{24} + \mathcal{O}\left[(\tilde{\omega}\Delta_t)^5\right]}$$



## Leapfrog Errors and Numerical Stability Continued (2)

It follows for the leapfrog method applied to a simple harmonic oscillator:

- For $\omega\Delta_t < 2$ the method is stable
- There is *no* amplitude error in the integration
- For $\omega\Delta_t \ll 1$ the phase error is

  Actual phase: $\psi \equiv \omega\Delta_t i$

  Simulated phase: $\tilde{\psi} \equiv \tilde{\omega}\Delta_t i \approx \omega\Delta_t i + \frac{(\omega\Delta_t)^3}{24}i$

  Error phase: $\Delta\psi \equiv \tilde{\psi} - \psi \approx \frac{(\omega\Delta_t)^3}{24}i$

Note: i to get to a fixed time $\sim \Delta_t^{-1}$ and therefore phase errors decrease as $\mathcal{O}(\Delta_t^2)$

// Example: $\omega = 2\pi/\tau$

| Time step | Steps for a $\pi$ phase error |
|---|---|
| $\Delta_t = 0.1\tau$ | $24\pi/(0.1\cdot 2\pi)^3 \approx 3\times 10^2$ |
| $\Delta_t = 0.01\tau$ | $24\pi/(0.01\cdot 2\pi)^3 \approx 3\times 10^5$ |

//

## Leapfrog Errors and Numerical Stability Continued (3)

Contrast: Numerical and Actual Orbit: Simple Harmonic Oscillator

Numerical orbit (dashed ellipse)

Exact orbit (solid ellipse)

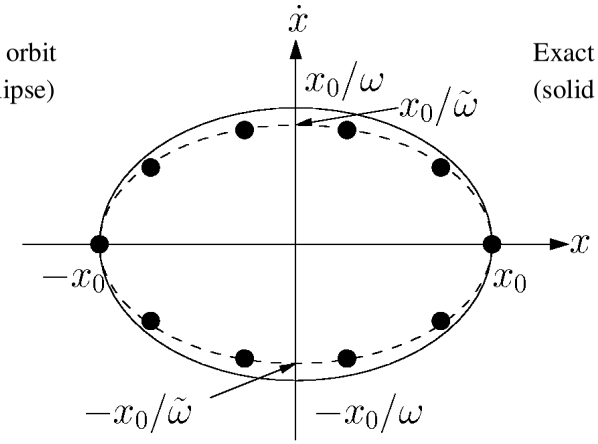


Emittance = (Phase Space Area)/$\pi$

Exact: $\varepsilon = x_0^2/\omega$

Numerical: $\tilde{\varepsilon} = x_0^2/\tilde{\omega}$

$$\frac{\tilde{\varepsilon}}{\varepsilon} \approx 1 - \frac{(\omega\Delta_t)^2}{24}$$



## Leapfrog Errors and Numerical Stability Continued (4)

The numerical orbit conserves phase space area regardless of the number of steps taken! The slight differences between the numerical and actual orbits can be removed by rescaling the angular frequency to account for the discrete step

- More general analysis of the leapfrog method shows it has "symplectic" structure, meaning it preserves the Hamiltonian nature of the dynamics
- Symplectic methods are important for long tracking problems (typical in accelerators) to obtain the right orbit structure
  - Runge-Kutta methods are not symplectic and can result in artificial numerical damping in long tracking problems



## Example: Contrast of Non-Symplectic and Symplectic Advances

Contrast: Numerical and Actual Orbit for a Simple Harmonic Oscillator

use scaled coordinates (max extents unity for analytical solution)

Symplectic Leapfrog Advance:

5 steps per period, 100 periods

10 steps per period, 100 periods

Cosine-type initial conditions

Sine-type initial conditions

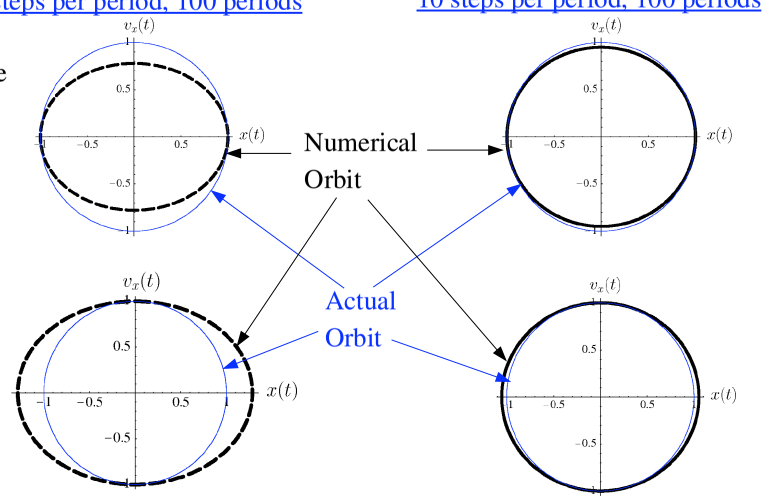




## Example: Contrast of Non-Symplectic and Symplectic Advances (2)

Contrast: Numerical and Actual Orbit for a Simple Harmonic Oscillator

Non-Symplectic 2nd Order Runge-Kutta Advance: (see earlier notes on RK advance)

6 steps per period, 10 periods

20 steps per period, 50 periods

Cosine-type initial conditions

Sine-type initial conditions

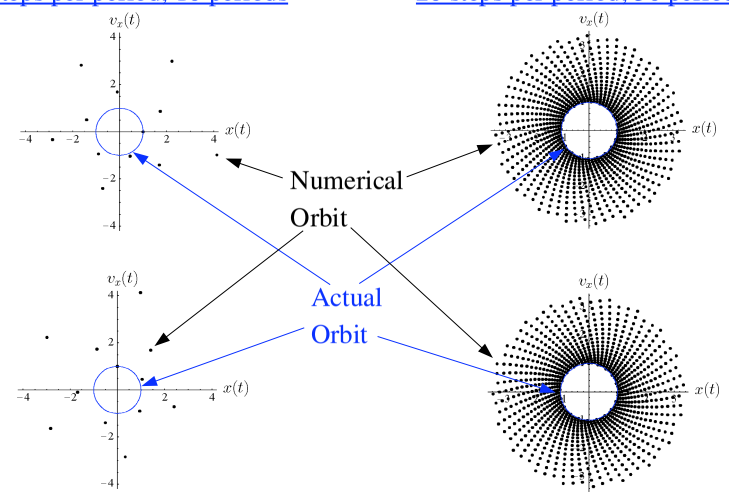

## Example: Contrast of Non-Symplectic and Symplectic Advances (3)

Contrast: Numerical and Actual Orbit for a Simple Harmonic Oscillator

Non-Symplectic 4th Order Runge-Kutta Advance: (analog to notes on 2nd order RK adv)

5 steps per period, 20 periods

10 steps per period, 200 periods

Cosine-type initial conditions

Sine-type initial conditions

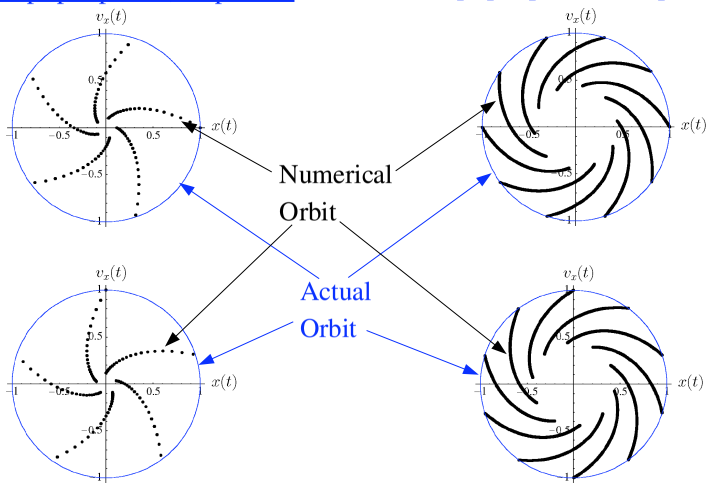




## Example: Leapfrog Stability Applied to the Nonlinear Envelope Equation in a Continuous Focusing Lattice

For linear equations of motion, numerical stability requires:

$$k\Delta_s < 2$$

Here, $k$ is the wave number of the phase advance of the quantity evolving under the linear force. The continuous focusing envelope equation is nonlinear:

$$\frac{d^2 r_x}{ds^2} + k_{\beta 0}^2 r_x - \frac{2Q}{r_x + r_y} - \frac{\varepsilon_x^2}{r_x^3} = 0$$

$$\frac{d^2 r_y}{ds^2} + k_{\beta 0}^2 r_y - \frac{2Q}{r_x + r_y} - \frac{\varepsilon_y^2}{r_y^3} = 0$$

Several wavenumbers $k$ can be expressed in the envelope evolution:

$k_\beta = \sigma / L_p$ .... Depressed Particle Betatron Motion

$k_{\beta 0} = \sigma_0 / L_p$ .... Undepressed Particle Betatron Motion

$k_Q \equiv \sqrt{k_{\beta 0}^2 + 3k_\beta^2}$ .... Quadrupole Envelope Mode

$k_B \equiv \sqrt{2k_{\beta 0}^2 + 2k_\beta^2}$ .... Breathing Envelope Mode



## Example: Leapfrog Stability and the Continuous Foc. Envelope Equation (2)

Expect that $k_{\beta 0}\Delta_s < 2$ for the fastest (largest $k$) component determines stability.

Numerical simulations for an initially matched envelope with: $\sigma/\sigma_0 = 1/2$

| $k_\beta \Delta_s$ | $k_{\beta 0}\Delta_s$ | $k_Q \Delta_s$ | $k_B \Delta_s$ | Stable? |
|---|---|---|---|---|
| 0.500 | 1.00 | 1.32 | 1.58 | Yes |
| 0.600 | 1.20 | 1.59 | 1.90 | Yes |
| 0.630 | 1.26 | 1.67 | 1.99 | Yes |
| 0.635 | 1.27 | 1.68 | 2.01 | No |
| 0.640 | 1.28 | 1.69 | 2.02 | No |

The highest $k$-mode, the breathing mode, appears to determine stability, i.e. $k_B \Delta_s < 2$ is the stability criterion. Other values of $\sigma/\sigma_0$ produce results in agreement with this conclusion.



## Example: Leapfrog Stability and the Continuous Foc. Envelope Equation (3)

Numerical simulations an initially matched envelope with: $\sigma_0 = 80°$, $\sigma/\sigma_0 = 1/2$

Note that numerical errors seed small amplitude mismatch and that the plot scale to the left is ~ $10^{-13}$, corresponding to numerical errors.

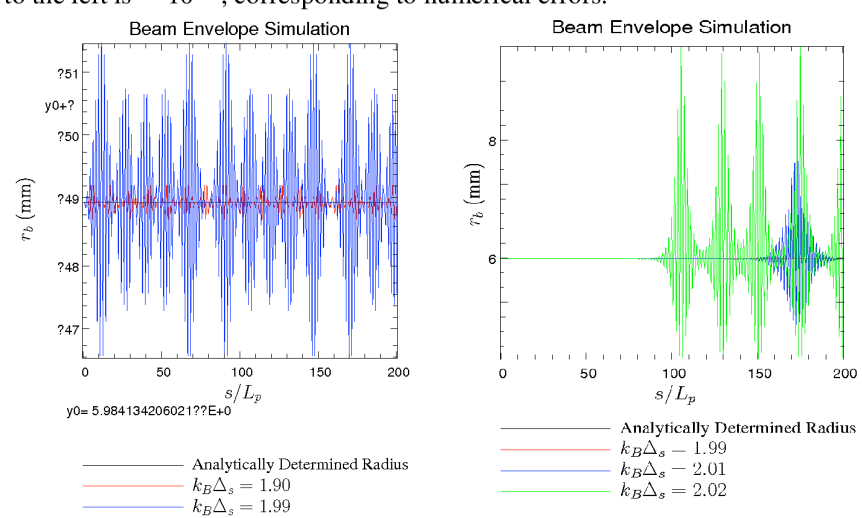

## Comments of 2D and 3D Axisymmetric Particle Moves

To be added:

Comments on moving ring particles:
- 3D axisymmetry => particles rings, 3D axisymmetry => particles are infinite cylindrical shells.
- Angular momentum will be conserved for such particles (can rotate)
- Easier to do in many cases using x-y movers



## S4C: Field Solution

The self-consistent calculation of beam-produced self-fields is vital to accurately simulate forces acting on particles in intense beams

$$\mathbf{F} = q\left(\mathbf{E} + \mathbf{v} \times \mathbf{B}\right)$$

- Techniques outlined here are also applicable to distribution methods

Fields can be resolved into externally applied and self (beam generated) components

$$\boxed{\begin{aligned}\mathbf{E} &= \mathbf{E}_a + \mathbf{E}_s \\ \mathbf{B} &= \mathbf{B}_a + \mathbf{B}_s\end{aligned}}$$

$\mathbf{E}_a,\ \mathbf{B}_a$ applied fields generated by magnets and electrodes
- Sometimes calculated at high resolution in external codes and imported or specified via analytic formulas
- Sometimes calculated from code fieldsolve via applied charges and currents and boundary conditions

$\mathbf{E}_s,\ \mathbf{B}_s$ self fields generated by beam charges and currents
- At high beam intensities can be a large fraction (on average) of applied fields
- Important to calculate with realistic boundary conditions



## Electrostatic Field Solution

For simplicity, we restrict analysis to electrostatic problems to illustrate methods:

$\mathbf{B} = \mathbf{B}_a$ $\quad$ $\mathbf{B}_a$ specified via another code or theory

$\mathbf{E} = \mathbf{E}_a + \mathbf{E}_s$ $\quad$ $\mathbf{E}_a$ due to biased electrodes and $\mathbf{E}_s$ due to beam space-charge

The Maxwell equations to be solved for $\mathbf{E}$ are

$$\boxed{\begin{aligned}\nabla \cdot \mathbf{E} &= \frac{\rho}{\epsilon_0} \qquad + \text{ boundary conditions on } \mathbf{E} \\ \nabla \times \mathbf{E} &= 0\end{aligned}}$$

$\nabla \times \mathbf{E} = 0$ implies that we can always take $\mathbf{E} = -\nabla\phi$ and so

$$\boxed{\begin{aligned}\nabla^2\phi &= -\frac{\rho}{\epsilon_0} \qquad + \text{ boundary conditions on } \phi \\ \mathbf{E} &= -\nabla\phi\end{aligned}}$$



## Electrostatic Field Solution: Typical Problem

As an example, it might be necessary to solve (2D) fields of a beam within an electric quadrupole assembly.

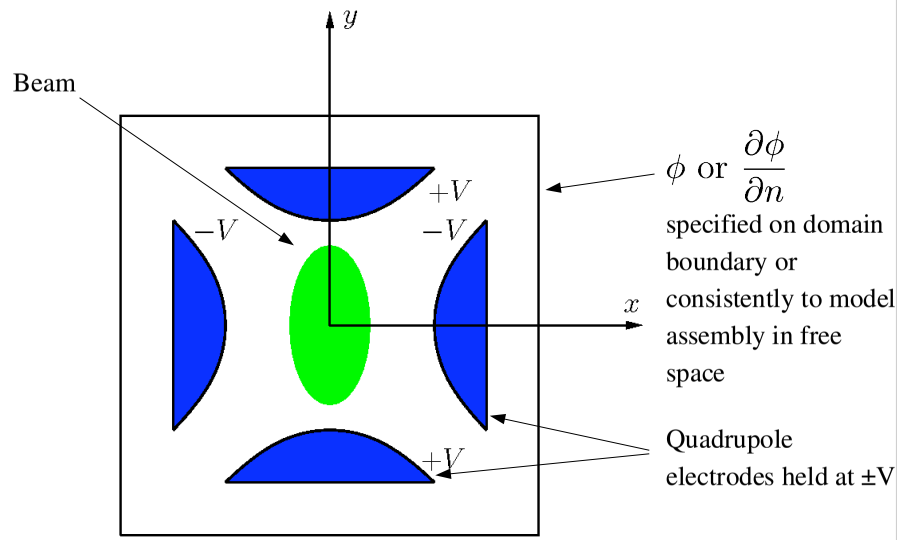

## Electrostatic Field Solution by Green's Function

Formally, the solution to $\phi$ can be constructed with a Green's function, illustrated here with Dirichlet boundary conditions:

$$\nabla^2 G(\mathbf{x},\mathbf{x}') = -4\pi\delta(\mathbf{x}-\mathbf{x}')$$
$$G(\mathbf{x},\mathbf{x}')|_{\mathbf{x}'_b} = 0$$
$$\mathbf{x}'_b \equiv \mathbf{x}' \text{ on boundaries}$$

Definitions:

$$\frac{\partial}{\partial n} \equiv \hat{\mathbf{n}} \cdot \frac{\partial}{\partial \mathbf{x}}$$

$\hat{\mathbf{n}} \equiv$ Unit normal vector to boundary surface

This yields

$$\phi(\mathbf{x}) = \frac{1}{4\pi\epsilon_0}\int_V d^3x'\ \rho(\mathbf{x}')G(\mathbf{x},\mathbf{x}') - \frac{1}{4\pi}\oint_S d^2x'\ \phi(\mathbf{x}')\frac{\partial G(\mathbf{x},\mathbf{x}')}{\partial n'}$$

Self-field component $\equiv \phi_s$ $\qquad$ Applied field from electrode potentials $\equiv \phi_a$

$$\mathbf{E}_s = -\frac{\partial \phi_s}{\partial \mathbf{x}} \qquad \mathbf{E}_a = -\frac{\partial \phi_a}{\partial \mathbf{x}}$$



## Electrostatic Field Solution by Green's Function (2)

Applied Field:

$\phi_a$ can be calculated in advance and need not be recalculated if transverse geometry does not change

- Can be analytical in simple situations

Self Field:

Let: $q_M$, $\mathbf{x}_i =$ Macro-particle charge and coordinate

$N_p =$ Macro-particle number

$$\phi_s = \frac{1}{4\pi\epsilon_0}\int d^3x'\ \rho(\mathbf{x}')G(\mathbf{x},\mathbf{x}') = \frac{q_M}{4\pi\epsilon_0}\sum_{i=1}^{N_p}\int d^3x'\ \delta(\mathbf{x}'-\mathbf{x}_i)G(\mathbf{x},\mathbf{x}')$$

$$\phi_s = \frac{q_M}{4\pi\epsilon_0}\sum_{i=1}^{N_p} G(\mathbf{x},\mathbf{x}_i)$$

Then the field at the ith macro-particle is (self-field term removed):

$$\mathbf{E}_{si} = \left.\frac{\partial \phi_s}{\partial \mathbf{x}}\right|_{\mathbf{x}=\mathbf{x}_i} = \frac{q_M}{4\pi\epsilon_0}\sum_{\substack{j=1\\ j\neq i}}^{N_p}\left.\frac{\partial G(\mathbf{x},\mathbf{x}_j)}{\partial \mathbf{x}}\right|_{\mathbf{x}=\mathbf{x}_i}$$



## Electrostatic Field Solution by Green's Function (3)

The Green's Function expression for $\phi_a$ will, in general, be a numerically intensive expression to evaluate at *each* macroparticle

- $N_p(N_p - 1)$ terms to evaluate and G itself will in general be complicated and may require many costly numerical operations for each term, limiting $N_p$
- Small $N_p$ for which this procedure is practical will result in a noisy field
  - Enhanced, unphysically high, close approaches (collisions) with poor statistics can change the physics
- Special "fast multipole" methods based on Green's functions can reduce the scaling to ~$N_p$ or ~$N_p ln(N_p)$.
  - Coefficient is large and smoothing is not easily implemented, often rendering such methods inferior to gridded methods to be covered shortly

// Example: Self fields in free space

$$G(\mathbf{x},\mathbf{x}') = \frac{1}{|\mathbf{x}-\mathbf{x}'|}\ ; \quad \mathbf{E}_{si} = \frac{q_M}{4\pi\epsilon_0}\sum_{\substack{j=1\\ j\neq i}}^{N_p}\frac{(\mathbf{x}_i-\mathbf{x}_j)}{|\mathbf{x}_i-\mathbf{x}_j|^3}$$

//



## Field Solution on a Discrete Grid

An alternative procedure is needed to

1) Calculate fields efficiently by disretization of the Maxwell equations
2) Smooth interactions to compensate for limited particle numbers

Approach: Solve the Maxwell Equations on a discrete spatial grid and then smooth the interactions calculated from the gridded field.

Discretization: 2D uniform grid (1D and 3D analogous)

$$x_i = x_{min} + i\Delta_x \quad \Delta_x = (x_{max} - x_{min})/n_x \quad i = 0,1,2,...,n_x$$
$$y_j = y_{min} + j\Delta_y \quad \Delta_y = (y_{max} - y_{min})/n_y \quad j = 0,1,2,...,n_y$$

$$\left.\begin{aligned}\mathbf{E}_{ij} &= \mathbf{E}(x_i,y_j)\\ \phi_{ij} &= \phi(x_i,y_j)\\ \rho_{ij} &= \rho(x_i,y_j)\end{aligned}\right\}$$

Field components, potential, and charge are gridded

Comments:

- $\rho_{ij}$ must be calculated from macro-particles, not necessarily on grid points
- Fields will ultimately be needed at marco-particle coordinates, not on grid

These issues will be covered later under "particle weighting"

## Field Solution on a Discrete Grid: Example Problem, Beam in an Electric Quadrupole

Beam in an electric quadrupole lattice (2D)

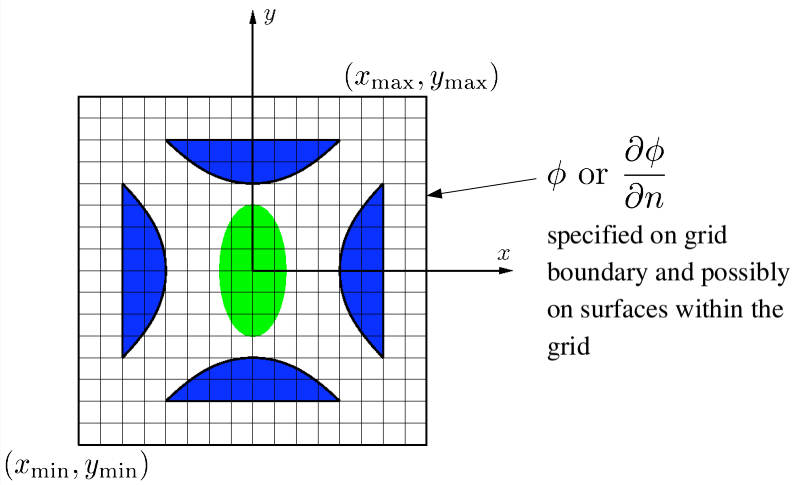




## Gridded Field Solution: Discretized Poisson Eqn.

For low order differencing, the Poisson Equation becomes

$$\frac{\phi_{i+1,j} - 2\phi_{i,j} + \phi_{i-1,j}}{\Delta_x^2} + \frac{\phi_{i,j+1} - 2\phi_{i,j} + \phi_{i,j-1}}{\Delta_y^2} = -\frac{\rho_{i,j}}{\epsilon_0}$$

with the gridded field components calculated as

$$E_{x_{ij}} = \frac{\phi_{i+1,j} - \phi_{i-1,j}}{2\Delta_x}$$

$$E_{y_{ij}} = \frac{\phi_{i,j+1} - \phi_{i,j-1}}{2\Delta_y}$$

Boundary conditions must also be incorporated as constraint equations

Dirichlet Conditions: $\phi$ specified on surfaces

Neumann Conditions: $\frac{\partial \phi}{\partial n}$ specified on surfaces



## Gridded Field Solution: Discretized Dirichlet Boundary Cond

Dirichlet Conditions: $\phi$ specified on surface

Example: $\phi = V = \text{const}$ at right grid edge

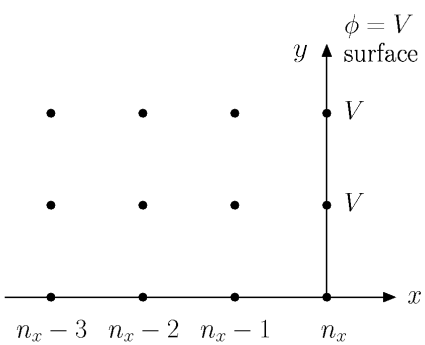


$\phi_{n_x,j} = V = \text{const}$

For $i = n_x - 1$ cells

$$\frac{V - 2\phi_{n_x-1,j} + \phi_{n_x-2,j}}{\Delta_x^2} + \frac{\phi_{n_x-1,j+1} - 2\phi_{n_x-1,j} + \phi_{n_x-1,j-1}}{\Delta_y^2} = -\frac{\rho_{n_x-1,j}}{\epsilon_0}$$



## Gridded Field Solution: Discretized Neumann Boundary Cond

Neumann Conditions: $\frac{\partial \phi}{\partial n}$ specified on surfaces

Example: $\frac{\partial \phi}{\partial n} = G = \text{const}$ at right grid edge

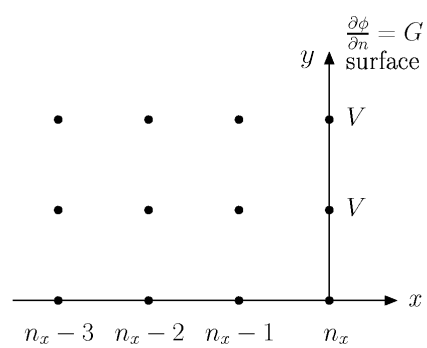


Use 1st order forward difference formula at surface

$$\frac{\phi_{n_x-1,j} - \phi_{n_x,j}}{\Delta_x} = G$$

## Solution of Discretized Poisson Eqn -- Direct Matrix Method

The finite-differenced Poisson Equation and the boundary conditions can be expressed in matrix form as:

$$\boxed{\overline{\mathbf{M}} \cdot \mathbf{\Phi} = \mathbf{S}}$$

$\overline{\mathbf{M}} =$ Coefficients matrix from local finite differences. This matrix will be sparse, i.e., most elements will equal zero

$\mathbf{\Phi} =$ Vector of potentials at grid points

$\mathbf{S} =$ "Source" terms resulting from beam charge deposited on the grid $(\rho_{ij})$ and known potentials from boundary condition constraints

Formal solution found by matrix inversion:

$$\boxed{\mathbf{\Phi} = \overline{\mathbf{M}}^{-1} \cdot \mathbf{S}}$$

Direct inversion of $\overline{\mathbf{M}}^{-1}$ is not practical due to the large dimension of the problem

- $\overline{\mathbf{M}}$ will in general be sparse due to use of local, low-order finite differencing
- Many fast, numerically efficient inversion methods exist for sparse matrices
  - Specific method best used depends on type of differencing and BC's



## Example Discretized Field Solution

To illustrate this procedure, consider a simple 1D example with Dirichlet BC's

$$\frac{d^2\phi}{dx^2} = -\frac{\rho}{\epsilon_0} \qquad \phi(x_l) = V_l \quad \text{left BC}$$
$$\phi(x_r) = V_r \quad \text{right BC}$$

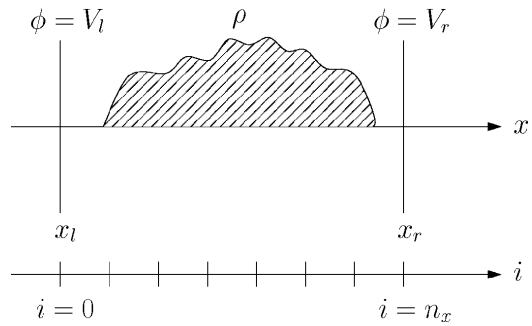


Discretize:

$$\frac{\phi_{i+1} - 2\phi_i + \phi_{i-1}}{\Delta x^2} = -\frac{\rho_i}{\epsilon_0}$$

$$\phi_0 = V_l$$
$$\phi_{n_x} = V_r$$

$$x_i = x_l + i\Delta_x, \quad \Delta_x = (x_r - x_l)/n_x; \quad i = 0, 1, 2, ..., n_x$$

Note: $\rho_0$ , $\rho_{n_x}$ irrelevant

- Correspond to surface terms that fix boundary condition potentials



## Example Discretized Field Solution (2)

The 1D discretized Poisson equation and boundary conditions can be expressed in matrix form as:

$$\begin{bmatrix} -2 & 1 & & & & & 0 \\ 1 & -2 & 1 & & & & \\ & 1 & -2 & 1 & & & \\ & & \ddots & \ddots & \ddots & & \\ & & & 1 & -2 & 1 & \\ & & & & 1 & -2 & 1 \\ 0 & & & & & 1 & -2 \end{bmatrix} \cdot \begin{bmatrix} \phi_1 \\ \phi_2 \\ \phi_3 \\ \vdots \\ \phi_{n_x-3} \\ \phi_{n_x-2} \\ \phi_{n_x-1} \end{bmatrix} = -\frac{\Delta_x^2}{\epsilon_0} \begin{bmatrix} \rho_1 + \frac{\epsilon_0}{\Delta_x^2} V_l \\ \rho_2 \\ \rho_3 \\ \vdots \\ \rho_{n_x-3} \\ \rho_{n_x-2} \\ \rho_{n_x-1} + \frac{\epsilon_0}{\Delta_x^2} V_r \end{bmatrix}$$

Matrix has tri-diagonal structure and can be rapidly inverted to find the $\phi_i$

- Sparse matrices need not be stored in full (waste of memory)



## S4: Particle Methods – Field Solution Methods on Grid

Many other methods exist to solve the discretized field equations. These methods fall into three broad classes:

1) Direct Matrix Methods
- Fast inversion of sparse matrix

2) Spectral Methods
- Fast Fourier Transform (FFT)
  - Periodic boundary conditions
  - Sine transform ($\phi = 0$ on grid boundary)
  - FFT + capacity matrix for arbitrary conductors
  - Free space boundary conditions

3) Relaxation Methods
- Successive over-relaxation (SOR)
  - General boundary conditions and structures
- Multigrid (good, fast, and accurate method for complicated boundaries)

## Field Solution Methods on Grid Continued (2)

Sometimes methods in these three classes are combined. For example, one might employ spectral methods transversely and invert the tri-diagonal matrix longitudinally.

Other discretization procedures are also widely employed, giving rise to other classes of field solutions such as:

- Finite elements
- Variational
- Monte Carlo

Methods of field solution are central to the efficient numerical solution of intense beam problems. It is not possible to review them all here. But before discussing particle weighting, we will first overview the important spectral methods and FFT's



## Spectral Methods and the FFT

The spectral approach combined with numerically efficient Fast Fourier Transforms (FFT's) is commonly used to efficiently solve the Poisson Equation on a discrete spatial grid

- Approach provides spectral information on fields that can be used to smooth the interactions
- Efficiency of method enabled progress in early simulations
  - Computers had very limited memory and speed
- Method remains important and can be augmented in various ways to implement needed boundary conditions
  - Simple to code with numerical libraries
  - Efficiency still important ... especially in 3D geometries



## Spectral Method: Discrete Fourier Transform

Illustrate in 1D for simplicity (multidimensional case analogous)

$$\boxed{\frac{d^2\phi}{dx^2} = -\frac{\rho}{\epsilon_0}}$$

Continuous Fourier Transforms (Reminder)

$$\boxed{\begin{aligned} \tilde{\phi}(k) &= \int_{-\infty}^{\infty} dx\, e^{ikx}\phi(x) & \tilde{\rho}(k) &= \int_{-\infty}^{\infty} dx\, e^{ikx}\rho(x) \\ \phi(x) &= \int_{-\infty}^{\infty} \frac{dk}{2\pi}\, e^{-ikx}\tilde{\phi}(k) & \rho(x) &= \int_{-\infty}^{\infty} \frac{dk}{2\pi}\, e^{-ikx}\tilde{\rho}(k) \end{aligned}}$$

Transform Poisson Equation: $k^2\tilde{\phi}(k) = \dfrac{\tilde{\rho}(k)}{\epsilon_0}$

$$\boxed{\phi(x) = \int_{-\infty}^{\infty} \frac{dk}{2\pi} e^{-ikx}\frac{\tilde{\rho}(k)}{\epsilon_0 k^2}}$$

Similar procedures work to calculate the field on a finite, discrete spatial grid

- Develop by analogy to continuous transforms



## Discrete Fourier Transform (2)

Discretize the problem as follows:

$$x_j = x_{min} + j\Delta_x; \quad \Delta_x = \frac{x_{max} - x_{min}}{n_x}; \quad j = 0, 1, 2, ..., n_x$$

$$\phi_j \equiv \phi(x_j)$$

$n_x + 1$ grid points

$n_x$ distinct values (periodic)

$$k_n \equiv \frac{2\pi n}{n_x \Delta_x} \qquad n = -\frac{n_x}{2}, ..., 0, ..., \frac{n_x}{2}$$

The discrete transform is the defined by analogy to the continuous transform by:

$$\tilde{\phi}(k_n) = \int_{-\infty}^{\infty} dx\, e^{ik_n x}\phi(x) \iff \boxed{\begin{aligned} \tilde{\phi}_n &\equiv \Delta_x \sum_{j=0}^{n_x} e^{ik_n(x_j - x_{\min})}\phi_j \\ &= \Delta_x \sum_{j=0}^{n_x} \exp\left(\frac{i2\pi nj}{n_x}\right)\phi_j \end{aligned}}$$

## Discrete Fourier Transform (3)

| Grid | | Transform |
|---|---|---|
| $\phi_j$ | $\Longleftrightarrow$ | $\tilde{\phi}_n$ |
| $(n_x + 1$ values$)$ | | $(n_x + 1$ complex values$)$ |

Note that $\tilde{\phi}_n$ is periodic in $n$ with period $n_x$

$$\tilde{\phi}_{-n} = \tilde{\phi}_{n_x - n}$$

- Let $n = 0, 1, 2, ..., n_x$ so $n$ and $j$ have the same ranges

Then an inverse transform can be constructed *exactly*:

$$\boxed{\phi_j = \frac{1}{n_x \Delta_x} \sum_{n=0}^{n_x} \exp\left(-\frac{i2\pi nj}{n_x}\right) \tilde{\phi}_n}$$

- This exact inversion is proved in the problems by summing a geometric series



## Spectral Methods: Aliasing

The discrete transform describes a periodic problem if indices are extended

- Discretization errors (aliasing) can occur

Figure to be edited:

$$\lim_{x \to \pm\infty} \phi(x) = 0$$

Plots will be replaced with real transforms based on a Gaussian distribution in future versions of the notes

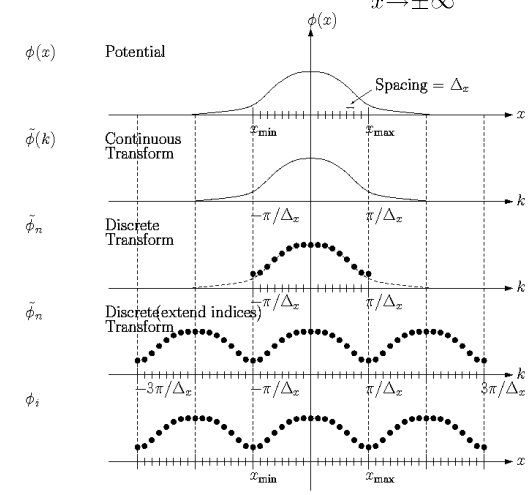




## Discrete Transform Formulas

Application of the Discrete Fourier Transform to solve Poisson's Equation:

$$E_x = -\frac{d\phi}{dx} \quad \Longleftrightarrow \quad E_{xj} = -\frac{\phi_{j+1} - \phi_{j-1}}{2\Delta_x}$$

$$\frac{d^2\phi}{dx^2} = -\frac{\rho}{\epsilon_0} \quad \Longleftrightarrow \quad \frac{\phi_{j+1} - 2\phi_j + \phi_{j-1}}{\Delta_x^2} = -\frac{\rho}{\epsilon_0}$$

Applying the discrete transform yields:

$$\boxed{\tilde{E}_{xn} = i\kappa_n \tilde{\phi}_n \qquad \kappa_n = k_n \left[\frac{\sin(k_n \Delta_x)}{k_n \Delta_x}\right] \equiv k_n \mathrm{dif}(k_n \Delta_x) \qquad k_n \equiv \frac{2\pi n}{(n_x + 1)\Delta_x}}$$

Poisson's Equation becomes:

$$\boxed{\tilde{\phi}_n = \frac{\tilde{\rho}_n}{\epsilon_0 K_n^2} \; ; \quad K_n^2 \equiv k_n^2 \mathrm{dif}^2(k_n \Delta_x/2) = k_n^2 \left[\frac{\sin(k_n \Delta_x/2)}{k_n \Delta_x/2}\right]^2}$$

Note: factors of $K_n^2$ need only be calculated once per simulation (store values)



## Derivation of Discrete Transform Eqns.

/// Example Derivation of a formula for the discrete transformed E-field:

Discretized E-field $\quad E_{xj} = -\dfrac{\phi_{j+1} - \phi_{j-1}}{2\Delta_x}$

Transforms

$$\phi_j = \frac{1}{(n_x + 1)\Delta_x} \sum_{n=0}^{n_x} \exp\left(-\frac{i2\pi nj}{n_x + 1}\right) \tilde{\phi}_n$$

$$E_{xj} = \frac{1}{(n_x + 1)\Delta_x} \sum_{n=0}^{n_x} \exp\left(-\frac{i2\pi nj}{n_x + 1}\right) \tilde{E}_{xn}$$

Substitute transforms into difference formula:

$$2\Delta_x \sum_{n=0}^{n_x} \exp\left(-\frac{i2\pi nj}{n_x + 1}\right) \tilde{E}_{xn}$$

$$= -\sum_{n=0}^{n_x} \exp\left(-\frac{i2\pi nj}{n_x + 1}\right) \tilde{\phi}_n \left\{\exp\left(-\frac{i2\pi n}{n_x + 1}\right) - \exp\left(\frac{i2\pi n}{n_x + 1}\right)\right\}$$

$$= \Delta_x \sum_{n=0}^{n_x} \exp\left(-\frac{i2\pi nj}{n_x + 1}\right) \tilde{E}_{xn} = i \sum_{n=0}^{n_x} \exp\left(-\frac{i2\pi nj}{n_x + 1}\right) \sin\left(\frac{2\pi n}{n_x + 1}\right) \tilde{\phi}_n$$

$$\Delta_x \sum_{n=0}^{n_x} \exp\left(-\frac{i2\pi nj}{n_x+1}\right) \tilde{E}_{xn} = i \sum_{n=0}^{n_x} \exp\left(-\frac{i2\pi nj}{n_x+1}\right) \sin\left(\frac{2\pi n}{n_x+1}\right) \tilde{\phi}_n$$

This equation must hold true for each term in the sum proportional to

$\exp\left(-\frac{i2\pi nj}{n_x+1}\right)$ to be valid for a general j.

$$\Rightarrow \tilde{E}_{xn} = \frac{i}{\Delta_x} \sin\left(\frac{2\pi n}{n_x+1}\right) \tilde{\phi}_n$$

$$k_n = \frac{2\pi n}{(n_x+1)\Delta_x}$$

$$\Rightarrow \boxed{\begin{aligned} \tilde{E}_{xn} &= ik_n \left[\frac{\sin(k_n\Delta_x)}{k_n\Delta_x}\right] \tilde{\phi}_n \\ &= ik_n \mathrm{dif}(k_n\Delta_x)\tilde{\phi}_n \end{aligned}}$$

///



## Spectral Methods: Discrete Transform Field Solution

Typical discrete Fourier transform field solution (not optimized)

| Forward Transform | | Multiply | | Inverse Transform | | Finite Difference | | |
|---|---|---|---|---|---|---|---|---|
| $\rho_j$ | $\longrightarrow$ | $\tilde{\rho}_n$ | $\longrightarrow$ | $\tilde{\phi}_n$ | $\longrightarrow$ | $\phi_j$ | $\longrightarrow$ | $E_{xj}$ |
| | DFT | | $\cdot\frac{1}{K_n^2}$ | | IDFT | | | |

- $K_n^2$ factors can be calculated once and stored to increase numerical efficiency



## Discussion of Spectral Methods and the FFT

The Fast Fourier Transform (FFT) makes this procedure numerically efficient

- Discrete transform (no optimization), ~$(n_x + 1)^2$ complex operations
- FFT exploits symmetries to reduce needed operations to ~ $(n_x + 1)ln(n_x + 1)$
  - Huge savings for large $n_x$
- The needed symmetries exist only for certain numbers of grid points. In the simplest manifestations: $n_x + 1 = 2^p$, $p = 1, 2, 3, ...$
  - Reduced griding freedom
  - Other manifestations allow $n_x + 1 = 2^p$ and products of prime numbers for more possibilities

The FFT can be combined with other procedures such as capacity matrices to implement boundary conditions for interior conductors, etc.

- This allows rapid field solutions in complicated geometries when capacity matrix elements can be pre-calculated and stored

FFT is the fastest method for simple geometry

- Simple to code using typical numerical libraries for FFT's



## S4D: Weighting: Depositing Particles on the Field Mesh and Interpolating Gridded Fields to Particles

We have outlined methods to solve the electrostatic Maxwell's equations on a discrete spatial grid. To complete the description we must:

- Specify how to deposit macro-particle charges and current onto the grid
- Specify how to interpolate fields on the spatial grid points to the macroparticle coordinates (not generally on the grid) to apply in the particle advance
- Smooth interactions resulting from the small number of macro-particles to reduce artificial collisions resulting from the use of an unphysically small number of macro-particles needed for rapid simulation

This is called the *particle weighting* problem

## Weighting (2)

Particle weighting problem for electrostatic fields

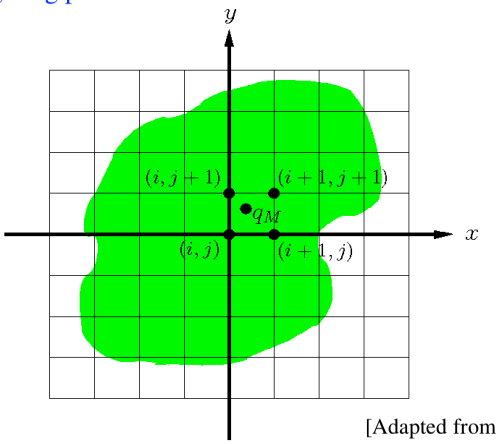


[Adapted from Birdsall and Langdon]

It is found that it is usually better to employ the same weighting schemes to deposit both the macro-particle charges and currents on the mesh and to extrapolate the fields at gridded points to the macro-particles

- Avoids unphysical self-forces where the particle accelerates itself



## Weighting Methods

Many methods of particle weighting exist. They can be grouped into 4 categories:

1) Nearest Grid Point
2) Cloud in Cell (CIC)
   - Shaped particles
   - PIC method, linearly shaped particles
3) Multipole
   - Dipole, subtracted dipole, etc.
4) Higher order methods
   - Splines
   - ***k***-space cutoffs in discrete transforms
   - ⋮

Possible hybrid methods also exist. We will illustrate methods 1) and 2) for electrostatic problems. Descriptions of other methods can be found in the literature.



## Weighting: Nearest Grid Point

1) Nearest Grid Point: Assign charges to the nearest grid cell

- Fast and simple: Show for 1D; 2D and 3D generalization straightforward
- Noisy

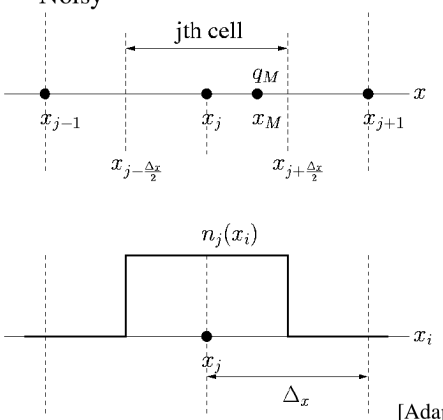


$q_M =$ Charge of macro-particle

$x_M =$ Coordinate of macro-particle

$x_j =$ Closest grid cell

Charge Deposition:

$$q_j = q_M$$

Field "Interpolation":

$$E_x|_{x=x_M} = E_{xj}$$

[Adapted from Birdsall and Langdon]

Comments:

- Currents can be interpolated to grid similarly for electromagnetic solving and/or diagnostics



## Weighting : Cloud in Cell

2) Cloud in Cell: Shaped macro-particles pass freely through each other

- Smoother than Nearest Grid Point, but more numerical work
- For linear interpolation results in simple, commonly used "Particle in Cell" (PIC) method

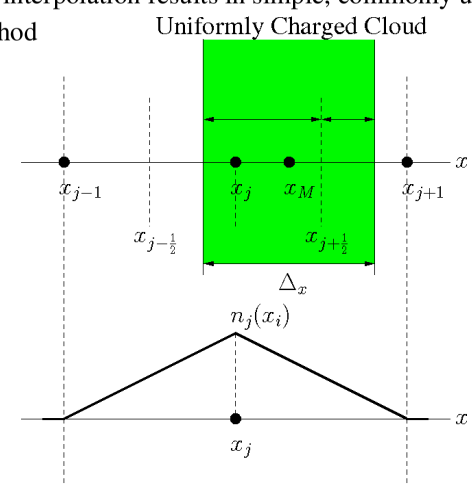


[Adapted from Birdsall and Langdon]

## Cloud in Cell (2)

$q_M$ , $x_M$ = Charge and coordinate of macro-particle

$x_j$ = Closest grid cell

Charge Deposition:

$$q_j = q_M \left[ \frac{\Delta_x - (x_M - x_j)}{\Delta_x} \right] = q_M \frac{x_{j+1} - x_M}{\Delta_x}$$

$$q_{j+1} = q_M \left[ \frac{x_M - x_j}{\Delta_x} \right]$$

Field Interpolation:

$$E_x|_{x=x_M} = \left[ \frac{x_{j+1} - x_M}{\Delta_x} \right] E_j + \left[ \frac{x_M - x_j}{\Delta_x} \right] E_{j+1}$$

Comments:

- Linear interpolation results in triangularly shaped particles
- Shape smooths interactions reducing collisionality
  - Vlasov evolution with limited number of shaped particles
- Simple shape is fast to calculate numerically
- Currents can be interpolated to grid similarly for electromagnetic solving and/or diagnostics



## Weighting: Area Weighting

In a 2D cloud-in-cell system, weighting is accomplished using rectangular "area weighting" to nearest grid points

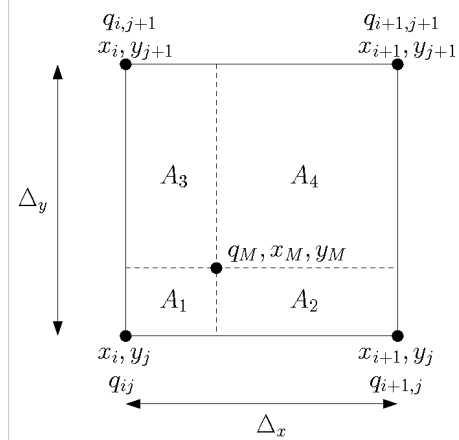


$q_M$ = Macro-particle charge

$(x_M, y_M)$ = Macro-particle coordinates

$q_{ij}$ = Mesh charges



## Area Weighting (2)

Charge Deposition:

$$q_{ij} = \left(1 - \frac{A_1}{\Delta_x \Delta_y}\right) q_M \qquad A_1 = (x_M - x_i)(y_M - y_j)$$

$$q_{i+1,j} = \left(1 - \frac{A_2}{\Delta_x \Delta_y}\right) q_M \qquad A_2 = (x_{i+1} - x_M)(y_M - y_j)$$

$$q_{i,j+1} = \left(1 - \frac{A_3}{\Delta_x \Delta_y}\right) q_M \qquad A_3 = (x_M - x_i)(y_{j+1} - y_M)$$

$$q_{i+1,j+1} = \left(1 - \frac{A_4}{\Delta_x \Delta_y}\right) q_M \qquad A_4 = (x_{i+1} - x_M)(y_{j+1} - y_M)$$

Field Interpolation:

$$\mathbf{E} = \frac{A_4}{\Delta_x \Delta_y} \mathbf{E}_{ij} + \frac{A_3}{\Delta_x \Delta_y} \mathbf{E}_{i+1,j} + \frac{A_2}{\Delta_x \Delta_y} \mathbf{E}_{i,j+1} + \frac{A_1}{\Delta_x \Delta_y} \mathbf{E}_{i+1,j+1}$$

Comments:

- Easily generalized to 3D using volumes
- Currents can be interpolated to grid similarly for electromagnetic solving and/or diagnostics



## Higher Order Weighting: Splines

To be added: Slide on Splines to
illustrate what is meant by higher order methods
Make Points:
- Requires more numerical work and harder to code
- Some schemes can introduce neg probability problems
- Should evaluate against simpler low order methods using same computer power to see which method wins.

## S4E: Computational Cycle for Particle-In-Cell Simulations

We now have (simplified) notions of the parts that make up a Particle-In-Cell (PIC) simulation of Vlasov beam evolution

1) Particle Moving
2) Field Solver on a discrete grid
3) Weighting of particle and fields to and from the grid

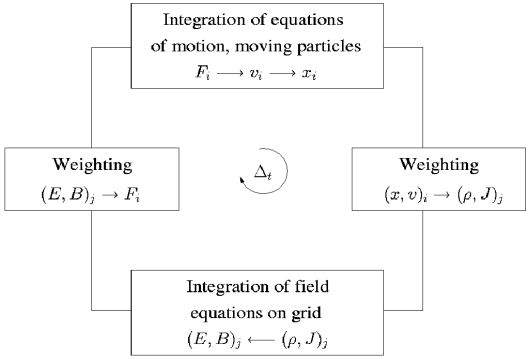


[Adapted from Birdsall and Langdon]



## Computational Cycle for Particle-In-Cell Simulations Contd.

Comments:

- Diagnostics must also be accumulated for useful runs (see S5)
  - Particles (coordinates and velocities) and fields will need to be synchronized (common time) when diagnostics are accumulated
- Initial conditions must be set (particle load, see S6)
  - Particle and field variables may need appropriate de-synchronization to initialize advance



## S5: Diagnostics

Diagnostics are *extremely* important. Without effective diagnostics even a correct and well converged simulation is useless. Diagnostics must be well formulated to display relevant quantities in a manner that increases physical understanding by highlighting important processes. This can be difficult since there can be a variety of issues and multiple effects taking place simultaneously.

Diagnostics can be grouped into two broad categories:

1) Snapshot Diagnostics
   - Examples: Particle distribution projections at a particular values of s or t
   - Data can be saved to generate plots after the run or just the needed plots can be generated during the run using linked graphics packages etc.
2) History Diagnostics
   - Examples: moments for the statistical beam centroid, envelope, and emittances
   - Data for history plots must be accumulated and saved over several simulation advance steps



See handwritten notes from USPAS 06 for remaining diagnostics slides

- Will be updated in future versions of the notes

## S6: Initial Distributions and Particle Loading

To start the large particle or distribution simulations, the initial distribution function of the beam must be specified.

- For direct Vlasov simulations the distribution need simply be deposited on the phase-space grid

For PIC simulations, an appropriate distribution of macro-particle phase-space coordinates must be generated or "loaded" to represent the Vlasov distribution

Discussion:

In realistic accelerators, focusing elements are *s*-varying. In such situations there are no known smooth equilibrium distributions.

- The KV distribution is an exact equilibrium for linear focusing fields, but has unphysical (singular) structure in 4-dimensional transverse phase-space

Moreover, it is unclear in most cases if the beam is even best thought of as an equilibrium distribution as is typical in plasma physics. In accelerators, the beam in generally injected from a source and may only reside in the machine (especially for a linac) for a small number of characteristic oscillation periods and may not fully relax to an equilibrium like state within the machine.



## Initial Distributions: Source-to-Target Simulations

The lack of known, physically reasonable equilibria and the fact that the beams are injected from a source motivates so-called "source-to-target" simulations where particles are simulated off the source and tracked to the target. Such first principles simulations are most realistic if carried out with the actual focusing fields, accelerating waveforms, alignment errors, etc. Source-to-target simulations are highly valuable to measure expected machine performance. However, ideal source-to-target simulations can rarely be carried out due to:

- Source is often incompletely described
  - Example: important alignment and material errors may not be known
- Source may contain physics not adequately in imperfectly modeled
  - Example: plasma injectors with complicated material physics, etc.
- Computer limitations:
  - Memory required and simulation time
  - Convergence and accuracies
  - Limits of numerical methods applied
    Ex: singular description needed for Child-Langmuir model of space-charge limited injection



## Initial Distributions: Types of Specified Loads

Due to the practical difficulty of always carrying out simulations off the source, two alternative methods are commonly applied:

1) Load an idealized initial distribution
   - Specify at some specific time
   - Based on physically reasonable theory assumptions
2) Load experimentally measured distribution
   - Construct/synthesize a distribution based on experimental measurements

Discussion:

The 2nd option of generating a distribution from experimental measurements, unfortunately, often has practical difficulties:

- Real diagnostics often are far from ideal 6D snapshots of beam phase-space
  - Distribution must be reconstructed from partial data
  - Typically many assumptions must be made in the synthesis process
- Process of measuring the beam can itself change the beam
- It can sometimes be helpful to understand processes and limitations starting from cleaner, more idealized initial beam states



Discussion Continued:

Because of the practical difficulties of loading a distribution based exclusively on experimental measurements, idealized distributions are often loaded:

- Employ distributions based on reasonable, physical ansatzes
- Use limited experimental measures to initialize:
  - Energy, current, rms equivalent beam sizes and emittances
- Simpler initial state can often aid insight:
  - Fewer simultaneous processes can allow one to more clearly understand how limits arise
  - Seed perturbations of relevance when analyzing resonance effects, instabilities, halo, etc.

A significant complication is that there are no known exact smooth equilibrium distribution functions valid for periodic focusing channels:

- Approximate theories valid for low phase advances may exist
  Davidson, Struckmeier, and others

Formulate a simple approximate procedure to load an initial distribution that reflects features one would expect of an equilibrium

## Initial Distributions Based on Continuous Focusing Equilibria

Simple psudo-equilibrium initial distribution:

- Use rms equivalent measures to specify the beam
  - Natural set of parameters for accelerator applications
- Map rms equivalent beam to a smooth, continuous focused matched beam
  - Use smooth core models that are stable in continuous focusing:
  - Waterbag Equilibrium
  - Parabolic Equilibrium
  - Thermal Equilibrium
  - ⋮

  } See Notes on: *Transverse Equilibrium Distributions*
- Transform continuous focused beam for rms equivalency with original beam specification
  - Use KV transforms to preserve uniform beam Courant-Snyder invariants

Procedure will apply to any s-varying focusing channel

- Focusing channel need not be periodic
- Beam can be initially rms equivalent matched or mismatched if launched in a periodic transport channel
- Can apply to both 2D transverse and 3D beams



## Procedure for Initial Distribution Specification

Assume focusing lattice is given:

$$\kappa_x(s), \quad \kappa_y(s) \quad \text{specified}$$

Strength usually set by specifying undperessed phase advances $\sigma_{0x}, \quad \sigma_{0y}$

Step 1:

For each particle (3D) or slice (2D) specify 2nd order rms properties at axial coordinate *s*

Envelope coordinates/angles:

$$r_x(s) = 2\langle x^2\rangle_\perp^{1/2} \qquad r'_x(s) = 2\langle xx'\rangle_\perp / \langle x^2\rangle_\perp^{1/2}$$

$$r_y(s) = 2\langle y^2\rangle_\perp^{1/2} \qquad r'_y(s) = 2\langle yy'\rangle_\perp / \langle y^2\rangle_\perp^{1/2}$$

Emittance:

$$\varepsilon_x(s) = 4[\langle x^2\rangle_\perp \langle x'^2\rangle_\perp - \langle xx'\rangle_\perp^2]^{1/2}$$

$$\varepsilon_y(s) = 4[\langle y^2\rangle_\perp \langle y'^2\rangle_\perp - \langle yy'\rangle_\perp^2]^{1/2}$$

Perveance:

$$Q = \frac{q\lambda(s)}{2\pi\epsilon_0 m\gamma_b^3(s)\beta_b^2(s)c^2}$$



## Procedure for Initial Distribution Specification (2)

If the beam is rms matched, we take:

$$r''_x + \kappa_x r_x - \frac{2Q}{r_x + r_y} - \frac{\varepsilon_x^2}{r_x^3} = 0 \qquad \kappa_x(s+L_p) = \kappa_x(s)$$

$$\kappa_y(s+L_p) = \kappa_y(s)$$

$$r''_y + \kappa_y r_y - \frac{2Q}{r_x + r_y} - \frac{\varepsilon_y^2}{r_y^3} = 0 \qquad r_x(s+L_p) = r_x(s)$$

$$r_y(s+L_p) = r_y(s)$$

- Not necessary even for periodic lattices
  - Procedure applies to mismatched beams



## Procedure for Initial Distribution Specification (3)

Step 2:

Define an rms matched, continuously focused beam in each transverse *s*-slice:

| Continuous | s-Varying | |
|---|---|---|
| $r_b(s) =$ | $\sqrt{r_x(s)r_y(s)}$ | Envelope Radius |
| $\varepsilon_b(s) =$ | $\sqrt{\varepsilon_x(s)\varepsilon_y(s)}$ | Emittance |
| $Q(s) =$ | $Q(s)$ | Perveance |

Define a (local) matched beam focusing strength in continuous focusing:

$$\cancelto{0}{r''_b} + k_{\beta 0}^2 r_b - \frac{Q}{r_b} - \frac{\varepsilon_b^2}{r_b^2} = 0$$

$$\rightarrow \quad k_{\beta 0}^2(s) = \frac{Q(s)}{r_b^2(s)} + \frac{\varepsilon_b^2(s)}{r_b^4(s)}$$

## Procedure for Initial Distribution Specification (4)

Step 3:

Specify an rms matched continuously focused equilibrium consistent with step 2:

Specify an equilibrium function:

$$f_\perp(x,y,x',y') = f_\perp(H_\perp) \qquad H_\perp = \frac{1}{2}\mathbf{x}_\perp'^2 + \frac{1}{2}k_{\beta 0}^2\mathbf{x}_\perp^2 + \frac{q\phi}{m\gamma_b^3\beta_b^2c^2}$$

and constrain parameters used to define the equilibrium function with:

$$\lambda = q\int d^2x \int d^2x' \; f_\perp(H_\perp) \qquad \text{Line Charge <--> Perveance}$$

$$r_b^2 = \frac{4\int d^2x \int d^2x' \; x^2 f_\perp(H_\perp)}{\int d^2x \int d^2x' \; f_\perp(H_\perp)} \qquad \text{rms edge radius}$$

$$\frac{\varepsilon_b^2}{r_b^2} = \frac{4\int d^2x \int d^2x' \; x'^2 f_\perp(H_\perp)}{\int d^2x \int d^2x' \; f_\perp(H_\perp)} \qquad \text{rms edge emittance}$$

- Constraint equations are generally highly nonlinear and must be solved numerically
  - Allows specification of beam with natural accelerations variables



## Procedure for Initial Distribution Specification (5)

Load N particles in x,y,x',y' phase space consistent with continuous focusing equilibrium distribution $f_\perp(H_\perp)$

Step A (set particle coordinates):

Calculate beam radial number density $n(r)$ by (generally numerically) solving the Poisson/stream equation and load particle $x,y$ coordinates:

$$x = r\cos\theta$$

$$y = r\sin\theta$$

- Radial coordinates $r$: Set by transforming uniform deviates consistent with $n(r)$
- Azimuthal angles θ: Distribute randomly or space for low noise

Step B (set particle angles):

Evaluate $f_\perp(U,r)$ with $U = \sqrt{x'^2 + y'^2}$ at the particle $x$, $y$ coordinates loaded in step A to calculate the angle probability distribution function and load $x'$, $y'$ coordinates:

$$x' = U\cos\xi$$

$$y' = U\sin\xi$$

- Radial coordinate $U$: Set by transforming uniform deviates consistent with $f_\perp(U,r)$
- Azimuthal coordinate ξ: Distribute randomly or space for low noise



## Procedure for Initial Distribution Specification (6)

Step 4:

Transform continuous focused beam coordinates to rms equivalency in the system with s-varying focusing:

$$x = \frac{r_x}{r_b}x_i \qquad y = \frac{r_y}{r_b}y_i$$

$$x' = \frac{\varepsilon_x}{\varepsilon_b}\frac{r_b}{r_x}x_i' + \frac{r_x'}{r_b}x_i \qquad y' = \frac{\varepsilon_y}{\varepsilon_b}\frac{r_b}{r_y}y_i' + \frac{r_y'}{r_b}y_i$$

Here, $\{x_i\}$, $\{y_i\}$, $\{x_i'\}$, $\{y_i'\}$ are coordinates of the continuous equilibrium loaded

- Transform reflects structure of Courant-Snyder invariants



## Comments on Procedure for Initial Distribution Specification

- Applies to both 2D transverse and 3D beams
- Easy to generalize procedure for beams with centroid offsets
- Generates a charge distribution with elliptical symmetry
  - Sacherer's results on rms equivalency apply
  - Distribution will reflect self-consistent Debye screening
- Equilibria are only pseudo-equilibria since transforms are not exact
  - Nonuniform space-charge results in errors
  - Transform consistent with preserved Courant-Snyder invariants for uniform density beams
  - Errors largest near the beam edge - expect only small errors for very strong space charge where Debye screening leads to a flat density profile with rapid fall-off at beam edge
- Many researchers have presented or employed aspects of the improved loading prescription presented here, including:

  I. Hofmann, GSI — M. Reiser, U. Maryland — M. Ikigami, KEK

  E. Startsev, PPPL — Y. Batygin, SLAC

## PIC simulations with the WARP code (see S9) were carried out to verify that the loading procedure results in less fluctuations and waves in self-consistent Vlasov evolutions from the load

Show evolutions from a matched load in a periodic FODO quadrupole transport lattice:

pseudo-thermal

semi-Gaussian (for contrast)

Find:

- Works well for $\sigma_0 \lesssim 85^\circ$
  - Should not work where beam is unstable and all distributions are expected to become unstable for $\sigma_0 >\sim 85^\circ$ see:

    Experiment: Tiefenback, Ph.D. Thesis, U.C. Berkeley (1986)

    Theory: Lund and Chawla, Proc. 2005 Part. Accel. Conf.
- Works better when matched envelope has less "flutter"
  - Solenoids: larger lattice occupancy $\eta$
  - Quadrupoles: smaller $\sigma_0$
  - Not surprising since less flutter" corresponds to being closer to continuous focusing



## WARP PIC Simulation (see S9) Results – Pseudo Thermal Equilibrium

$$\sigma_0 = 70^\circ, \quad L_p = 0.5 \text{ m}, \quad \varepsilon_x = \varepsilon_y = 50 \text{ mm-mrad}$$

$$\sigma/\sigma_0 = 0.2$$

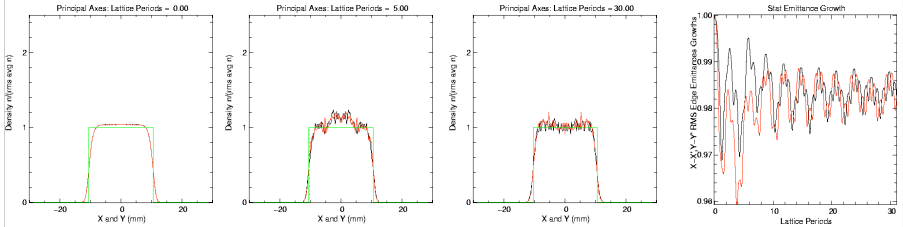


$$\sigma/\sigma_0 = 0.7$$

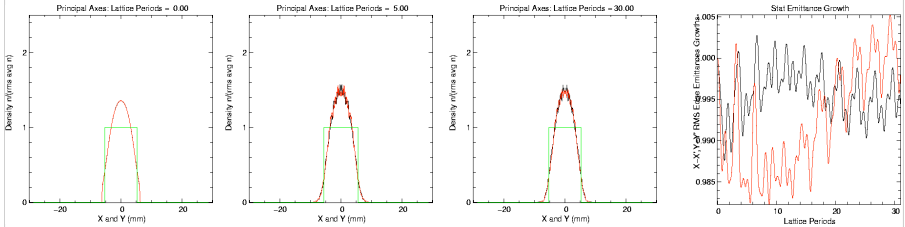




## WARP PIC Simulation (see S9) Results – Semi-Gaussian (for contrast)

$$\sigma_0 = 70^\circ, \quad L_p = 0.5 \text{ m}, \quad \varepsilon_x = \varepsilon_y = 50 \text{ mm-mrad}$$

$$\sigma/\sigma_0 = 0.2$$

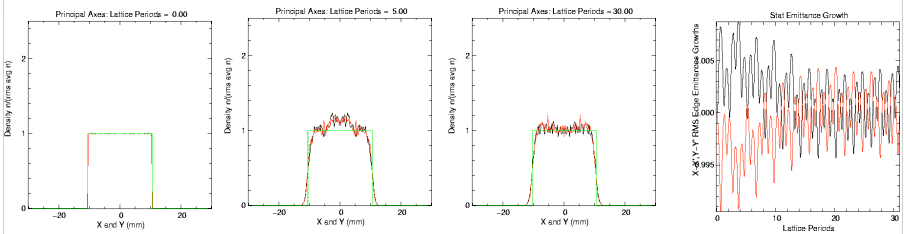


$$\sigma/\sigma_0 = 0.7$$

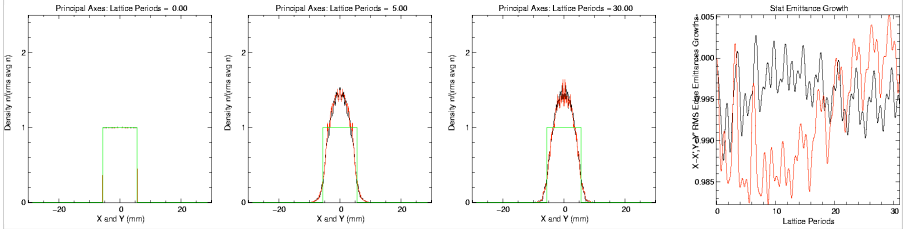




See handwritten notes from USPAS 06 for remaining distribution loading slides

- Will be updated in future versions of the notes

## Initial Loads: The Semi-Gaussian Distribution

See handwritten notes from USPAS 06

- Will be updated in future versions of the notes



## S7: Numerical Convergence

Numerical simulations must be checked for proper resolution and statistics to be confident that answers obtained are correct and physical:

Resolution of discretized quantities

- Time $t$ or axial s step of advance
- Spatial grid of fieldsolve
- For direct Vlasov: the phase-space grid

Statistics for PIC

- Number of macroparticles used to represent Vlasov flow to control noise

Increased resolution and statistics generally require more computer resources (time and memory) to carry out the required simulation. It is usually desirable to carry out simulations with the minimum resources required to achieve correct, converged results that are being analyzed. Unfortunately, there are no set rules on adequate resolution and statistics. What is required generally depends on:

- What quantity is of interest
- How long an advance is required
- What numerical methods are being employed .....



## General Guidance on Numerical Convergence Issues

Although it is not possible to give detailed rules on numerical convergence issues, useful general guidance can be given:

- Find results from similar problems using similar methods when possible
- Analyze quantities that are easy to interpret and provide good measures of convergence for the use of the simulation
  - Some moments like rms emittances:

$$\epsilon_x = 4\left[\langle\tilde{x}^2\rangle_\perp\langle\tilde{x}'^2\rangle_\perp - \langle\tilde{x}\tilde{x}'\rangle_\perp^2\right]^{1/2} \qquad \tilde{x} \equiv x - \langle x\rangle_\perp \qquad \tilde{x}' \equiv x' - \langle x'\rangle_\perp$$

  can provide relatively sensitive and easy to interpret measures of relative phase-space variations induced by numerical effects when plotted as overlaid time (or $s$) evolution "histories"
- Benchmark code against problems with known analytical solutions and properties
  - Apply a variety of numerical methods to judge which applies best
- Benchmark code against established, well verified simulation tools
  - Use different numerical methods expected to be more or less accurate



- Recheck convergence whenever runs differ significantly or when different quantities are analyzed
  - What is adequate for one problem/measure may not be for another
  - Ex: rms envelope evolution easier to converge than collective modes
- Although it is common to increase resolution and statistics till quantities do not vary, it is *also* useful to purposefully analyze poor convergence so characteristics of unphysical errors can be recognized
  - Learn characteristic signature of failures to resolve effects so subtle onset issues can be recognized more easily
- Expect to make *many* setup, debugging, and convergence test runs for each useful series of simulations carried out

See handwritten notes from USPAS 06 for remaining slides

- Will be updated in future versions of the notes



## S8: Practical Considerations: A: Overview

Intense beam simulation problems can be highly demanding on computer resources – particularly for realistic higher dimensional models. The problem size that can be simulated is dictated by computer resources available in fast memory and the run time required to complete the simulation

- Fast Memory (RAM)
- Wall Clock Run Time (Computer Speed)

Both of these can depend strongly on the architecture of computer system that the problem is run on:

- Serial Machine
- Parallel Machine

can strongly influence the size of the problem that can be simulated. We will present rough estimates of the computer memory required for simulations and provide some guidance on how the total simulation time can scale on various computer systems. The discussion is limited to PIC and direct Vlasov simulations.



## S8B: Practical Considerations: Fast Memory

Fast computer memory (RAM) dictates how large a problem can be simulated

- If a problem will not fit into fast memory (RAM), computer performance will be severely compromised
- Writes to hard disks are slow

There are 3 main contributions to the problem size for typical PIC or direct Vlasov simulations:

1) Particle Phase Space Coordinates (PIC)
   or Discretized Distribution Function (Direct Vlasov)
2) Gridded Field
3) General Code Overhead

These three contributions to memory required are discussed in turn

Particle and field quantities are typically stored in double precision:

| | Representation | Digits (Floating Point) | Bytes Memory |
|---|---|---|---|
| | Single Precision | 8 | 4 |
| Most problems | Double Precision | 16 | 8 |



## Estimates of Required Fast Memory

1) Particle Phase Space Coordinates (PIC):

$B$ = bytes of floating point number (typically 8 for double precision)

$N_p$ = number macro particles (0 for direct Vlasov)

$D$ = dimension of variables characterizing particles

$$\boxed{\text{Memory} = B * N_p * D \text{ Bytes}}$$

The dimension D depends on the specific type of PIC simulation and methods employed

/// Common Examples of $D$:

3D PIC: $D = 7$

$x,\ y,\ z$

$p_x,\ p_y,\ p_z,\ \gamma^{-1}$

2D Transverse Slice PIC: $D = 5$

$x,\ y$

$p_x,\ p_y, \gamma^{-1}$ + $p_z$ ($D$=6) some models

$\gamma^{-1}$ is often included often to optimize the mover

///

## Estimates of Required Fast Memory

1) Discretized Distribution Function (Direct Vlasov):

$B$ = bytes of floating point number (typically 8 for double precision)

$N_{pm}$ = number mesh points of grid describing the discretized particle phase space

$$\text{Memory} = B * N_{pm} \quad \text{Bytes}$$

The value of $N_{pm}$ depends critically on the dimensionality of the phase space

// Examples of $N_{pm}$ scaling for a uniform phase-space meshes:

| Problem | Phase Space | $N_{pm}$ | Scaling ($n_x = n_{p_x} \equiv n$ etc) |
|---|---|---|---|
| 1D $\parallel$ | $z - p_z$ | $n_z n_{p_z}$ | $n^2$ |
| 2D $\perp$ Slice | $x - p_x,\ y - p_y$ | $n_x n_y n_{p_x} n_{p_y}$ | $n^4$ |
| 2D Slice | $x - p_x,\ y - p_y,\ p_z$ | $n_x n_y n_{p_x} n_{p_y} n_{p_z}$ | $n^5$ |
| 3D | $x - p_x,\ y - p_y\ z - p_z$ | $n_x n_y n_{p_x} n_{p_y}$ | $n^6$ |

$$n_x = \text{number mesh points in } x \text{ etc.}$$

Rapid growth of $N_{pm}$ with dimensionality severely limits tractability of problems



Memory required for a double precision ($B$ = 8) uniform phase-space grid with 100 zone discretization per degree of freedom:

$$n_x = n_{p_x} \equiv n = 100 \text{ etc.}$$

$$\text{D} = \text{dimension of phase-space}$$

$$\text{Memory} = 8 * n^D \text{ Bytes}$$

| Problem | $D$ | Memory (Bytes) (n = 100) |
|---|---|---|
| 1D $\parallel$ | 2 | $80 \times 10^3 \sim 80$ KB |
| 2D $\perp$ Slice | 4 | $80 \times 10^6 \sim 80$ MB |
| 2D Slice | 5 | $80 \times 10^9 \sim 80$ GB |
| 3D | 6 | $8 \times 10^{12} \sim 8000$ GB |

//

Rapidly increasing problem size with phase-space dimension $D$ practically limits what can be simulated on direct Vlasov models with reasonable resolution *even on large parallel computers*:

- Irregular phase-space grids that place resolution where it is needed can partially alleviate scaling problem
- Optimal methods must also only grid minimal space exterior to the oscillating beam core in alternating gradient lattices



2) Gridded Field:

Required memory for a gridded field solve depends on the class of field solve (electrostatic, electromagnetic), mesh size, and numerical method employed. For a concrete illustration, consider *electrostatic* problems using a simple FFT field solve:

- Discrete Fourier Transform complex, but transform is of real functions. Proper optimization allows use of transforms using only real $\phi$ and $\rho$ arrays
- Electric field is typically not stored and is calculated for each particle only where it is needed. Spatial grid location need not be stored.
  - Some methods store gridded E to optimize specific problems

$N_{fm}$ = number mesh points of field spatial grid

$$\text{Memory} = 2 * B * N_{fm} \quad \text{Bytes}$$

Factor of 2 for: $\rho, \phi$



Number of mesh points $N_{fm}$ depends *strongly* on the dimensionality of the field solve and the structure of the mesh

- Generally more critical to optimize storage and efficiency (see next section) of fieldsolvers in higher dimensions

Examples for uniform meshes:

$$N_{fm} = n_z \quad \text{1D (Longitudinal)}$$
$$= n_x n_y \quad \text{2D (Transverse Slice)}$$
$$= n_x n_y n_z \quad \text{3D}$$

$$n_x = \text{number mesh points in } x \text{ etc.}$$

3) General Code Overhead:

System memory is also used for:

- Scratch arrays for various numerical methods (fieldsolvers, movers, etc.)
- History accumulations of diagnostic moments
- Diagnostic routines
- Graphics packages, external libraries, etc.
  - Graphics packages can be large!

$$\text{Memory} = M_{overhead} \quad \text{Bytes}$$

Characteristic of packages used, size of code, and methods employed. But typical numbers can range 1 MB – 20 MBytes

Summary: Total Memory Required:

For illustrative example, add contributions for electrostatic PIC

$$\text{PIC:} \quad \text{Tot Memory} = B * (N_p * D + 2 * N_{fm}) + M_{overhead} \quad \text{Bytes}$$

$$\text{Direct Valsov:} \quad \text{Tot Memory} = 2 * B * (N_{pm} + N_{fm}) + M_{overhead} \quad \text{Bytes}$$

Reminder: Machine fast memory (RAM) capacity *should not be exceeded*

- Storing data on disk and cycling to RAM generally too slow!



## S8C: Practical Considerations: Run Time

Run time can depend on many factors including:

- Type of problem
- Dimensionality of problem and number of particles and/or mesh points
- Numerical methods employed (particle moving, fieldsolve, ....)
- Moments and diagnostics accumulated
- Architecture/speed of computer system

It is not possible to give fully general guidance on estimating run times. However, to better characterize the time required, it can be useful to benchmark the code on the computer to be employed in terms of:

$$t_{step} = \text{Time for an “ordinary” run step}$$

Generally, parts of the code that more time is spent in should be more carefully optimized to minimize total run time. Care should generally be applied with:

- Particle mover
- Field solver
- Frequent diagnostics such as moments



Diagnostics, loaders, problem setup routines, etc. can often be coded with less care for optimization since they are only executed infrequently. However:

- Diagnostics often take a large amount of development time
  - Often better to code as simply as possible!

Software profiling tools can be useful to best understand where “bottlenecks” occur so effort on optimization can be appropriately directed for significant returns.



## Dimenstionality plays a strong role in required run time

Some general guidance for electrostatic PIC Simulations:

1D: (Longitudinal typical)

Fieldsolve generally fast: small fraction of time compared to moving particles

- Green's function methods can be used (Gauss Law)

2D: (Transverse slice typical)

Fieldsolve typically a small fraction of time relative to moving particles if fast gridded methods are applied (like FFT based methods)

- Special boundary conditions can increase the fraction

| Method | Numerical Work |
|---|---|
| FFT with Periodic BC | Small fraction of particle moving |
| FFT with Capacity Matrix | . |
| SOR | . |
| . | . |
| Green's Function | Dominates particle moving |

3D:

Fieldsolve typically comparable in time or dominates time for particle moving even if fast, gridded methods are applied

- Fieldsolve efficiency of *critical* importance in 3D to optimize run time
- Whole classes can be taught just on methods of 3D electrostatic field solves for Poission's equation

Some general guidance for Direct Vlasov Simulations:

The rapid growth of the problem size with the phase space-dimension and available fast computer memory can severely limit problem sizes that can be simulated:

- Numerical work can be significant to advance the discretized distribution over characteristics
- Size of gridded field arrays can be very large leading to slow advances
  - Uniform mesh: $D$



The type of computer system employed can also strongly influence run time

- Processor Speed
- Memory Speed
  - RAM
  - Fast, optimized cache memory
- System Architecture (see next section)
  - Serial
  - Parallel
- Library Optimization
  - Especially for parallel machines



## S8D: Practical Considerations: Machine Architectures

Problems may be simulated on:

1) Serial Machines
   - Single processor or an independently run processor on a multi-processor machine (example: most present multi-"core" processors)
2) Parallel Machine
   - Multi-processors coordinated to work as a large single processor
   - Usually employ independent memory for each processor making up the machine but sometimes uses shared memory among processors

Serial machines represent traditional computers (PCs workstations, etc), whereas parallel machines are generally less familiar.

Overview of parallel simulations:

In recent years parallel machines have significantly improved with libraries that allow more "natural" problem formulation with less effort and they are enabling significantly larger simulations to be carried out

- Several 100 million particles typically practical to simulate on large machines



## Typical Parallel Machine Architecture

Beam problems may often be conveniently partitioned among processors in terms of axial slices. Schematic example (5 processors):

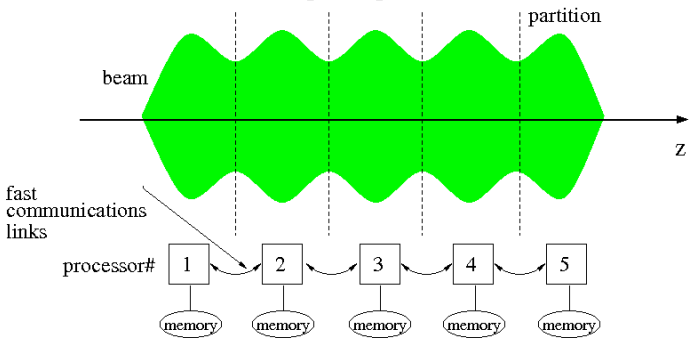


- Sharing of data at boundaries is necessary for fieldsolve
- Problems with axial velocity spread will generally require sorting of particles to maintain the load balance between processors
  - Processors should ideally all perform an equal amount of work since the slowest will dictate the total time of the advance step

Ideal parallelization will result in a linear speedup with processor number

- Actual speedup less due to:
  - Overhead in data transfers
  - Lack of ideal load balance causing processors to wait on the slowest one that the problem is partitioned among

$$\tau_{\text{step}} = \text{Time "ordinary" step in compuational cycle}$$

$$t_{\text{sim}} = \frac{\text{Simulation Time}}{\tau_{\text{step}}}$$

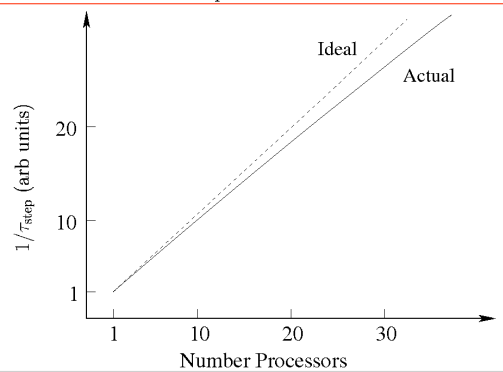




Even with the significant advances in problem size and speed promised by parallel computers, the solution of realistic 3D beam problems with direct (not gridded) fields remains far too large a problem to simulate with present coputer systems. Thus, for detailed simulations, we often push computer resources to the maximum extent possible.

- Better numerical algorithms
- Parallelization
- ....



## S9: WARP Code Overview

See handwritten notes from USPAS 06 for remaining slides

- Will be updated in future versions of the notes



## S10: Example Simulations

Examples to this point have mostly been simply formulated to illustrate concepts. Here, we present results from more complex simulations carried out in support of experiments, theory, and for machine design. Simulations highlighted include:

- Electrostatic Quadrupole Injector
- Multi-beamlet Injector
- Collective Mode Effects
- Detailed Transport Lattice Design
- Transport Limits in Periodic Quadrupole Focusing Channels
- Electron Cloud Effects for Ion Beam Transport

All these simulations, as well as many of the preceding illustrations in the lecture notes, were produced with the WARP code described in S9. Only select issues from the problems are highlighted.

## Example: Electrostatic Quadrupole Injector

See handwritten notes from USPAS 06 for remaining slides

- Will be updated in future versions of the notes



These slides will be corrected and expanded for reference and any future editions of the US Particle Accelerator School class:
*Beam Physics with Intense Space Charge*, by J.J. Barnard and S.M. Lund

Corrections and suggestions are welcome. Contact:

Steven M. Lund
Lawrence Berkeley National Laboratory
BLDG 47 R 0112
1 Cyclotron Road
Berkeley, CA 94720-8201

SMLund@lbl.gov
(510) 486 – 6936

Please do not remove author credits in any redistributions of class material.



## Acknowledgments

Sven Chilton (UCB, LLNL) assisted in the development of part of these lecture notes and in generating some of the numerical examples and figures

Special thanks are deserved for Alex Friedman, Dave Grote, and Jean-Luc Vay of the Lawrence Livermore and Lawrence Berkeley National Laboratories for help with these notes and extensively educating the authors in simulation methods.

Rami Kishek (UMD) assisted teaching a version of this class and contributed to the notes. Irving Haber (UMD), Christine Celata (LBL), and Bill Fawley (LBL) helped educate the authors on various simulation methods.

Michiel de Hoon helped with an early version of the lectures and with example Lagrangian methods.



## References: For more information see:

### Numerical Methods

Forman S. Acton, *Numerical Methods that Work*, Harper and Row Publishers, New York (1970)

Steven E. Koonin, *Computational Physics*, Addison-Wesley Publishing Company (1986)

W. Press, B. Flannery, S. Teukolsky, W. Vetterling, *Numerical Recipes in C: The Art of Scientific Computing*, Cambridge University Press (1992).

### Particle Methods

C.K. Birdsall and A.B. Langdon, *Plasma Physics via Computer Simulation*, McGraw-Hill Book Company (1985).

R.W. Hockney and J.W. Eastwood, *Computer Simulation using Particles*, Institute of Physics Publishing (1988).

§5 Diagnostics:

Depend on what is analyzed. Typical choices:

- Moments – statistical sums over the particle distribution (slices and full beam), often plotted as time histories as the beam evolves in the accelerator:

centroid: $x_c = \langle x \rangle_\perp$ .....

RMS Widths: Beam Size $r_x = 2\langle (x-x_c)^2 \rangle^{1/2}$, ..... etc.

Emittance: $\varepsilon_x = 16\left[\langle (x-x_c)^2\rangle\langle (x'-x_c')^2\rangle - \langle (x-x_c)(x'-x_c')\rangle^2\right]^{1/2}$,

etc.

Here; $\langle \cdots \rangle_\perp = \frac{1}{N_s}\sum_{i}^{\text{slice}} \{\cdots\}_i$ ..... etc.

Slice emittance "history"

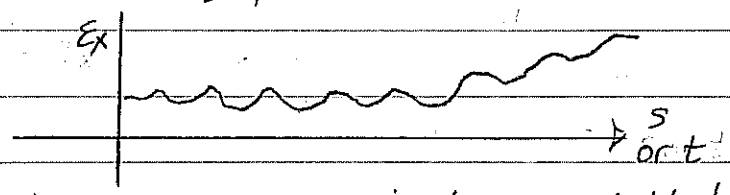


- Particle phase-space projections plotted as snapshots in time ($x$-$x'$, $y$-$y'$, $x$-$y$, $x'$-$y'$, .....).

At some value of s or t

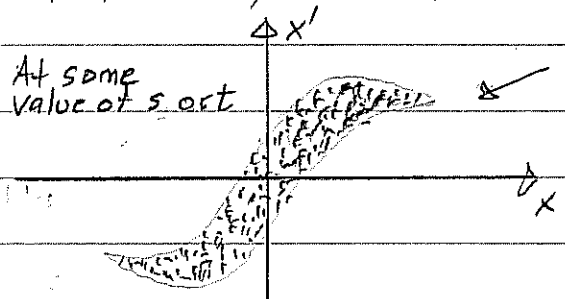


Scatter plot of enough macro-particles to visualize the phase-volume and structure of the beam.

Plotting snapshots at periodic locations allows vizualization of the evolution of beam distortions:

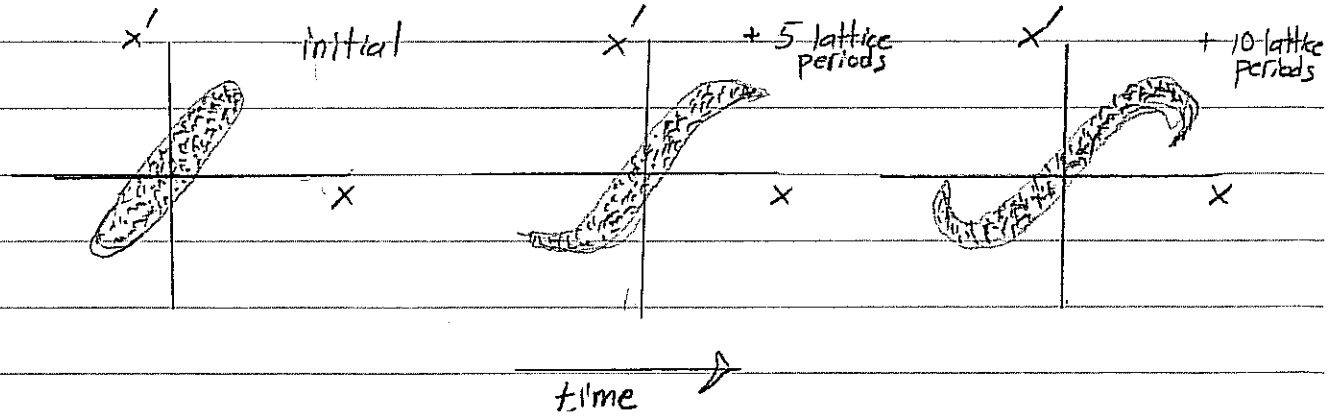

- <u>Field</u> Diagnostics:

Contours of self and applied fields illustrate field structure.

Examples:

1) Total potential contors of $\phi$ (self and applied) of an elliptical beam in an electric quadrupole formed by 4 biased rods.

same $\phi$ contours with beam particles plotted

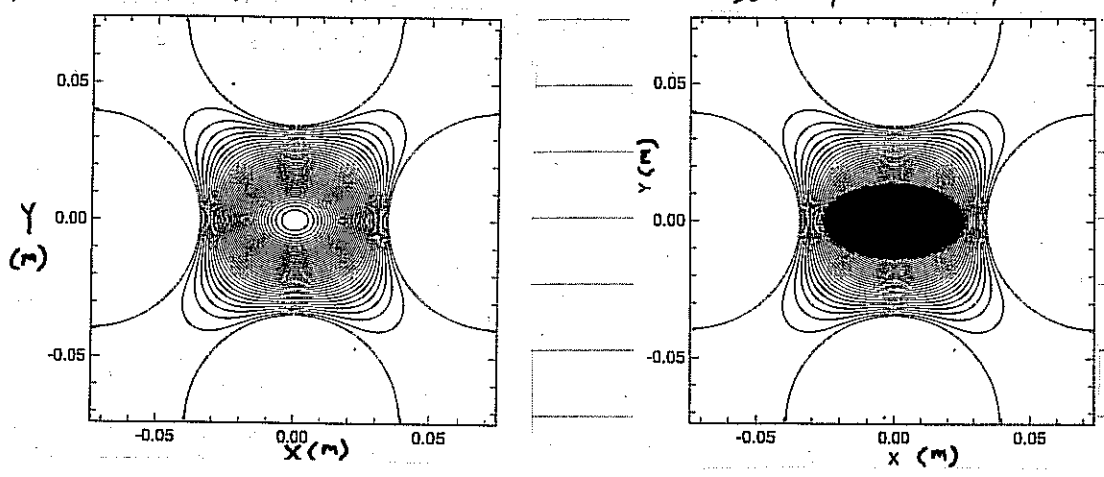


2) <u>Applied Field</u> Scalar magnetic potential contours of a permanant magnet lense illustrate the structure of applied field nonlinearities:

8 Block Permanent Magnet Quadrupole.

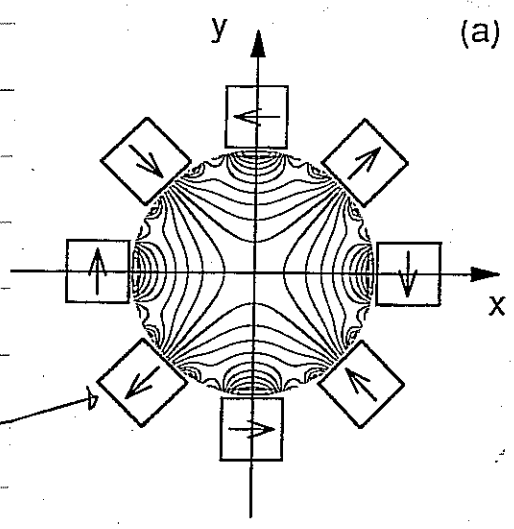


Note: contours deviate from hyperbolic near apeture edge.

Numerous other field diagnostics are possible:

- Field energy, multipole moments,

# §6 Particle Loads

To start the simulation, one must specify and "load" the initial distribution function.

In realistic accelerators, focusing elements are s-varying. In such situations there are in general no known equilibrium distribution functions. Moreover, it is unclear in most cases if the beam is even best thought of as an equilibrium + perturbations as is typical in plasma physics. Rather, in accelerators, the beam is injected from a source and may only reside in the machine (especially a linac) for a small number of characteristic oscillation periods and may not fully relax to an equilibrium-like state. In such situations, so-called "source-to-target" simulations where the particles are simulated off the source and tracked to the target can be most realistic if carried out with realistic focusing fields, accelerating waveforms, alignment errors, etc.

Unfortunately, such idealized source-to-target simulations can rarely be carried out due to computer limitations.

- Memory limits
- Numerical convergance and accuracy ...

Two ways around this limitation:

1) Load experimentally measured distribution at some point in the machine and advance as an initial condition.
2) Load an idealized initial distribution.

The 1st option can have practical difficulties:

- Diagnostics often are far from an ideal 6D "snapshot" of the beam phase-space.
  - Much information typically lost.
- Process of measuring the beam can itself change the beam.

Most commonly, some experimental measures such as:

- rms beam sizes $r_x, r_y, r_x', r_y'$
- rms emittances $\varepsilon_x, \varepsilon_y$

are loaded in the form of idealized distributions.

It can be insightful to initialize the beam in a simplified manner

- Fewer simultaneous processes can allow one to more clearly see how limits arise.
- Seed perturbations of relevance when analyzing resonance effects, instabilities, halo, etc.

In these situations it is often useful to load a round, continuously focused distribution such as:

- Thermal Equilibrium
- Waterbag
- KV

and then transform the particle coordinates to "match" the local focusing structure of the lattice using a local KV envelope solution:

$$\frac{d^2}{ds^2} r_x(s) + \kappa_x(s) r_x(s) - \frac{2Q(s)}{r_x(s)+r_y(s)} - \frac{\varepsilon_x^2(s)}{r_x^3(s)} = 0$$

$$\frac{d^2}{ds^2} r_y(s) + \kappa_y(s) r_y(s) - \frac{2Q(s)}{r_x(s)+r_y(s)} - \frac{\varepsilon_y^2(s)}{r_y^3(s)} = 0$$

$\kappa_x(s), \kappa_y(s)$ = lattice focusing constants
$Q(s)$ = local perveance (specified)
$\varepsilon_x(s), \varepsilon_y(s)$ = local emittances (specified)

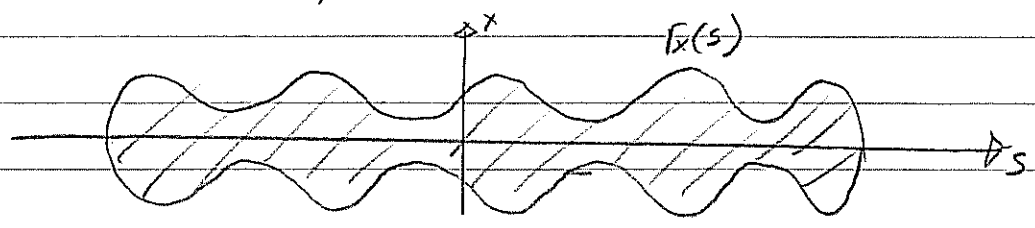

## Procedure:

**1st**

Load in each $\perp$ slice round, continuous distribution:

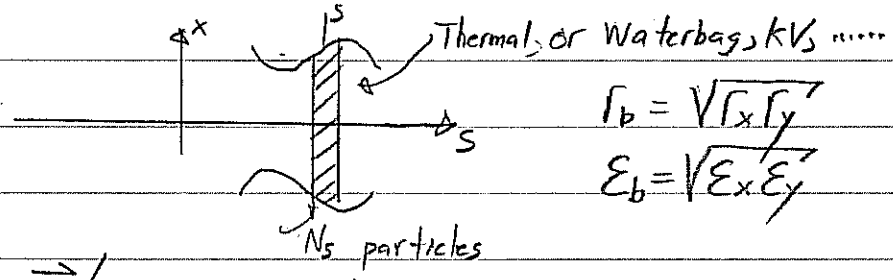


$$r_b = \sqrt{r_x r_y}$$
$$\varepsilon_b = \sqrt{\varepsilon_x \varepsilon_y}$$

$\Rightarrow \quad \vec{X}_i, \vec{X}_i'$ specified

**2nd**

Transform the spatial coordinates to match the elliptical envelope structure

$$x_i \longrightarrow \frac{r_x}{r_b} x_i$$

$$y_i \longrightarrow \frac{r_y}{r_b} y_i$$

**3rd**

Transform the local thermal velocity spreads to obtain the right average thermal force.

$$x_i' \longrightarrow \frac{\varepsilon_x}{\varepsilon_b} \frac{r_b}{r_x} x_i'$$

$$y_i' \longrightarrow \frac{\varepsilon_y}{\varepsilon_b} \frac{r_b}{r_y} y_i'$$

**4th**

Add the correct coherent velocity to match the needed envelope angle.

$$x_i' \longrightarrow x_i' + r_x' \frac{x_i}{r_x}$$

$$y_i' \longrightarrow y_i' + r_y' \frac{y_i}{r_y}$$

// Aside – The semi-Gaussian Distribution

It is not necessary to always load something based on a transformation of an equilibrium distribution to get a good quiescent load. Note that for high space-charge intensities:

- Beam space charge will be more or less uniform out to the edge, where the density will rapidly fall to zero.

- If the beam is injected off a uniform tempeture source or has relaxed, one expects roughly uniform thermal velocity spread across the cross-section of the beam.

This suggests the so-called "semi-Gaussian" load specified as follows:

- Uniform density within an elliptical beam envelope.

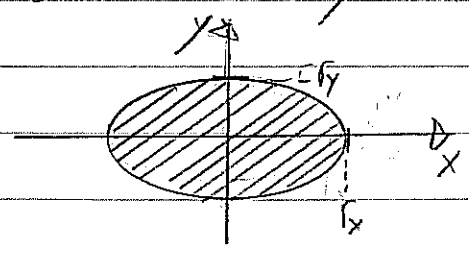


$x_i, y_i$ uniformly distributed for $(x/r_x)^2 + (y/r_y)^2 \leq 1$.

- Gaussian distributed thermal velocity spread with the correct coherent velocity to match the needed envelope angles

$$x_i' = r_x' \frac{x_i}{r_x} + \frac{\varepsilon_x}{2r_x} \tilde{r}_{x_i}$$
$$y_i' = r_y' \frac{y_i}{r_y} + \frac{\varepsilon_y}{2r_y} \tilde{r}_{y_i}$$

$\tilde{r}_{x,y_i}$ Gaussian distributed with unit variance $\left(\frac{1}{N_s}\sum_i^{slice} \tilde{r}_{x,y_i}^2 = 1\right)$

The semi-Gaussian load results in "squared" initial x-x' and y-y' phase space projections:

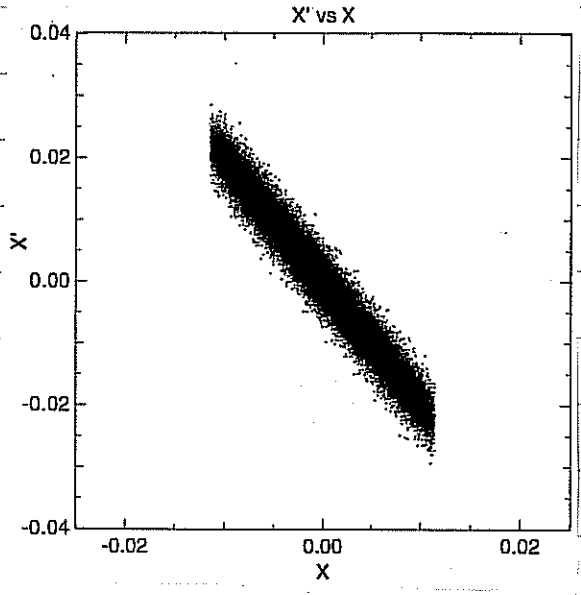


Initial load in a symmetric FODO AG Quadrupole transport lattice

The unphysical edges typically relax rapidly without perturbing the low order RMS structure of the beam (envelope match, emittance, etc.).

1 lattice period advance

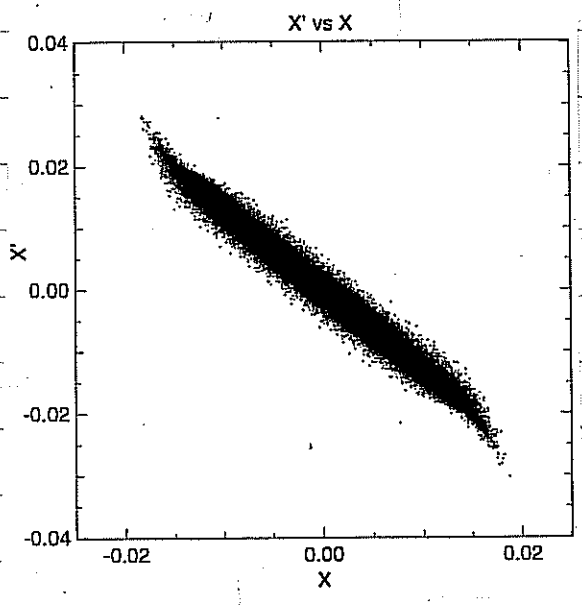


4 lattice period advance

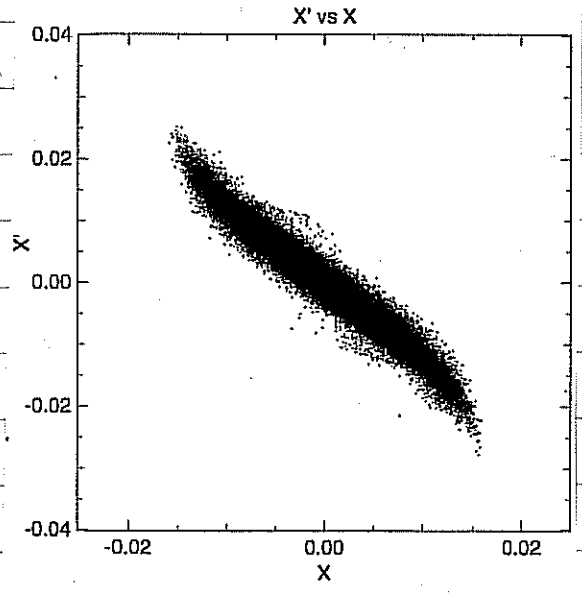


Numerous other loading techniques exist to address specific issues. //

## §7 Numerical Convergence

Numerical simulations must be checked for proper resolution and statistics to be confident that answers obtained are correct and physical.

Resolution on discritized quantities
- Time step in particle advance
- Spatial grid for fields

Statistics (number of macroparticles) to control noise.

More resolution and statistics require more computer time and memory. To be practical, one generally wishes to solve problems with the minimum resources required to achieve correct, converged answers. Unfortunately, there are no set rules on what resolution and statistics are required. This depends on what one is examining, how long the simulations are run, what numerical methods are employed, ....

Some general guidance:

- The statistical rms emittances:

$$\varepsilon_x = 4\left[\langle x^2\rangle_\perp \langle x'^2\rangle_\perp - \langle xx'\rangle_\perp^2\right]^{1/2}$$

$$\varepsilon_y = 4\left[\langle y^2\rangle_\perp \langle y'^2\rangle_\perp - \langle yy'\rangle_\perp\right]^{1/2}$$

often prove to be sensitive and easy to interpret measures of numerical differences when plotted as overlaid time histories.
  - picks up small phase space distortions induced by numerical errors.

general guidance continued ....

- To get started, find results from similar problems using similar methods.

- Benchmark code and methods against problems with known analytical solutions, established codes using both similar and different numerical methods, ....

- Recheck numerical convergence whenever runs differ significantly <u>or</u> when differing quantities are analyzed.

  - What is adequate for one measure of the beam (say image charge structure) may not be for another (say collective modes).

- Although it is common to increase resolution and statistics till relevant quantities do not vary, it is <u>also useful to purposefully analyze poor resolution and statistics regimes so the characteristics of unphysical numerical errors can be recognized.</u>

- Expect to make many setup, convergence, and debugging runs for each useful series of simulations carried out.

Specific Numerical Convergence Comments:

Time Resolution.

These comments are applicable to both spatial or time steps of the particle advance. We will frame estimates in terms of timesteps.

- Particle coordinates should not move through more than one cell in a single step. This is a standard "Courant" condition:

$$\boxed{\begin{aligned} v_x \Delta_t &< \Delta_x \\ v_y \Delta_t &< \Delta_y \\ v_z \Delta_t &< \Delta_z \end{aligned}}$$

for all particles.

- Enough steps should be taken to resolve variations in applied field structures.

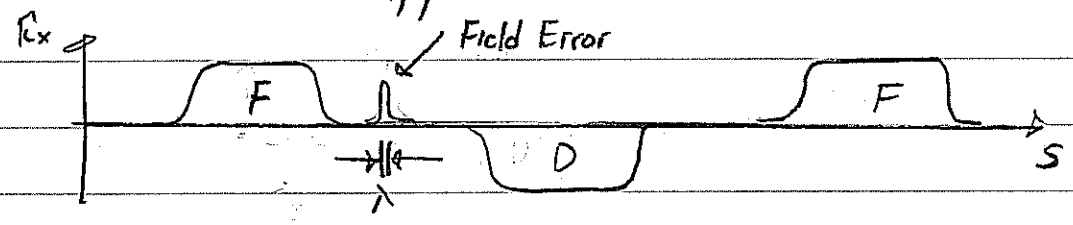


$$\boxed{v_s \Delta_t < \lambda \quad ; \quad \lambda = \text{shortest wavelength of field structures to be modeled}}$$

- Phase variations in collective waves (if of interest) should be resolved. For a leap-frog mover this requires:

$$\boxed{\begin{aligned} &\omega = \text{mode frequency component} \\ &\frac{\omega \Delta_t}{2\pi} < \frac{1}{2} \end{aligned}}$$

## Spatial Resolution

For cold beams the beam edge can be sharp for most reasonable distribution functions:

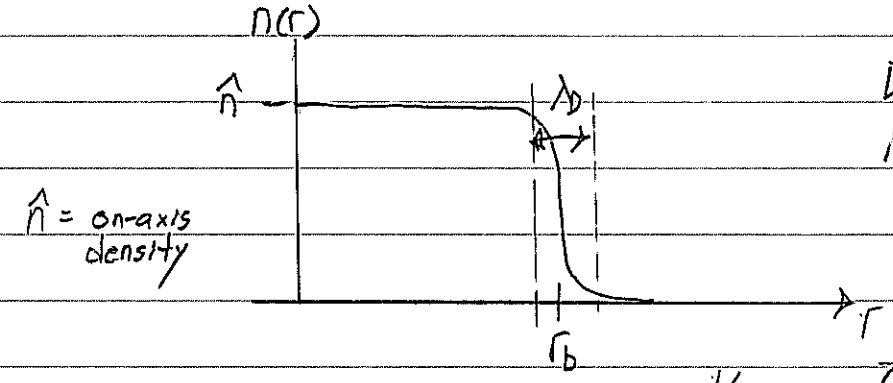


Density falls of in $\mathcal{O}(\lambda_D)$

Debye length: $\lambda_D = \dfrac{v_t}{\omega_p} = \left(\dfrac{\varepsilon_0 k_B T}{\hat{n} q^2}\right)^{1/2}$ $\qquad v_t = (k_B T/m)^{1/2}$, $\quad \omega_p = \left(\dfrac{q^2 \hat{n}}{\varepsilon_0 m}\right)^{1/2}$

$$r_b = \sim 5\lambda_D \rightarrow 30\lambda_D \quad \text{typical.}$$

To resolve edge physics, the mesh should have several cells across the rapid density variation near the edge of the beam.

$$\boxed{dx, dy < \frac{\lambda_{Dx,y}}{2} \qquad \lambda_{Dx,y} = \left(\frac{k_B T_{x,y}}{m}\right)^{1/2} \qquad T_{x,y} = \text{local kinetic temperature}}$$

The mesh should also resolve relevant spatial scales associated with processes of interest:

- If applied electrostatic fields are calculated from biased conductors, the mesh should resolve conductor structures or special corrections should be made.
- Self-field fluctuations induced by collective modes should be resolved.

Collective mode resolution: From Eigenfunctions to be presented later in the class:

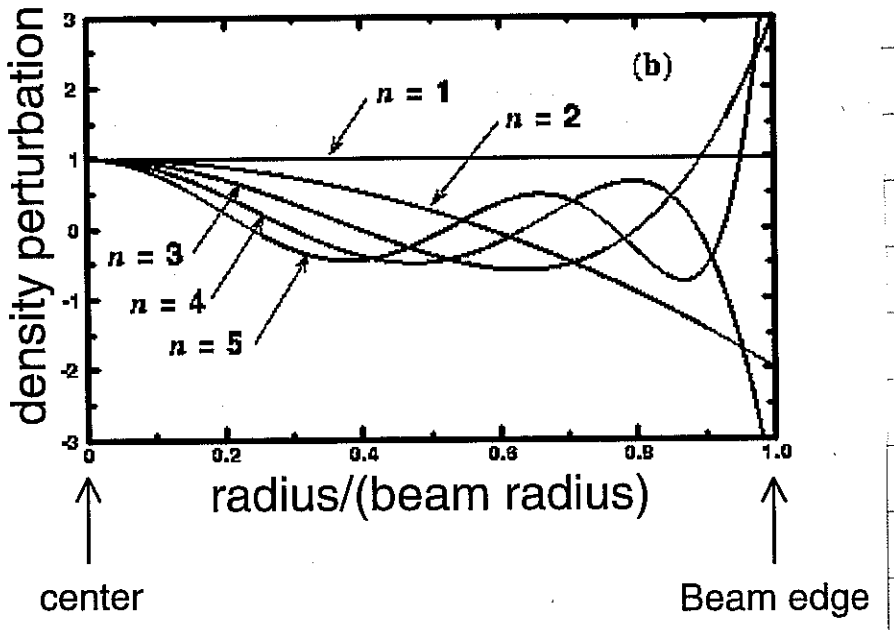


Collective mode density perturbations on a uniform density beam.

$\Rightarrow$ $dx, dy < \lambda$ ~ shortest characteristic wavelength of modes of interest.

Note that higher order modes (n larger) will become hard to resolve. Moreover, such perturbations also oscillate rapidly making time (s) stepsize resolution likewise difficult.

Statistics:

Collective effects typically require having a significant number of particles $N_D$ within the characteristic screening radius characterized by the Debye length:

$$\boxed{\begin{array}{ll} \text{2D:} & N_D = \sum_i \int_{\substack{\text{circle} \\ |\vec{x}|<\lambda_D}} d^2x\, \delta^{(2)}(\vec{x}-\vec{x}_i) \gg 1 \\ & \qquad \vec{x}_i = \text{macro-particle coordinate.} \\ \text{3D:} & N_D = \sum_i \int_{\substack{\text{sphere} \\ |\vec{x}|<\lambda_D}} d^3x\, \delta^{(3)}(\vec{x}-\vec{x}_i) \gg 1 \\ \text{where:} & \qquad v_t = (k_B T/m)^{1/2} \\ & \lambda_D = \dfrac{v_t}{\omega_p} = \left(\dfrac{\varepsilon_0 k_B T}{\hat{n} q^2}\right)^{1/2} \qquad \omega_p = \left(\dfrac{q^2 \hat{n}}{\varepsilon_0 m}\right)^{1/2} \\ & \sum_i \Rightarrow \text{sum over all macro particles.} \end{array}}$$

In simulations of higher order collective modes it may also be necessary to have a significant number of particles per cell on a mesh that resolves the relevant spatial variations of mode induced self-field fluctuations.

$$\boxed{\begin{array}{ll} \text{2D:} & N_{cell} = \sum_i \int_{\text{cell}} d^2x\, \delta^{(2)}(\vec{x}-\vec{x}_i) \gg 1 \\ \text{3D:} & N_{cell} = \sum_i \int_{\text{cell}} d^3x\, \delta^{(3)}(\vec{x}-\vec{x}_i) \gg 1 \end{array}}$$

- Larger $N_{cell}$ prevents local self-fields from being noise dominated.
- Larger $N_{cell}$ leads to larger $N_D$, typically $N_D > N_{cell}$ since $\lambda_D$ must be resolved on the grid.

Good statistics are <u>only</u> needed in the beam core with the possible exception of certain beam-halo problems and near the beam edge.

- Most beams will only occupy a fraction of the full grid.

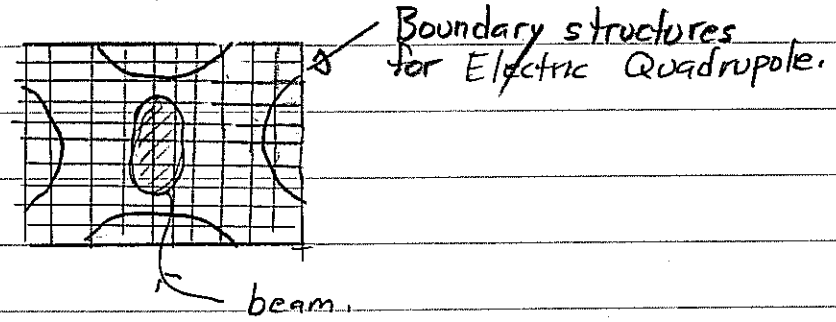


statistics should be evaluated in the cells that the beam occupies rather than average grid measures.

No comprehensive rules exist for how good the statistics must be. <u>Individual problems must be checked and verified.</u> Some general comments:

- What is adequate will typically depend on what is analyzed
  - Image fields may be resolved with few particles
  - Collective waves may take many particles if low noise (interpetable) diagnostic projections are needed.
- Longer runs generally require increased statistics
- Poor statistics result in unphysical collisionality that is often characterized by a linear rise in beam emittances with simulation time.

# Classes of Particle Simulations.

How important is smoothing?

3D Beam: $N \sim 10^{10} - 10^{14}$ particles typical

Simulations: $N \lesssim 10^{8}$ practical (modern parallel computers), typical $10^{3} - 10^{6}$

Each simulation particle may represent: $10^{3} \rightarrow 10^{11}$ particles in the real beam for 3D simulations.

- Smoothing involved with particle weightings are key to obtaining physical answers and limiting collisionality.

Is the situation really this bad?

- Lower dimensonal models typically simulated.

## 3D Model

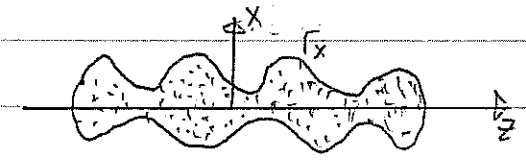


N point particles with smoothed interactions

Phase Space:

$x, y, z$
$p_x, p_y, p_z$ } 6D

Physical charge – point charges

$$\rho = \sum_i q\, \delta(x-x_i)\,\delta(y-y_i)\,\delta(z-z_i)$$

Smoothed charge

$$\rho = \sum_i q_M\, f(x-x_i, y-y_i, z-z_i)$$

$q_M$: Macro particle charge

$f$: smoothed shape function

## 2D ⊥ Thin Slice Model

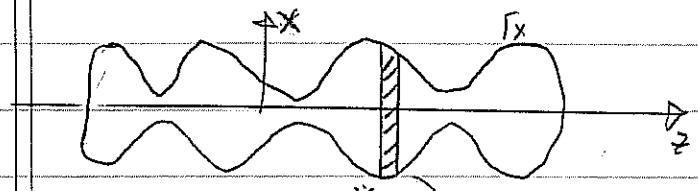


N line charges with smoothed interactions.

Thin slice

$\frac{\partial}{\partial z} \ll \nabla_\perp$

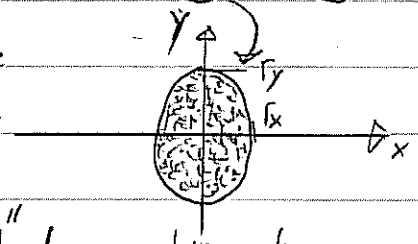


Phase Space:

$x, y$ } 4D + possible 1D
$p_x, p_y$ } $p_z$

4D or 5D

"Physical" charge - line charges

$$\rho = \sum_i \lambda_p \delta(x-x_i)\delta(y-y_i)$$

Smoothed charge -

$$\rho = \sum_i \lambda_M f(x-x_i, y-y_i)$$

$\lambda_M$: Macro particle line charge

$f$: smoothing function

The slice must be tracked in $s$ with each particle moving the same increment in $s$ with each step so that a slice maps to a slice.

- If $p_z$ is included the velocity distribution must be assumed "frozen in".

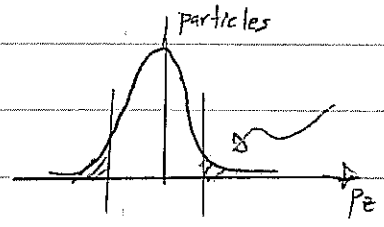


parts that would leave assumed replenished by particles from adjacent slices.

- Response to acceleration may be modeled with

- "Thick" slice models also possible with periodic boundary conditions on the "slice" to try to recover some 3D effects of a long pulse in a periodic lattice.

## 2D r-z Model

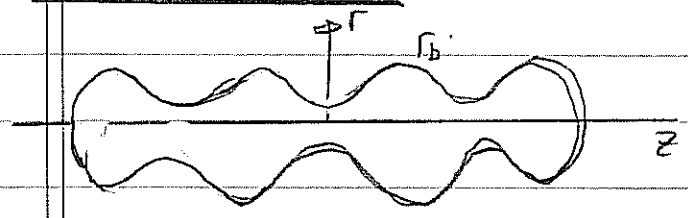


N charged Rings with smoothed interactions

$\partial/\partial\theta = 0$ Axisymmetric

Phase Space.

$\left.\begin{matrix} r, z \\ p_r, p_z \end{matrix}\right\}$ 4D + possible 1D $p_\theta$ (angular mom.)

4D or 5D.

physical charge – cylindrical rings

$$\rho = \sum_i \frac{Q_i}{2\pi} \frac{\delta(r-r_i)\,\delta(z-z_i)}{r_i}$$

smoothed charge

$$\rho = \sum_i \frac{Q_M}{2\pi} \frac{f(r-r_i,\, z-z_i)}{r_i}$$

$Q_M$ : Macro particle charge
$f$ : Smoothing function.

- Used to model solenoidal transport of an initial axisymmetric beam.
- Sometimes used to model AG beams with an approximately equivalent, s-dependant focusing force. $\vec{x}_\perp'' = k_{\beta 0}^2(s)\,\vec{x}_\perp + \cdots\cdots$

## 1D Axisymmetric Model

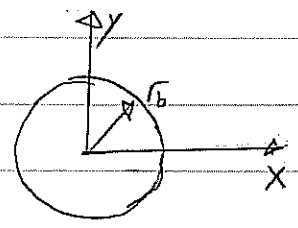


N charged cylinders with smoothed interactions

$\partial/\partial\theta = 0$

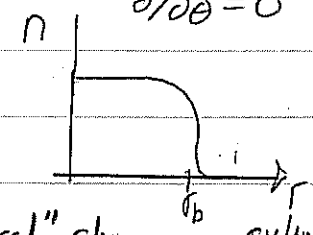


Phase – Space

$\left.\begin{matrix} r \\ p_r \end{matrix}\right\}$ 2D + possible $p_\theta, p_z$

2D to 4D

"physical" charge – cylindrical sheets

$$\rho = \sum_i \frac{Q_i}{2\pi} \frac{\delta(r-r_i)}{r_i}$$

smoothed charge

$$\rho = \sum_i \frac{Q_M}{2\pi} \frac{f(r-r_i)}{r_i}$$

$Q_M$ : Macro charge
$f$ : Smoothing function

- Simple model for continuously focused, axisymmetric beams

## 1D slab Model

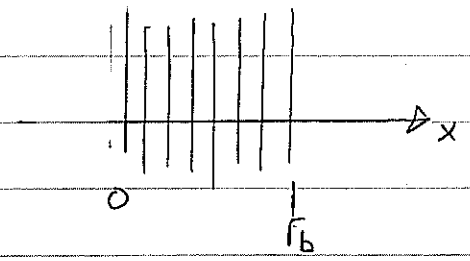


N charged slabs with smoothed interactions.

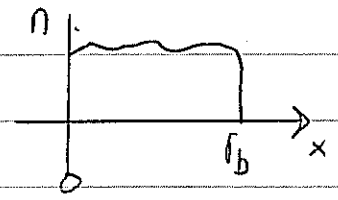


Phase-Space

$\left.\begin{matrix} x \\ p_x \end{matrix}\right\}$ 2D + possible $p_y, p_z$

2D to 4D

"physical" charge - sheets

$$\rho = \sum_i \sigma\, \delta(x - x_i)$$

smoothed charge

$$\rho = \sum_i \sigma_M\, f(x - x_i)$$

$\sigma_M$: macro particle charge
$f$: smoothing function

- Most simple model, but slab geometry is least physical.

---

It is not immediately clear how such different models can in many cases represent qualitatively similar collective interactions since force laws can change form with dimension. For example, in free space, we find that:

| Model | Free space: Field due to ith "particle" | |
|---|---|---|
| 3D | $\vec{E} = \dfrac{q_i (\vec{x} - \vec{x}_i)}{4\pi\varepsilon_0 \lvert\vec{x} - \vec{x}_i\rvert^3}$ | |
| 2D | $\vec{E} = \dfrac{\lambda_i q_i (\vec{x} - \vec{x}_i)}{2\pi\varepsilon_0 \lvert\vec{x} - \vec{x}_i\rvert^2}$ | $\lambda_i$ = line-charge "particle" |
| 1D | $E_x = \dfrac{\sigma_i}{2\varepsilon_0} \dfrac{(x - x_i)}{\lvert x - x_i\rvert}$ | $\sigma_i$ = sheet charge "particle" |

The reason these radically different interactions can give similar physics is that the screening associated with collective interactions is found to be similiar:

- Debye screening has similiar characteristics in each dimension.

showed 2D form, in class. Will show in final that the 3D scaling obtains the same Debye length definition.

$$\Rightarrow \quad \lambda_D = \frac{v_{thermal}}{\omega_p} = \left(\frac{\varepsilon_0 k_B T}{\hat{n} q^2}\right)^{1/2} \qquad v_t = (k_B T/m)^{1/2} \qquad \omega_p = \left(\frac{q^2 \hat{n}}{\varepsilon_0 m}\right)^{1/2}$$

- It is much easier to have a significant number of particles within the characteristic screening distances for lower dimensional problems.

  - Lower dimensional simulations can more easily resolve collective effects!
    (Sometimes people run 3D simulations for collective modes and present garbage answers due to resolution difficulties)

// Example

$q = Ze$ ions

$e = 1.6 \times 10^{-19}$ C

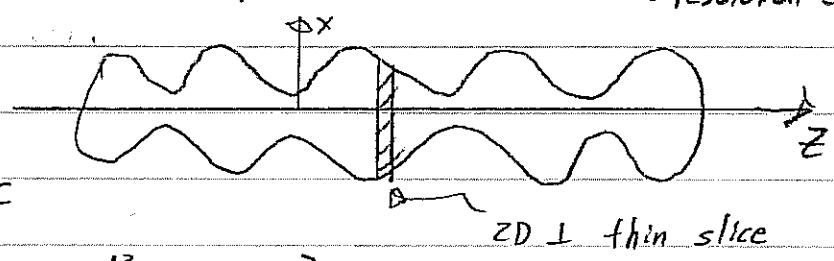


$\lambda \sim 10^{-13} \rightarrow 10^{-7}$ C/m  typical for intense beams

$$\frac{\#\text{ particles}}{\text{cm}} = \frac{\lambda}{Ze \cdot 100} \sim \frac{10^4}{Z} \rightarrow \frac{10^{10}}{Z} \qquad q = Ze$$

charge state

- Smoothing still important in lower dimensions and real beam is 3D

//

S.M. Lund Clay

89

# WARP Code Overview

Electrostatic Multi-dimensional PIC Code

WARP3d – $x, y, z, p_x, p_y, p_z$
Moves in t

Many Fieldsolvers!
SOR, Multigrid, FFT,
FFT + Tridiag, FFT + Cap Ma

WARPxy – $x, y, p_x, p_y, p_z$
Moves in s

WARPrz – $r, z, p_r, p_z, p_\theta$
Moves in t

WARPenv – envelope solver
used to seed / load PIC
$r_x, r_y, r_x', r_y'$
Advances in s

Hermes – Fluid II + Gridded
Space Charge Field

- Common diagnostic tools built around gist. graphics
- Run with python interpreter

Example Script
"ag-slice.py"

# 3D PIC simulations are being used to guide retrofits of an existing ESQ injector at LBL

## 1st principles, mid-pulse 3D simulations have been carried out to guide injector retrofits aimed at decreasing beam aberrations

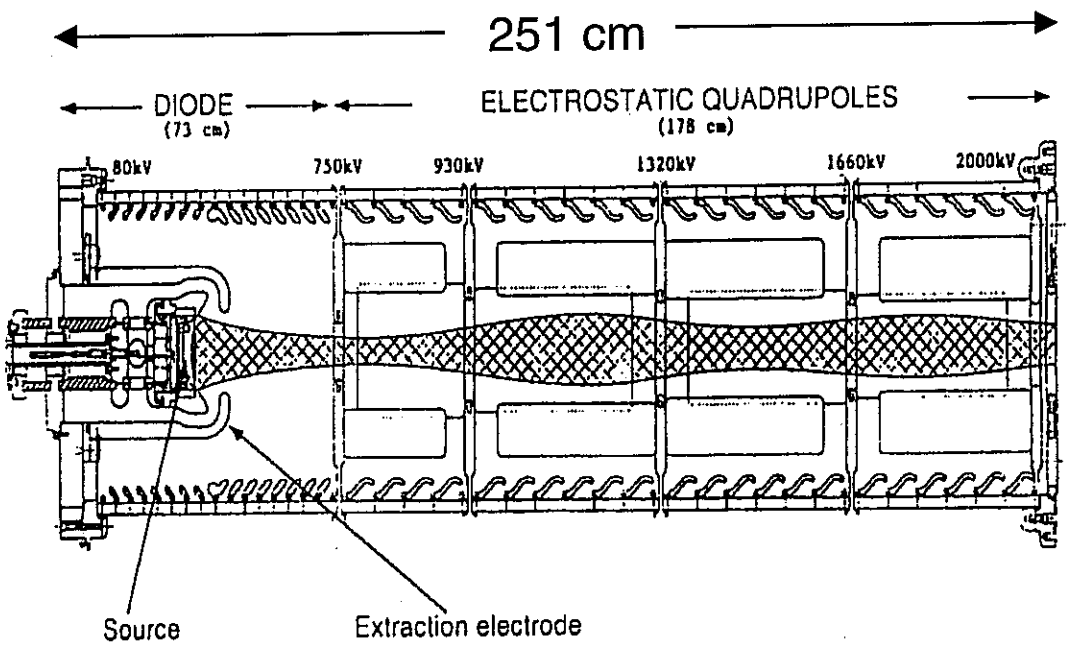


Multi-Shot Film Images of Beam at Injector Exit

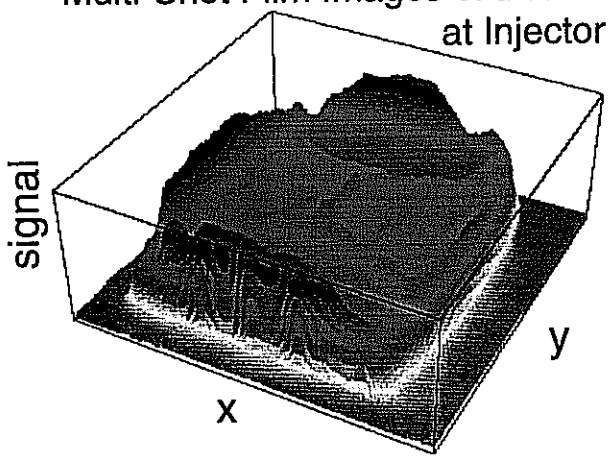


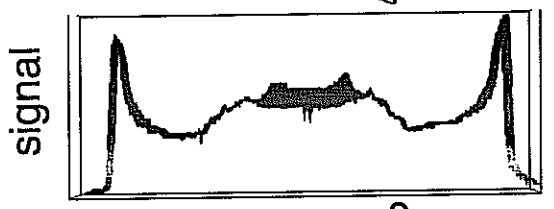


## Parameters expected at exit of retrofitted injector:

| | | |
|---|---|---|
| **Energy:** | **E = 1.71 MeV** | |
| **Current:** | **I = 692 mA, K** | |
| **Emittance:** | **$\varepsilon_n$ = 1.1 $\pi$ mm-mrad** | **rms edge measure** |
| | **~ 0.7 $\pi$ mm-mrad** | **measure eliminating empty entrained space** |
| **Envelope:** | **r_x = 56.3 mm** | **r_x' = 53.8 mrad** |
| | **r_y = 55.7 mm** | **r_y' = -44.8 mrad** |



810 Example PIC Simulations

S.M. Lund 54

# HCX Injector: Simulations show distribution distortions in the retrofitted injector should be more modest

## Mid-pulse distribution projections at exit plane of injector

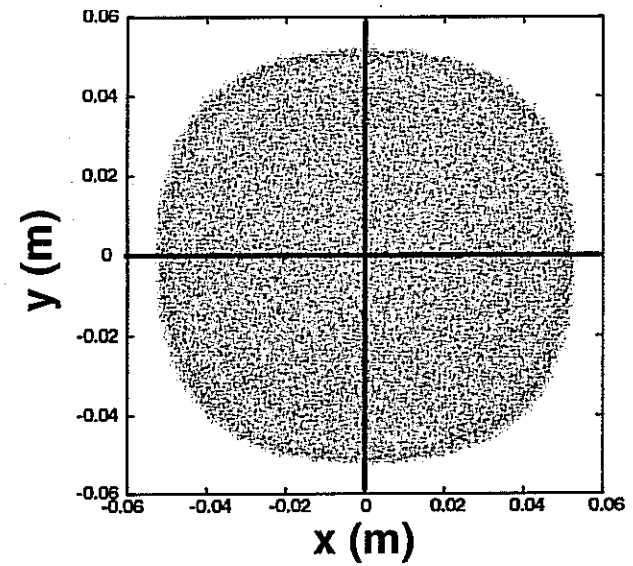


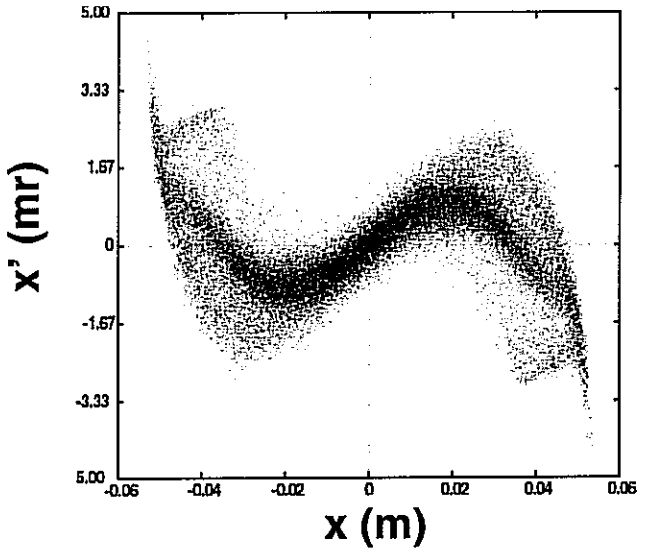


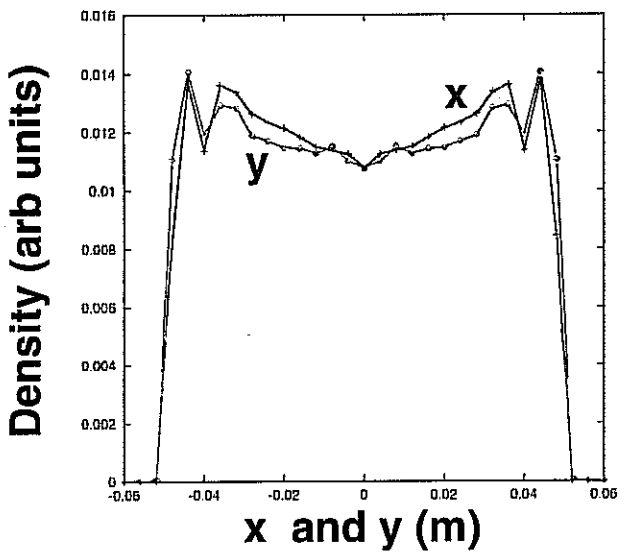


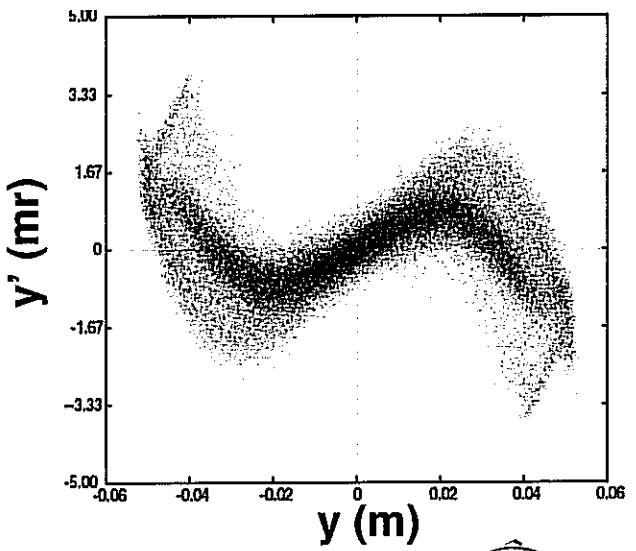


Overall convergence and divergence angles removed to illustrate distortions



SM, Lund 35/

# Simulations show how waveform rise-time determines beam head mismatch

**Tuned 1d diode voltage waveform rise-time is 400 ns -- deviations from this lead to significant mismatch effects in the beam head and particle loss with resultant worries about breakdown, electron effects, etc.**

Rise-time $\tau$ = 800 ns

beam head particle loss < 0.1%

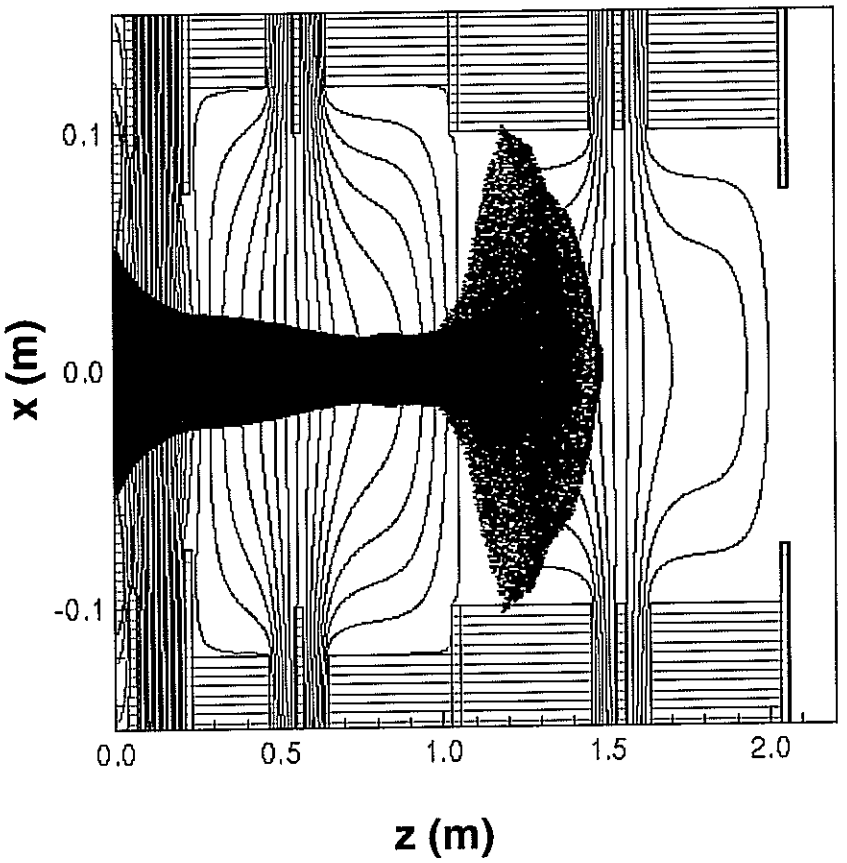


Rise-time $\tau$ = 400 ns

zero beam head particle loss

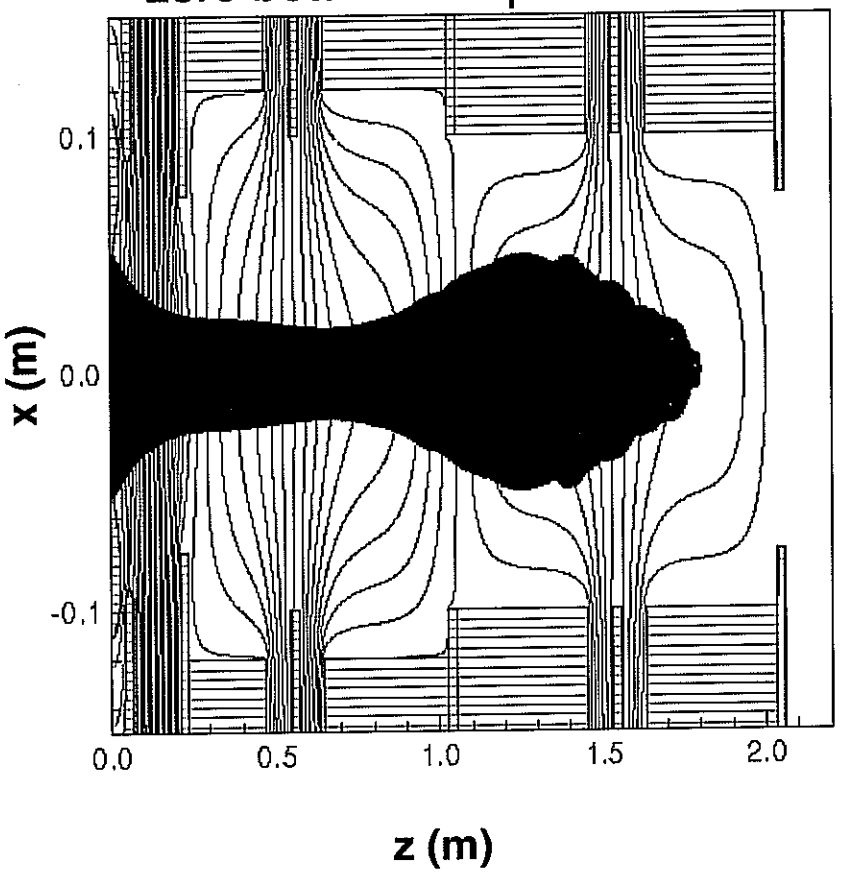




S.M. Lund 5/6/

# Initial distribution distortions will launch a spectrum of collective mode perturbations that evolve

**Kinetic and fluid theories have been employed to analyze perturbations on a uniform density intense-beam equilibrium [Lund and Davidson, Phys. Plasmas, 5 3028 (1998)]**

Small Amplitude Perturbations (arbitrary units, kinetic and fluid theory)

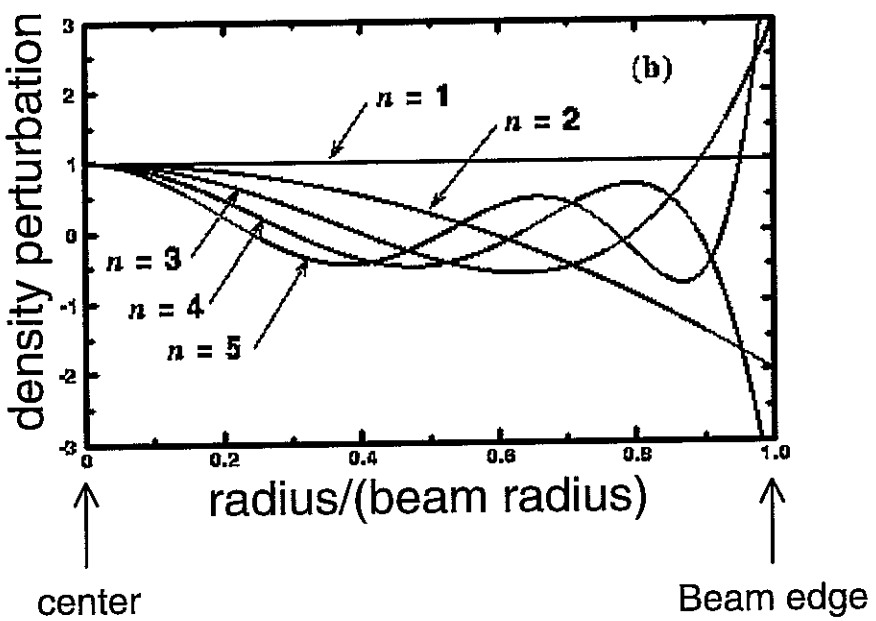


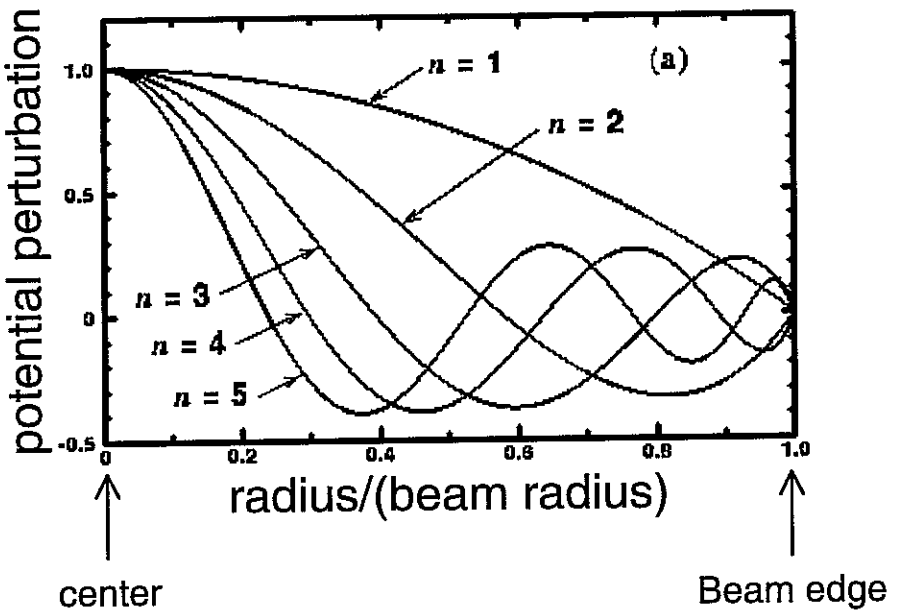


Mode Dispersion Relation (fast branch, from fluid theory)

$$\frac{\sigma_n}{\sigma_0} = \sqrt{2 + 2\left(\sigma/\sigma_0\right)^2 (2n^2 - 1)}$$

$\sigma_n$ = mode phase advance

n = 1,2,3, .....

Example:

$\sigma_0 = 80^o$, $\sigma/\sigma_0 = 0.2$

$\sigma_1 = 115^o$, $\sigma_5 = 182^o$, ....

S.M. Lund 57/

# Perturbations launched by initial distribution nonuniformities can phase-mix to a more uniform profile with increased emittance

## Mode spectrum launched can undergo a rapid cascade, settling to a smaller amplitude and lower order distortion

- Approximate conservation constraints employed to bound emittance increases resulting from full relaxation to a uniform profile [Lund, Lee, and Barnard, Proc. Linac 2000, pg. 290]
- How will such evolutions influence the range and interpretation of measurements

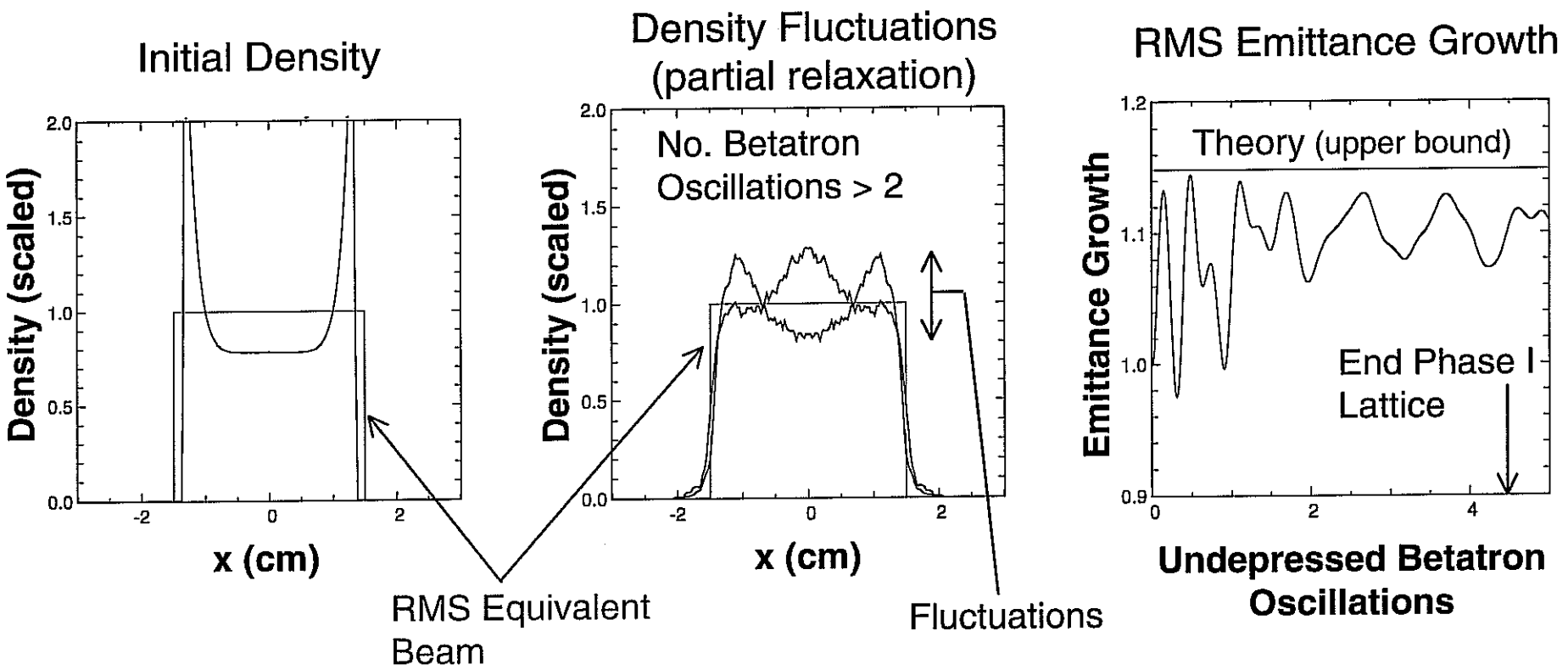




S.M. Lund 58/

# Analytic theory has been used to parametrically bound emittance growth due to the relaxation of space-charge nonunifomities

**Approximate conservation constraints can be employed to estimate maximal emittance increases resulting from the relaxation of an initial nonuniform density profile to a final, uniform profile [Lund, Lee, and Barnard, Proceedings Linac 2000, Monterey, CA, pg. 290]**

Initial Density

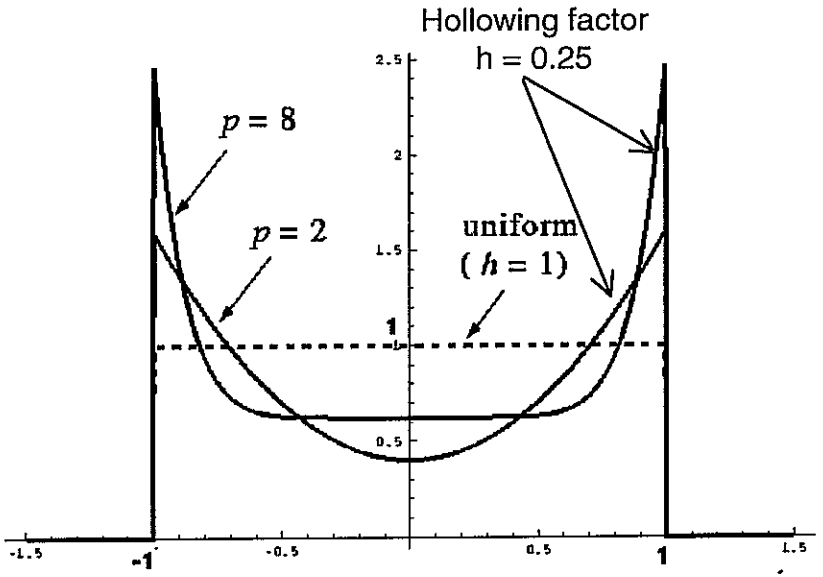


hollowing ~ $r^p$

h = ratio min to max density

Emittance Growth on Relaxation

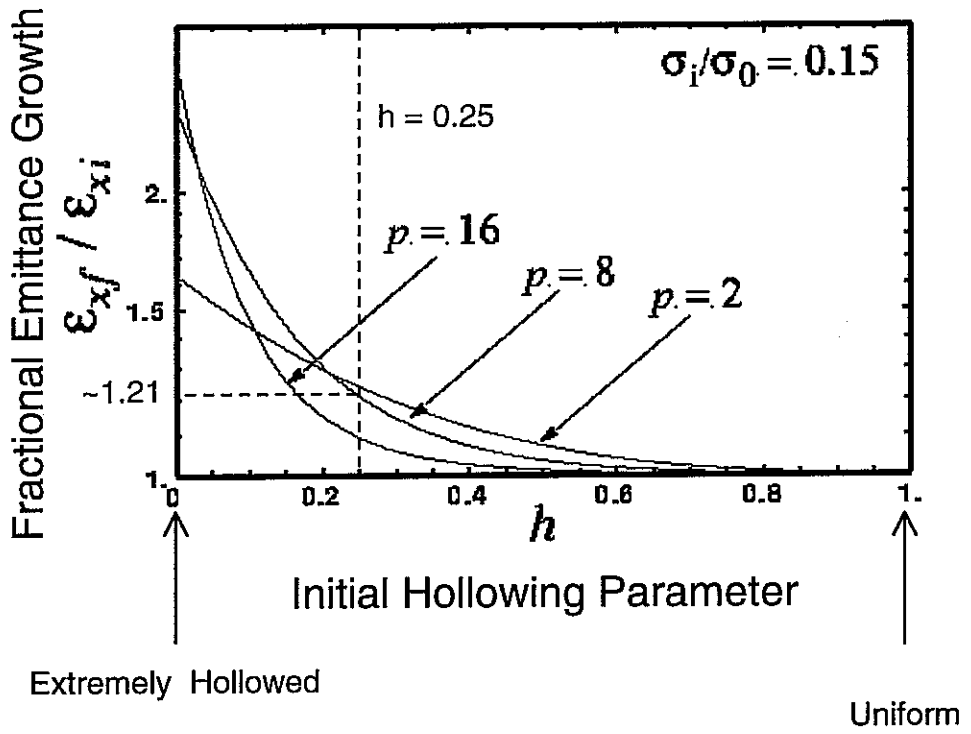


S.M. Lund 5/8/

# HCX Phase II: A wide range of parametric simulations have been carried out with realistic magnetic transport lattices

## A syncopated magnetic transport lattice of ~ 50 lattice periods has been designed

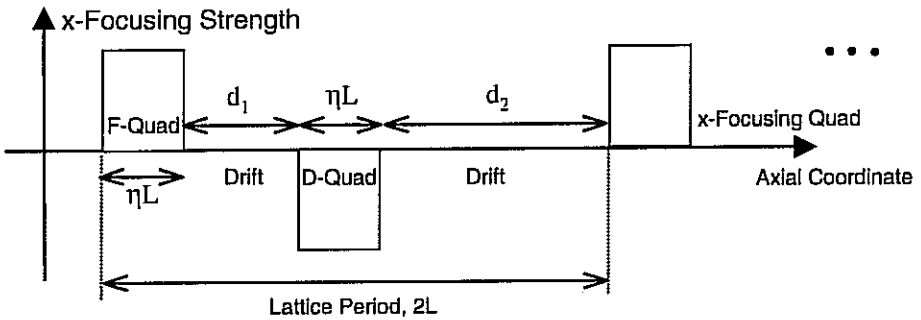


| | | HCX: |
|---|---|---|
| $\eta$ = Quadrupole Occupancy | $(0 < \eta < 1)$ | $\eta = 0.453$ |
| $\alpha$ = Syncopation Factor | $(0 < \alpha < 1)$ | $\alpha = 0.248$ |

Drifts:

$d_1 = \alpha(1-\eta)\eta L$

$d_2 = (1-\alpha)(1-\eta)\eta L$

## Superconducting magnetic quadrupoles have been designed and prototyped

$r_p = 29.5$ mm $\quad B_q' = 104$ T/m (max) $\quad B_q \sim 6$ Tesla (wire)

$\ell = 136$ mm $\quad \ell_{eff} = 101$ mm $\quad$ Integrated Field Error $< 15 \times 10^{-3}$

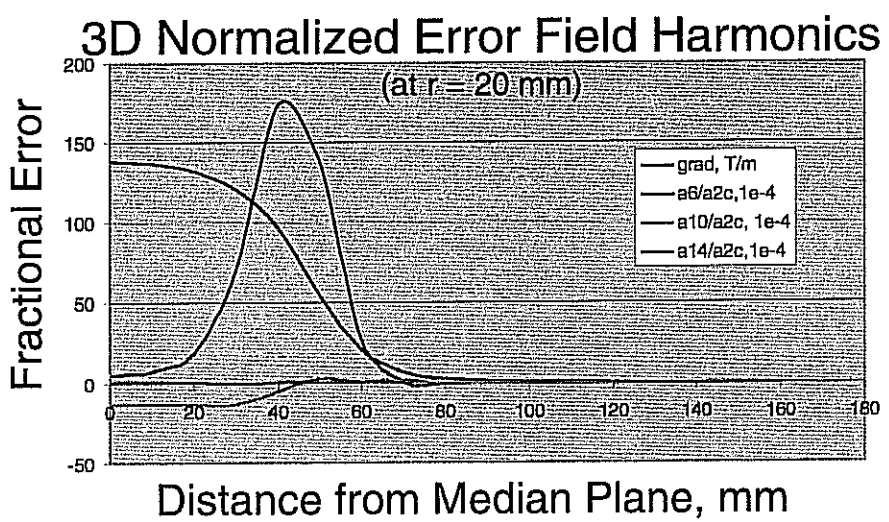


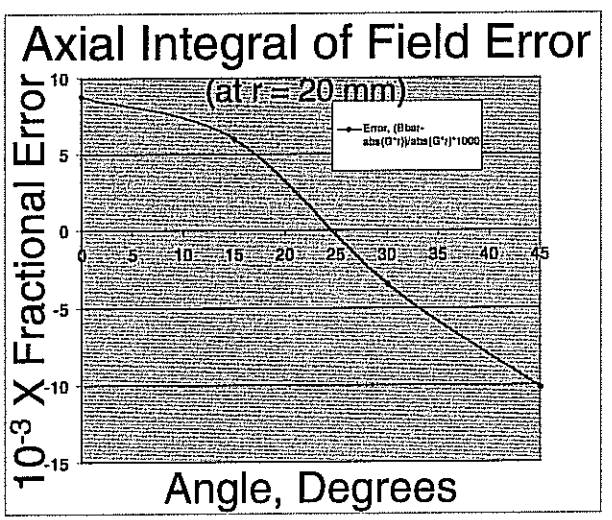




S.M. Lund 60/

# HCX Phase II: Processes influencing beam quality and control have been explored --- Example: Nonlinear applied fields and beam quality

**Full 3D magnetic field is resolved as:**

$$\vec{B} = \vec{B}_{quad} + \delta\vec{B} \qquad \delta\vec{B} \rightarrow s \cdot \delta\vec{B}$$

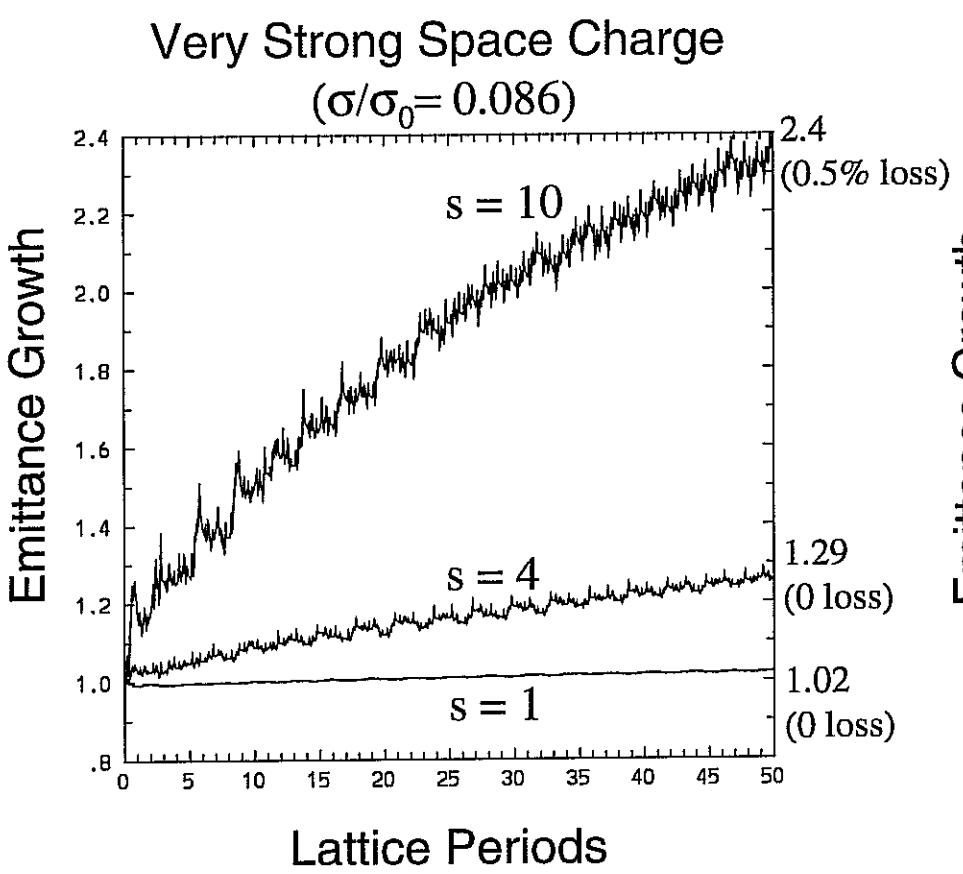


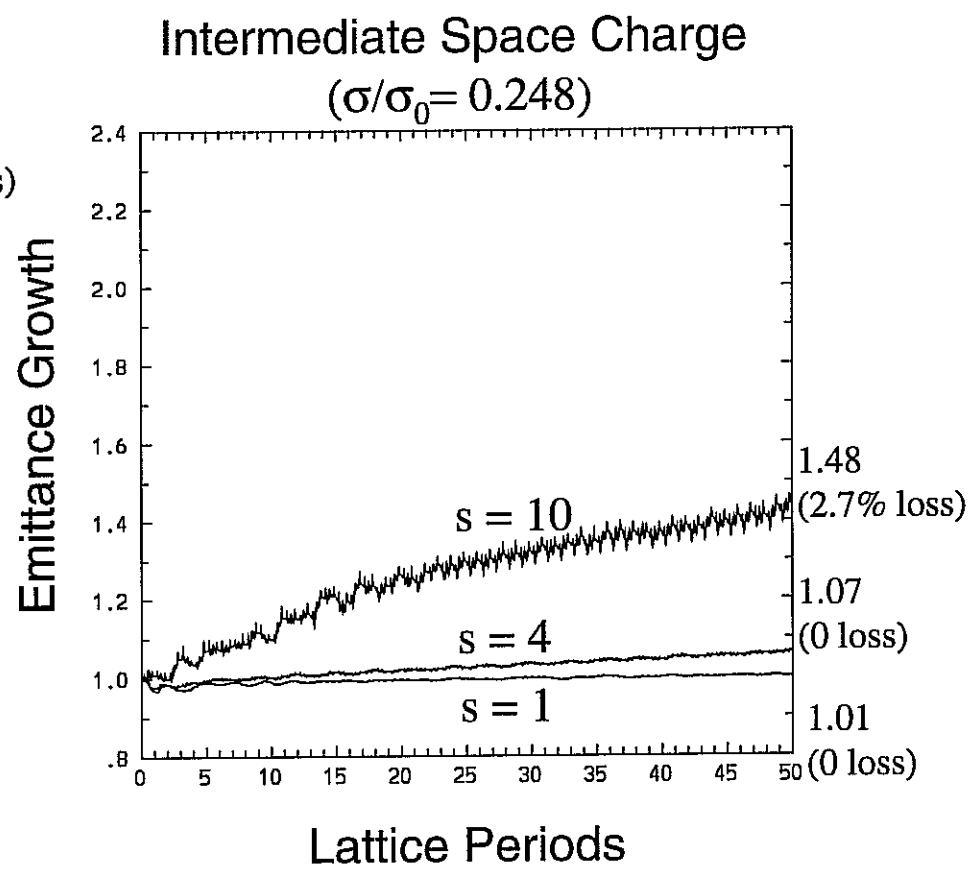


S.M. Lund 6/1/

S.M. Lund 62/



Initial KV Distribution

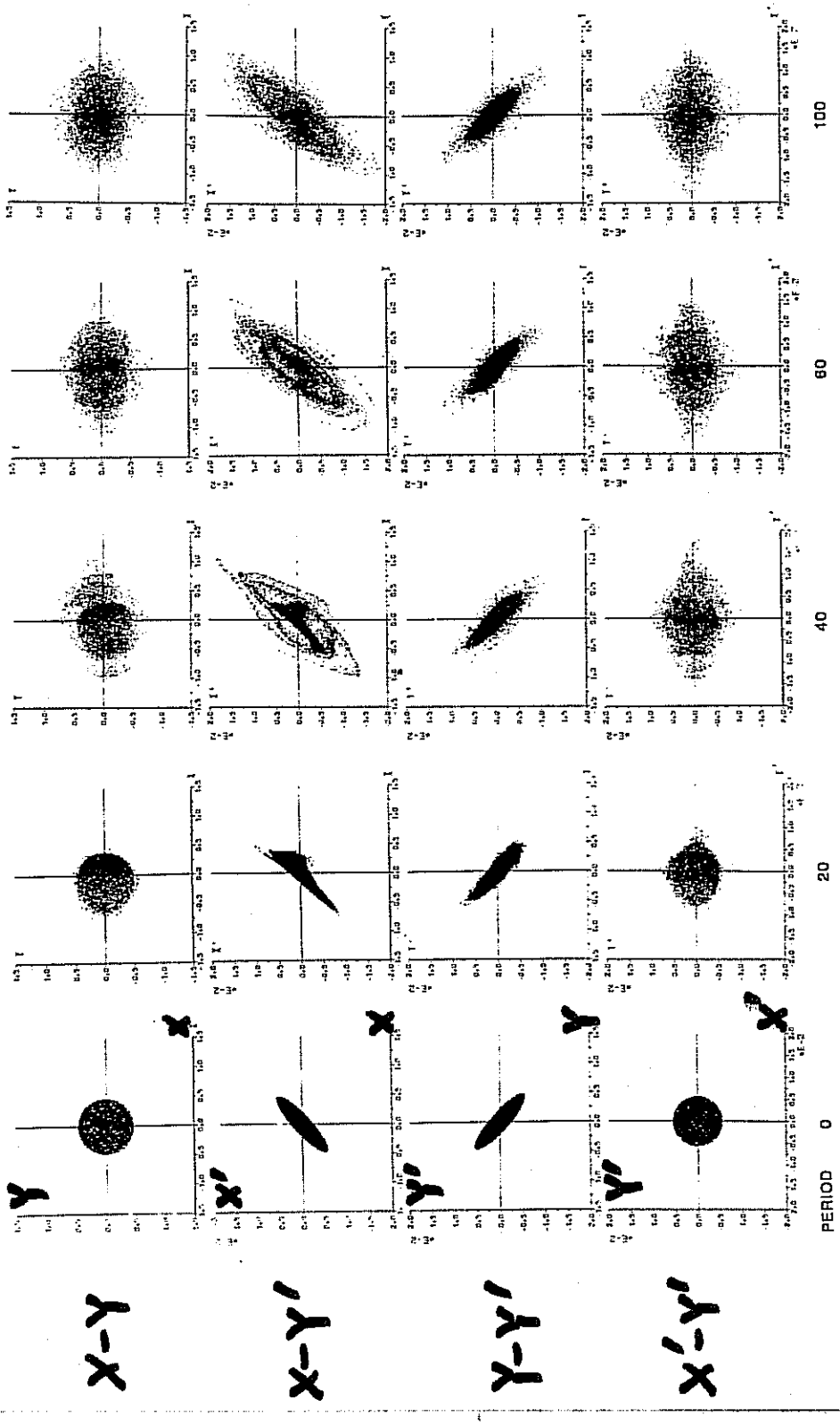


FIGURE 2 Transformation of an initial K-V distribution through the GSI FODO channel at $\sigma_0 = 90°$, $\sigma = 41°$.

J. Struckmeier, J. Klabunde, and M. Reiser, Part. Accel. 15, 47 (1984).

See also Reiser Text, pg 495.

# Initial Gaussian Distribution

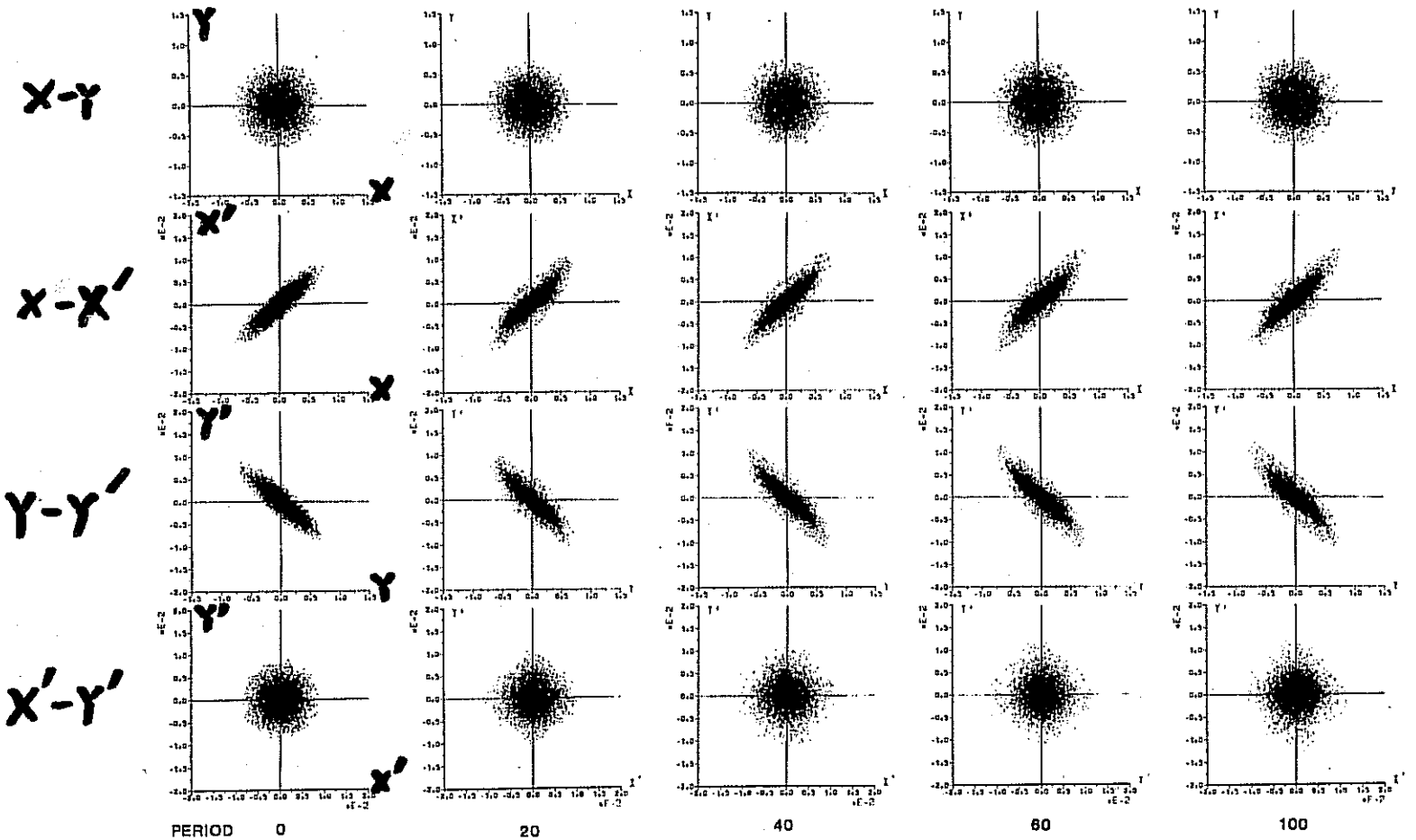


FIGURE 6 Transformation of an initial Gaussian distribution (rms-matched) through the GSI FODO channel at $\sigma_0 = 90°$, $\sigma = 41°$.

J. Struckmeier, J. Klabunde and M. Reiser, Part. Accel. 15, 47 (1984)

SM, Lund 63/

S.M. Lund 64



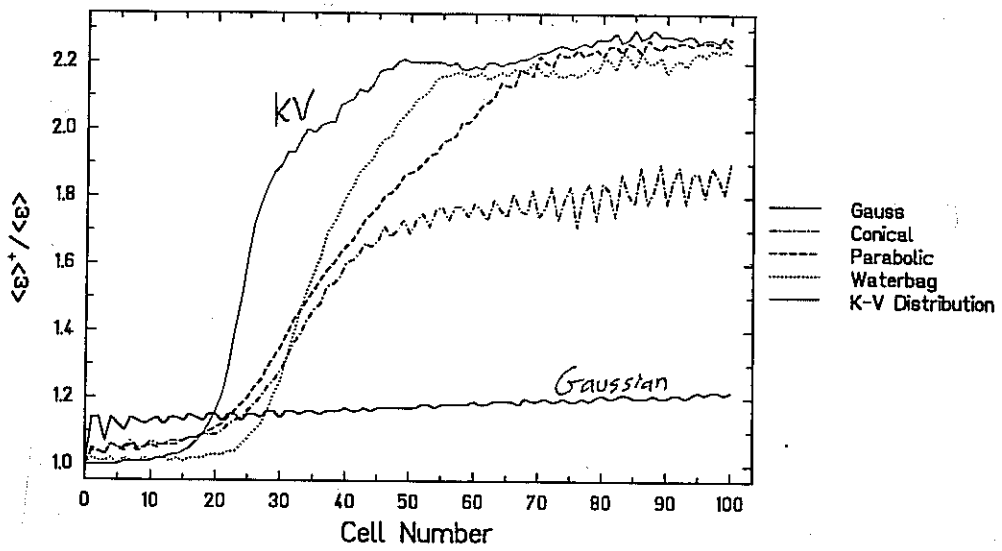


FIGURE 7 Emittance growth factors versus the number of cells obtained from particle simulations for initial K-V, waterbag, parabolic, conical and Gaussian distributions at $\sigma_0 = 90°$, $\sigma = 41°$.

From J. Struckmeier, J. Kabunde, and M. Reiser, Part. Accel. 15 47 (1984).

## Distribution Methods — Direct Gridded Solution of Vlasov's Equation.

Consider the Vlasov equation as an example.

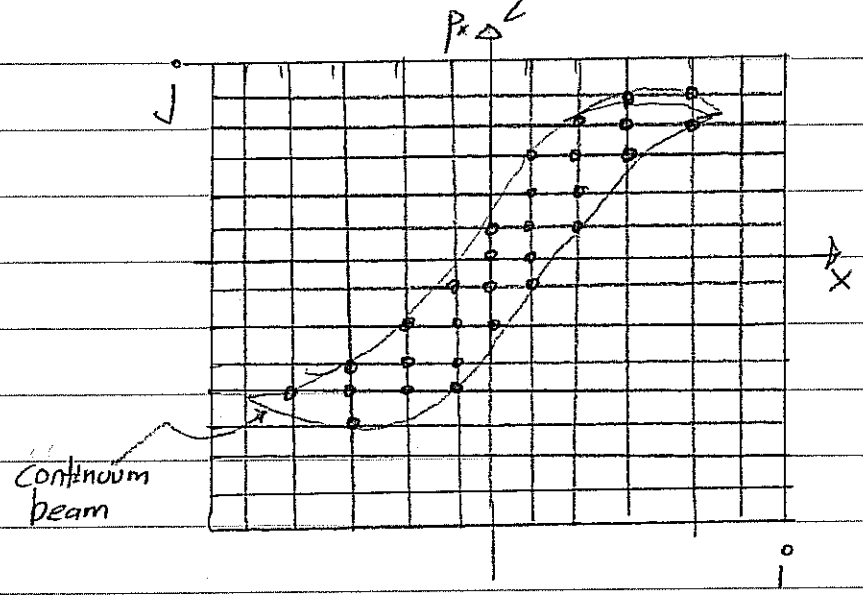


$$f(x_i, p_j, t) = f_{ij}(t)$$

The distribution is advanced at discrete grid points in time.

- Fields are typically solved using a discrete spatial mesh as for the particle methods described before.
  - Deposition on mesh is typically straightforward in Vlasov case (sum over momentum variables.

- The distribution advance cycle is different than for particle methods.
  - Numerical stability is key.
  - Characteristics and "semi-Lagrangian" methods can be employed.
  - Methods for solving for characteristics are familiar from dynamics/plasma physics.

# Direct Vlasov Methods:

S. M. Lund 661

## "Pros"

Reasons for Vlasov simulations:

- Low noise - only discretization effects without statistical effects
- Allows clear analysis of collective effects and tenuous distribution components.

## "Cons"

Reasons why Vlasov simulations are presently employed less than PIC:

- Extreme memory requirements for needed grid resolution in multi-dimensional phase space.
  - Beams often have sharp edges in phase space that move in responce to varying applied focusing forces.
- Numerical stability tends to be more difficult than in particle methods.

No time to illustrate Vlasov and other distribution methods in this introductory course. We hope to cover these methods and other numerical fieldsolve techniques in a later expanded version of this class.

However ..... it is easy to generalize from what we have learned!